MODELLING OF ENERGY REQUIREMENTS

BY A NARROW TILLAGE TOOL

A Thesis Submitted to the College of

Graduate Studies and Research

in Partial Fulfillment of the Requirements

for the Degree of Doctoral of Philosophy

in the Department of Agricultural and Bioresource Engineering

University of Saskatchewan

Saskatoon

By

Seyed Reza Ashrafi Zadeh

PERMISSION TO USE

In presenting this thesis in partial fulfillment of the requirements for a postgraduate degree from the University of Saskatchewan, the author agrees that the libraries of this university may make it freely available for inspection. The author further agrees that permission for copying of this thesis in any manner, in whole or in part, for scholarly purposes may be granted by the professor (s) who supervised my thesis work or, by the head of the department or the dean of the college in which my thesis work was done. It is understood that any copying or publication or use of this thesis or parts thereof for financial gain shall not be allowed without my written permission. It is also understood that due recognition shall be given to me and to the university of Saskatchewan in any scholarly use which may be made of any material in my thesis.

Requests for permission to copy or to make other use of material in this thesis in whole or part should be addressed to:

Head of the Department of
Agricultural and Bioresource Engineering
University of Saskatchewan
57 Campus Drive
Saskatoon SK S7N 5A9
Canada

ABSTRACT

The amount of energy consumed during a tillage operation depends on three categories of parameters: (1) soil parameters (2) tool parameters and (3) operating parameters. Although many research works have been reported on the effects of those parameters on tillage energy, the exact number of affecting parameters and the contribution of each parameter in total energy requirement have not been specified. A study with the objectives of specifying energy consuming components and determining the amount of each component for a vertical narrow tool, particularly at high speeds of operation, was conducted in the soil bin facilities of the Department of Agricultural and Bioresource Engineering, University of Saskatchewan.

Based on studies by Blumel (1986) and Kushwaha and Linke (1996), four main energy consuming components were assumed: (1) energy requirements associated with soil-tool interactions; (2) energy requirements associated with interactions between tilled and fixed soil masses; (3) energy requirements associated with soil deformation; and (4) energy requirements associated with the acceleration of the tilled soil. Energy requirement of a vertical narrow tool was calculated based on the draft requirement of the tool measured in the soil bin. The effects of three variables, moisture content, operating depth and forward speed, were studied at different levels: (1) moisture content at 14% and 20%; (2) depth at 40, 80, 120 and 160 mm; and (3) speed at 1, 8, 16 and 24 km h^{-1}. Total energy requirement was divided into these four components based upon the procedure developed in the research.

Regression equations for different energy components were developed based on experimental data of two replicates and then validated by extra soil bin experiments conducted at same soil and tool but different operational conditions. The set up of energy components data in the model development showed good correlation with the available experimental data for all four components. Coefficients of all regression equations showed a first order energy-moisture content relationship best applicable to those equations of energy components. For the acceleration component, energy-depth relationship at all speed levels resulted in an equation which included first and second

orders of depth. In contrast, if only two higher levels of speed were used in the regression model, the relationship between acceleration energy and depth resulted in the second order of depth. When experimental data of acceleration energy at 8, 16, and 24 km h^{-1} speeds were used in the regression equation, the acceleration energy-speed relationship resulted in both linear and quadratic relationships. It was concluded that for the tool and soil conditions used in the experiments, 8 km h^{-1} speed resulted in only linear relationship. On the other hand, 16 and 24 km h^{-1} speeds resulted in a quadratic relationship. Therefore, for all 3 speeds used in experiments, both linear and quadratic relationships were obtained. Considering that the tool was operating at high speeds, this research is expected to contribute valuable experimental data to the researchers working in the field of soil dynamics.

ACKNOWLEDGEMENTS

DEDICATION

This work is dedicated to my beloved country, Iran, and its great people, and as their representatives, it is dedicated to my wife Leila, and my sons, Abolfazl and Mohammad for their love and encouragement.

TABLE OF CONTENTS

ix

LIST OF TABLES

LIST OF FIGURES

LIST OF SYMBOLS

A_e	average cut area, m^2
$A_{soil..wedge}$	soil wedge surface area in front of the tool, m^2
A_{tool}	tool surface area engaged with soil, m^2
C	soil-soil cohesion, Pa
C_a	soil-tool adhesion, Pa
d	total working depth below the soil surface, m
E	tool energy requirement, J
g	acceleration due to gravity, 9.81 m s^{-2}
K_e	ratio of mean to maximum cutting force
K_v	coefficient of speed effect
N	normal force applied on the tool surface, N
N_a	an additional factor comprised in soil cutting forces, which accounts for the acceleration forces in the soil with varying tool speeds, but a fixed soil strength
N_{ca}	factor depends on soil-metal adhesion
N_γ, N_c, N_q	factors depend on soil frictional strength, soil geometry, and tool to soil Strength properties
P	total cutting force, N
P	quasi-static draft, N
P_1	force applied to the center wedge of the soil, N
P_2	force applied to the side crescent of the soil, N
P_A	inertia force of soil in acceleration, N
P_C	bottom-edge cutting force, N
P_F	frictional force along the cutting blade surface, N

P_G	compressive force of soil along the blade, N
P_{SH}	side-edge shear force, N
P_x	total draft of the tool, N
q	surcharge pressure vertically acting on the soil surface, N m^{-2}
$S_{cutting}$	soil cutting force, N
S_{shear}	soil shear force, N
v	tool speed, m s^{-1}
V	operating speed, m s^{-1}
V_d	soil disruption speed, m s^{-1}
w	tool width, m
α	tool rake angle, degrees
β	angle of the soil wedge rupture, degrees
ρ	soil bulk density, kg m^{-3}
δ	soil-metal friction angle, degrees
σ_n	normal pressure acting on the internal shear surface, kPa
τ	soil shear strength, N m^{-2}
τ_{max}	maximum shear strength along the soil to tool interface, kPa
ϕ	soil-soil friction angle, degrees

1.0   INTRODUCTION AND OBJECTIVES

1.1   Introduction

Agricultural engineering began to emerge as a branch of engineering in the early years of the twentieth century. From the beginning, agricultural engineers were concerned with efficiency in the application of energy in agriculture. While energy efficiency was not always an explicit goal, it was often a major driving force as improved machinery, power units, water systems, and other technologies evolved. For example, the steel plow reduced draft, and rubber tires on tractors improved traction. Both developments saved fuel and reduced operating costs. More recently, agricultural engineers have worked to improve the efficiency of electrical energy use in grain dryers, food processing systems, and a host of other applications. Thus, agricultural engineers have always been energy engineers in agriculture (Stewart 1979, as referenced by Hall and Olsen, 1992).

Agricultural tillage involves soil cutting, soil turning, and soil pulverization and thus demands high energy, not just due to the large amount of soil mass that must be moved, but also due to inefficient methods of energy transfer to the soil. The most widely used energy-transfer method is to pull the tillage tool through the soil. Various methods have been attempted to improve efficiency such as vibratory tillage tools. However, development of more efficient methods effectively depends upon the necessity for improved understanding of tillage tool mechanics. Complete tillage mechanics is far from being realized, although generalized relations have been proposed (Fornstrom et al. 1970).

Draft and energy requirements, based on current soil and operating conditions, are considered important parameters for design and manufacture of improved tillage

1

implements. Thus quantification of these parameters with respect to different soil failure patterns necessitates having good knowledge of soil-tool interaction.

During the 20th century, the appearance of new theories in the field of soil mechanics, mostly started by Terzaghi (1943), enabled new research in both areas of civil and agricultural engineering. The improvements, brought on by these theories, continued in the second half of the century as use of computers increased. In the field of soil-tool interaction, experimental and analytical models appeared during the 1940's. The finite element method (FEM), which originated in aviation engineering in the 1950's, was developed for soil cutting processes by Yong and Hanna (1977). This method has received much attention in recent decade to investigate soil-tool interactions (Shen and Kushwaha 1998).

Tillage tools apply forces to soil resulting soil failure for enhanced agricultural production; e.g., by increasing emergence, improving plant rooting, increasing infiltration, and controlling erosion (Ellison 1947; Lindstrom et al. 1990). The primary interest in tillage operations is the application of mechanical forces by machines to change the soil condition for agricultural production purposes (Schafer and Johnson 1982).

The force systems, applied by a tool, can cause the soil to yield by shear, compression, tension, and/or plastic flow. Yield or failure conditions in soil are much complex than in many engineering materials because soil conditions vary from a near liquid state to a brittle state. Shear failure and fracture for brittle materials have a clear meaning. Fracture by shear is also observed in soil. In some cases, however, fracture is not apparent in soils which may exhibit plastic flow and permanent deformation. The stress state that causes soil fracture or plastic flow is a measure of the soil shear strength. Thus, shear failure is some function of the stress state than just causes failure (Johnson et al. 1987). The amount of force required to shear the soil would change based upon soil conditions, tool specifications, and operational parameters employed during a tillage operation.

Depth of cut, width of cut, tool shape (including cutting edges), tool arrangement, and travel speed are factors that may affect draft and the energy utilization efficiency for a specific soil condition. The effects of these parameters vary with different types of

implements and with different soil conditions (Kepner 1972). Factors such as soil texture, soil moisture content, soil compaction, tool geometry, tool operating depth, tool forward speed, and tool rack angle obviously affect the energy requirement of a tillage operation. There has been much research that discusses the effect of these factors for different soil and tool conditions on tool energy requirement although each of them has some limitations in their applications (Nichols 1931; Payne 1956; Nikiforov and Bredun 1965; McKyes and Ali 1978; Koolen and Kuipers 1983).

In spite of the capability of various methods (Reece 1965; Godwin and Spoor 1977; Swick and Perumpral 1988; Chi and Kushwaha 1991) to model soil-tool interaction, researchers are still working on new models to compensate for some shortcomings of the current models. These methods are either complicated or ignoring some basic aspects that affect the results. For example, analytical methods are not able to account for all aspects of a real situation of a tillage operation as a dynamic process. Empirical methods are very costly due to the instrumentations which are required to record data precisely. These methods also cannot be implemented at any desired time and place since providing required instrumentation may not be possible, and in most cases, empirical methods represent only regional conditions. On the other hand, finite element methods are very professional methods to be implemented as they need good knowledge of mathematics and computer science. In addition, the predictions of FEM models are based on particular constitutive relationships. The parameters involved in such relationships are normally acquired through laboratory tests such as triaxial tests. Since soil in such laboratory tests undergoes situations that do not represent actual soil failure during tillage operations, those modeling methods need improvement. Therefore, it seems necessary to investigate new models for soil-tool interaction process in order to achieve better predictions of draft and energy requirements of different tillage implements during real operations. Since the application of soil mechanics in agriculture is complicated due to non-homogeneity of soil medium, further attempt to explore some aspects of soil dynamics in tillage, which have not received enough attention, should be undertaken.

In current research, efforts have been made to introduce a model that accounts for different energy consuming components of a narrow tillage tool. In this thesis, chapter 2

is a literature review that addresses fundamentals of soil mechanics regarding main issues such as speed, depth, soil and tool specifications affecting draft and energy requirements, operational conditions, and the interactions among these factors. In chapter 3, materials used for the tests, experimental procedure, and components of statistical analysis have been explained. Chapter 4 deals with the results of the experiments and the trends of draft and energy requirements of the tool, employed in this research, due to the change in moisture content, tool depth, and tool forward speed. In addition, soil mechanics theories have been implemented to justify those trends and to discuss regression equations determined for the energy components. In chapter five, suggestions for future research have been given based on the results obtained from this research.

1.1 Objectives

The overall objective of this research was to investigate energy requirement during a tillage operation. The specific objectives were:

1) To develop a mathematical model for the total energy requirement by evaluating energy requirement for four specified components as follows: (1) energy requirements associated with soil-tool interactions; (2) energy requirements associated with interactions between tilled and fixed soil masses; (3) energy requirements associated with soil deformation; and (4) energy requirements associated with the acceleration of the tilled soil.

2) To validate the model by experimental data from tests in a soil bin.

2.0   LITERATURE REVIEW

During a tillage operation various factors can affect energy requirement of a tool. These factors can be categorized in three main groups: (1) soil parameters (2) tool parameters and (3) operational parameters. To evaluate energy requirement of a tillage tool, energy requirement resulted from each group of factors should be taken into account in order to have an estimation of total energy requirement. Reece (1965) recognized that the mechanics of earthmoving is similar in many respects to the bearing capacity of shallow foundations on soil as described by Terzaghi (1943). According to Terzaghi's theory, the following equation was proposed by Reece (1965) as the universal earthmoving equation for describing the force required to cut the soil by a tool:

$$P = (\gamma g d^2 N_\gamma + cdN_c + c_a dN_a + qdN_q)w \tag{2.1}$$

where:

   P = total tool force, N

   γ = total soil density, N m^{-3}

   g = acceleration due to gravity, 9.81 m s^{-2}

   d = total working depth below the soil surface, m

   c = soil cohesion, N m^{-2}

   c_a = soil-tool adhesion, N m^{-2}

   q = surcharge pressure vertically acting on the soil surface, N m^{-2}

   w = tool width, m

N_γ, N_c, N_q = factors depend on soil frictional strength, soil geometry, and tool to soil Strength properties

According to the above equation, which is well accepted by researchers (Hittiaratchi-Reece 1967; Godwin-Spoor 1977; McKyes-Ali 1977; and Perumpral et al. 1983), the following factors affect force and consequently energy requirement by a tillage tool: soil bulk density, soil cohesion, soil frictional strength, geometry of cut soil, tool to soil adhesion and friction angle, tool operating depth, and tool width. This equation takes into account almost all affecting factors except for tool speed which manifests dynamic aspect of soil tillage. To compensate for this shortcoming of Reece equation, McKyes (1985) proposed another equation that basically was the same as Reece equation with a new term to account for the effect of tool speed on force requirement. Equations 2.2 and 2.3 present McKyes envelope with varying tool speeds, but fixed soil strength.

$$P = P_1 + 2P_2 = (\gamma g d^2 N_\gamma + cdN_c + c_a dN_{ca} + qdN_q + \gamma v^2 dN_a)w \tag{2.2}$$

$$N_a = \frac{\tan\beta + \cot(\beta + \phi)}{\left[\cos(\alpha + \delta) + \sin(\alpha + \delta)\cot(\beta + \phi)\right]\left[1 + \tan\beta\cot\alpha\right]} \tag{2.3}$$

where:

P = total cutting force, N

P_1 = force applied to the center wedge of the soil, N

P_2 = force applied to the side crescent of the soil, N

γ = total soil density, N m^{-3}

g = acceleration due to gravity, 9.81 m s^{-2}

d = total working depth below the soil surface, m

c = soil cohesion, N m^{-2}

C_a = soil-metal adhesion, N m^{-2}

q = surcharge pressure vertically acting on the soil surface, N m^{-2}

w = tool width, m

v = tool speed, m s^{-1}

N_γ, N_c, N_q = factors depend on soil frictional strength, soil geometry, and tool to
soil strength properties

N_{ca} = factor depends on soil-metal adhesion

N_a = an additional factor comprised in soil cutting forces, which accounts for the
acceleration forces in the soil with varying tool speeds, but a fixed soil
strength

α = rake angle

δ = soil-metal friction angle

ϕ = internal friction angle of soil

β = angle of the soil wedge

In the next sections, how the factors mentioned in Equations 2.1 through 2.3 affect draft and energy requirements of tillage tools are discussed. The affecting factors are discussed in three main groups as categorized above.

2.1   Soil Parameters

Soil physical and mechanical properties and soil dynamics properties have significant influences on the amount of energy requirement of a tillage operation. In this section, some of the most important soil physical and soil dynamic properties which affect draft and energy requirements of tillage tools are discussed.

2.1.1   Soil Physical Properties

Soil moisture content and soil texture affect mechanical behaviour and strength of soil. Soils at same mechanical and environmental conditions but different texture behave differently. Camp and Gill (1969) and smith (1964) reported that shear strength parameters of fine grained soils decreased with increasing moisture content. However, the soil density was concurrently decreasing as the moisture content was increased. Presence of water in void space of fine- grained soils can have a major impact on the engineering behaviour of the soil. Therefore, it is important to know not only how much

water is present, but also how it can affect engineering behaviours. As moisture content of a soil increases, the soil changes from a brittle solid to a plastic solid and eventually to a viscous liquid. Atterberg limits are moisture contents at certain limiting or critical stages of soil behaviour (Holtz and Kovacs 1981). These limits along with the natural moisture content are paramount in predicting the behaviour of fine-grained soils. The limits can be correlated to the engineering properties such as soil strength, compressibility, swelling potential, clay mineralogy, and stress history. Mckibben and reed (1952) reported that the effect of tool speed on draft was also influenced by the clay and moisture content.

Bulk density of a soil is a function of soil moisture at any given amount of compactive effort. As the soil wetness increases, the moisture weakens the inter-particle bonds, causing swelling and reducing internal friction making the soil more workable and compactable (Hillel 1980). However, as the soil wetness nears saturation, the fractional volume of expellable air is reduced and the soil can no longer be compacted to the same degree as before with the same compactive effort. The optimum moisture content is the point at which the soil wetness is just enough to expel all the air from the soil, and the corresponding density is the maximum dry density. Mouazen and Ramon (2002) reported that draft force of subsoiler was increased with wet and dry bulk densities where it decreased with soil moisture content. Draft force was changed linearly with moisture content where it was a quadratic function of wet bulk density and a cubic function of dry bulk density respectively. The decrease in draft with moisture content did not extend beyond a moisture content of 17%.

Mechanical behaviour of soil is influenced by any changes that occur in soil bulk density. This normally happens during tillage operations. Ayers (1987) studied the effect of soil moisture content and density effect on soil shear strength parameters of coarse grained soils during tillage operations. It was reported that cohesion and friction angle of those three loamy sand soils employed in the study increased with increasing soil density.

Tillage treatments are expected to affect soil response and crop yield. Erbach et al. (1992) evaluated the effect of no till, chisel plow, moldboard plow, and paraplow systems on three types of soil (poorly drained, medium, and fine textured) in Iowa.

Results showed that all tillage tools reduced bulk density and penetration resistance to the depth of operation. However, after planting, only the soil tilled with the paraplow remained less dense than before the tillage.

2.1.2 Soil Dynamic Properties

Dynamic properties of soil was defined as those soil properties which become manifest through soil movement (Gill and Vanden Berg 1968). According to this definition, if a block of soil starts moving on a flat surface, the resultant friction angle is a dynamic property of soil which does not appear unless soil starts moving. As well, when loose soil is compacted, its strength increases; therefore, soil strength is another dynamic property of soil.

As forward speed of a tillage tool increases, dynamic effects on the cutting force become more predominant because of two main effects: First, the need of continuous acceleration of new mass of soil as the tool travels, and second, alternation of soil strength at high rate of shear. Experience shows for the purely frictional soils (sandy), the strength of the soil does not vary a great deal with shear rate. For such a soil, inertial force involved in the accelerating the soil is the most important factor when operating speed increases. On the other hand, clay soils can possess marked changes in shear strength with increasing the shear rate, which outweigh inertial forces nearly completely at high velocities (McKyes 1985). Other researchers believe that there are more reasons for having higher draft at higher speeds.

Zhang and Kushwaha (1999) reported three mechanisms accounting for the draft increase with increase in operating depth: 1- soil inertial effect, 2- soil strength rate effect, and 3- wave propagation effect. The last effect comes from the research performed by Russians (Azyamova 1963; Katsygin 1969; Vetrov and Stanevski 1972) who noticed when the speed of a tillage tool exceeds some limits, the draft requirement of the tillage tool inversely decreases. This was attributed to the fact that as the tool speed increased faster than the wave of soil stress propagation, theoretically, the plastic zone of soil in front of the tool decreased or even disappeared, thus the soil cutting resistance decreased. Based on this research, they claimed that there should be an optimum speed at which the draft requirement would be lower.

According to many researchers stress-strain behaviour of soil is a function of time (Gill and Vandenberg 1968; Persson 1969; and Johnson 1972). Persson (1969) concluded that constitutive equations do not take into account for the rate of deformation. Flenniken et al. (1977) found that soil strength in dynamic unconfined compression was 3 to 5 times greater than quasi-static strength. Stafford and Tanner (1983) found that peak cohesion varied as the logarithm of the deformation rates above 1 m s^{-1}. These studies showed that dynamic tests should be employed to determine the dynamic response of soil. Vanden Berg (1961) emphasized that neither elastic nor plastic theory provided useable models of soil behaviour. Gill and Vanden Berg (1968) concluded elastic and plastic theories do not describe time dependency of soil deformation. They concluded viscoelastic theory as a promising theory to explain soil behaviour. Mohsenin (1970) described viscoelasticity as, a combined liquid-like and solid-like behaviour in which the stress-strain relationship was time dependent.

Measurement of dynamic properties of soil during tillage is very difficult because those physical measurements should be accomplished during the operation. There are concerns that mechanical devices cannot accurately measure those dynamic properties. The measuring device may react differently from the soil if for example it is softer or harder than the soil. In addition, the measuring device may influence soil reaction if it is one of those inserting device such as soil penetrometer (Gill and Vanden Berg 1968).

Results of same experiments but performed under different soil conditions cannot logically be compared to each other because the strength of soil is not the same for those experiments (Gill and Vanden Berg 1968). This problem would persist until measurement of soil strength during applying load to the soil becomes possible. Until then, the only way to compare the results of different tillage experiments is to assume constant soil strength during the operation. A closer relationship between the assumption and the reality would obtain better results. During last decades, many efforts have been made to develop mathematical equations to relate stress and strain in the soil medium. Only few of them have taken account for a soil strength which changes with time.

2.1.2.1 Soil Cohesion

Although the nature of cohesion is not fully understood, it can be considered as the strength of the soil that is not dependent on the applied force. Koolen and Kuipers (1983) defined it as bonding force among soil particles per unit area. They have counted it as a soil property which is affected by many factors including soil type, moisture content, and pore space. In soil mechanics, clay soils are classified as cohesive soils where sands are determined as non-cohesive or frictional soils, because sands may have no cohesion at all.

The increase of soil cohesion with increasing soil bulk density has been reported by several researchers (Mulqueen et al. 1977; Schmertmann 1975; Kuipers and Kroesbergen 1966; Smith 1964; Wes 1964). They expressed that this relationship is dependent on soil type and moisture content. It was concluded that normally, coarse grained soils (high sand fraction) exhibited higher friction angle values and fine grained soils (highly clay content) exhibited higher cohesion values. Stafford and Tanner (1983) found that peak cohesion varied as the logarithm of the deformation rates above 1 m s^{-1}.

2.1.2.2 Soil-soil Friction

During the tillage, part of energy requirement is expended to overcome the interlocking force of particles and their rolling and sliding on each other. Angle of internal friction (ϕ) exhibits the existence of friction force between soil particles. Its value is affected by soil porosity, moisture content, normal stress, and grain size distribution. Angle of internal friction is not affected by the rate of shear. Sandy soils are mostly named frictional soils because of their nature that usually have a larger angle of internal friction in comparison with the clays. In general, well-graded sands with a larger relative density and sharp edge particles have a larger angle of internal friction when compared to the uniform sands with lower density and round edge particles. In an unsaturated agricultural soil, angle of internal friction varies from $25°$ for moist, loose, fine texture soils to about $45°$ for dry, dense, coarse textured soils (Koolen and Kuipers 1983).

Payne (1956) measured cohesive and frictional properties of field soil using a torsional shear box. Approximate values of 33° and 3.5 kPa, and 33° and 21 kPa were determined for friction angle and cohesion of sandy loam and clay soils at depth of 10 cm respectively. McKyes (1978) employed draft measurements of Payne's tests (1956) to calculate same values by his own model. It was reported that the results of both methods were very close to each other.

2.1.2.3 Soil Cone Index

Cone index of agricultural soils is a very important factor that is measured in most tillage studies, and it indicates the resistance of soil to penetration. Since in each tillage activity, a tillage tool should be initially able to penetrate the soil, cone index values at different depths of different types of soils can help researchers to evaluate and compare soil mechanical strength and forces engaged in tillage operations. The ASAE Standards (2002) emphasizes that cone index does not provide specific soil values such as cohesion, angle of friction or coefficient of soil-metal friction.

Ayers and Perumpral (1982) in their research work evaluated the effect of soil density, moisture content, and soil type on cone index. They chose five different types of soil prepared with a determined percentage of zircon sand and clay. By using a drop hammer, all samples were compacted to an equal amount. In addition, each type of soil was provided with different levels of dry density and moisture content. The ASAE standard cone penetrometer with a base area of 3.2 cm^2 (0.5 in^2) was used and an Instron testing machine model TM-S3111 was used to conduct the penetration tests. Their results showed that, moisture content level which produced maximum dry density did not include maximum cone index. As well, samples with 100% sand had a significant lower cone index than samples including some clay. An increase in compaction level increased the maximum cone index attained for a soil mixed of 50% clay and 50% sand, and for all kinds of soils except for 100% sand, the effect of moisture content on relationship between dry density and cone index was consistent. Finally, in a soil mixture of 50% clay and 50% sand at low moisture contents of 2.2%, 4.4%, and 6.7%, cone index increased with dry density at a high rate. When moisture content reached higher amount of 8.8% and 11.8%, the relationship between cone index and dry density

became more linear. As moisture content increased, the increasing rate of cone index with dry density significantly decreased.

2.1.3 Soil Shear Strength

According to Gill and Vanden Berg (1968), soil strength is the ability or capacity of a particular soil in a particular condition to resist or endure an applied force. Tillage can cause soil failure by shear, compression, tension, or plastic flow. There is no doubt that shear is one of the most common methods of soil failure employed by many kinds of tillage implements. Many researchers have worked in this area investigating the characteristics of the shearing process. Johnson et al. (1978) evaluated methods and devices of shear measurements for agricultural soils. The most general envelope of shear strength was proposed by Coulomb as Equation 2.4:

$$\tau_{max} = C + \sigma_n \tan \phi \qquad (2.4)$$

This envelope is referred to as the Mohr-Coulomb envelope. The authors indicated that although the envelope cannot represent shear failure at all soil conditions, it is still valid enough to be a law. Mohr circles can be developed to determine C and ϕ graphically according to drawn stresses of σ_1, σ_2 and σ_3 which are obtained from practical tests. Based on this method, τ_{max} can be obtained for a number of normal stresses, σ_1, which are exerted to a defined soil sample. Having normal and maximum shear stresses (at failure point), Mohr circles are plotted as shown in Figure 2.1 where
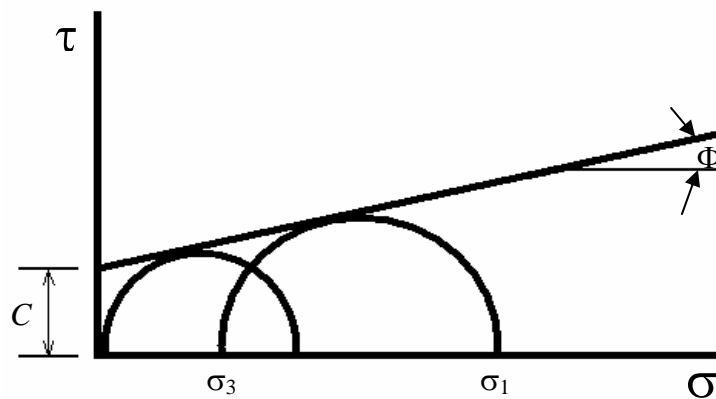
Figure 2.1 Schematic of Mohr- Coulomb's theory

14

a common tangent to the circles can give C and ϕ. The problem with the Mohr-Coulomb theory is that, it does not give one any information about soil behaviour before failure and does not discuss soil displacement caused by stress that affects soil failure.

An attempt was made by Nichols (1932), who related the shearing force of a soil to its plastic parameters and ambient moisture content. Raghavan et al. (1977) predicted the shear strength of a compacted clay soil based on consistency limits of the soil and they obtained a linear relationship between the shear strength and moisture content of the clay soil studied. Ohu et al. (1985) investigated the effect of organic matter contents on shear strength of compacted soils. They reported that soil shear strength increased with moisture content up to a maximum and then decreased at higher moisture contents.

2.1.4   Soil Compaction

Compaction is the densification of soils through the application of mechanical energy resulting in a reduction of air voids with little or no reduction in moisture content. Soil compaction is to some extent an unavoidable event that frequently occurs as a result of machinery traffic on agricultural soils. Although certain amount of soil compaction is required to ensure better contact between seeds and soil particles, any extra compaction increases soil strength and causes several problems. Many researchers have reported the harmful effects of soil compaction on soil structure including reduction of air filed void spaces, changes in soil matrix gaseous composition and increases in resistance to root growth (Soehne 1958; Taylor and Arkin 1981; Wells and Burt 1984; Plackett 1984; Bailey et al. 1988; Gupta et al. 1990; Janzen 1990; Bicki and Siemens 1991; Hakansson and Petelkau 1991; Lowery and Schuler 1991; Burt et al. 1992; Wood and Mangione 1993.

Laboratory tests are used to determine the optimum moisture content and maximum density to ensure that the desired design values for shear strength, compressibility, and permeability are met. Air is expelled from the soil rapidly whereas water, which has a viscosity 50-100 times greater than air, is expelled at a much slower rate. Therefore, compaction is defined as the compression of an unsaturated soil body due to a reduction in the free air volume (Hillel 1980).

Proctor established that the compaction of a soil is a function of the following four variables:

1. Dry density
2. Water content
3. Compactive effort
4. Soil type (gradation, presence of clay minerals, etc.) (Holtz and Kovacs 1981).

According to Gill and Vanden Berg (1968), compaction reduces soil permeability to water and aeration of the soil, increases the mechanical strength of the soil and therefore, reduces the metabolic activities of roots. All these effects may reduce the quality and quantity of food and fiber grown on the soil. In addition, a compacted soil requires higher amount of energy during tillage operations to break down aggregates and clods into smaller particles in order to provide a suitable seed bed.

2.1.5 Measurement of Soil Shear Strength Parameters

Several laboratory and in situ measurement methods and devices of soil shear strength parameters have been introduced in soil mechanics books. Among field measurement devices, the following devices have been widely used by the researchers: annular shear ring, shear graph, rectangular plate, shear vane, cone penetrometer, and pocket penetrometer.

Since current research has employed only laboratory measurement tests, the discussion will focus on laboratory tests particularly direct shear test.

2.1.5.1 Triaxial Test

Triaxial test, as the first shear strength test enable to measure pore-water pressure of soil during shear strength measurement, is still valid and very common although other tests with similar features have been developed. Results of this test can be individually used to predict the behaviour and characteristics of the soil, or they can be used to measure other characteristics of the soil such as consolidation and permeability characteristics. During the test, principle stresses as well as drainage can be controlled and pore water pressure is measured.

During a tillage operation sometimes soil undergoes a shearing at a high rate. To obtain soil parameters for such a dynamic situation, it is required to perform a high speed triaxial test on same soil sample in which soil experiences load at similar rates as it would encounter during the real tillage operation. There are, however, few problems associated with high speed triaxial testing as follows:

1. Since the length of soil specimens for such a test does not go usually longer than 100 to 150 mm, some more specific equipment will be required to do the test

2. In a high rate of applying load, it is almost impossible to apply a homogeneous load to the whole sample. It is expected to have more deformation inside the specimen adjacent to the loading ram than the rest of the specimen because of the viscoplastic effects.

3. Even in quasi-static tests, remoulded soils do not behave as in situ soil samples. The differences become more serious when the rate of shear stress increases during simulating a dynamic case. Different mechanisms act in real soils and in triaxial cells (Chancellor and Upadhyaya, 1994). Therefore, it is impossible to present a real behaviour of the soil in its original field without implementation of sophisticated corrections to interpret high speed triaxial tests. To date, no studies have been reported to support these kinds of corrections to use the high speed triaxial tests for agricultural soils.

2.1.5.2 Direct Shear Test

Direct shear test is an inexpensive, fast, and simple way to determine shear strength characteristics, especially those of granular materials (Holtz and Kovacs 1981). This test is conducted by placing a soil sample into a shear box similar to Figure 2.2 that is split with the bottom half fixed and the top half free to float. A loading block with a porous stone to allow drainage of water is placed on the sample, a normal load is applied and the loading block and top half of the box are clamped together allowing the two halves to separate slightly.
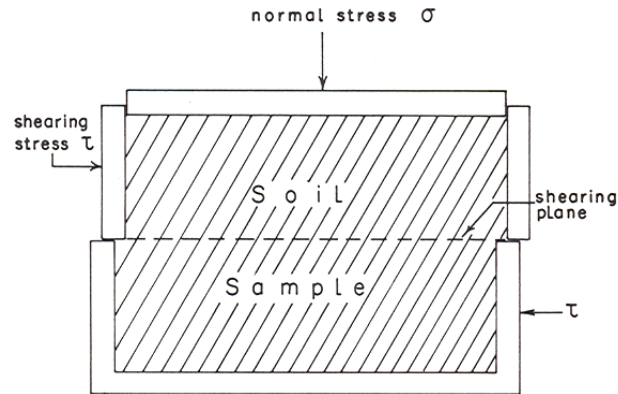
Figure 2.2 Direct Shear Apparatus (from Hillel 1980)

Shear box test is used to determine the angle of internal friction of a soil. As the horizontal displacement increases the shear force along the predetermined slip-plane also increases due to one half of the soil being restrained. Eventually, the soil reaches a maximum or peak shear stress and after the peak, the shear resistance decreases and failure occurs. Multiple tests are needed to determine the angle of internal friction. Tests are conducted with varying values of normal stress to determine the stress-displacement curves. From each curve, the maximum shear stress is plotted against the corresponding normal stress to determine the maximum shear stress vs. normal stress plot. This graph is generally linear and the inclination to the horizontal axis is equal to the angle of internal friction (ϕ) of the soil. If the soil sample is not pure sand $(C = 0)$, the intersection of the graph with the vertical axis will show the amount of soil cohesion (c). If soil-metal friction angle is desired, it can be measured by placing a plate made of the same metal as tool's metal between two halves of the apparatus during the test.

2.2   Tool Parameters

In a tillage operation different tool parameters influence energy requirement of the tool. Parameters such as tool type, tool shape and size, tool rake angle, tool sharpness, and tool material affect draft and energy requirements. In this section, mechanics of vertical tools has been discussed considering that soil bin experiments were conducted by a vertical narrow tool.

2.2.1 Mechanics of Vertical Tools

A vertical plane, perpendicular to the direction of movement represents a simple tillage tool. Payne (1956) developed a mechanics of this kind of tools based on the passive earth pressure theory of Rankine. The study started by observing the reaction of soil to a vertical tool as has been described in Figure 2.3. Payne assumed two categories of tools as wide and narrow vertical tools. For wide tools (tool width is at least twice of its operating depth), the side effect can be ignored since their surface area compared to the surface of bottom failure is ignorable whereas for narrow tools, side effect cannot be ignored. At the soil surface, principal stresses are divided into horizontal and vertical stresses for a wide vertical tool where at deeper points along the failure surface becomes in a shape of logarithmic spiral. For narrow tools, the shear failure surfaces are existing which pass along the sides of the tool and the bottom of the tool. These failure zones interrupt the bottom curved failure surface presented in Figure 2.3-A, and they will be at $(\frac{\pi}{4} - \frac{\varphi}{2})$ to the principal stresses. Vertical shear surfaces in narrow tools intersect each other as well as the curved bottom surface. Therefore, a wedge of soil adjacent to the tool is isolated from the rest of the soil block that was sheared from the soil mass. By changing the boundary condition of Rankine theory, the failure zone of a narrow tool was described as shown in Figure 2.3-A. It was expressed that isolated wedge would slowly come up the face of the vertical tool as the effect of applied forces on the inclined bottom surface. Efforts were made to describe the forces acting on the wedge since the wedge was the only block of soil in contact with the tool. In this way, he employed two behaviour equations including soil failure by shear (Equation 2.4) and soil-metal friction (Equation 2.5).

To determine the shape of the wedge as the first step to specify the location of the applied forces, the outputs of the equations were used in the same way as used by Soehne et al. (1958). The validity of the proposed shape of the wedge as illustrated in Figure 2.3-A was confirmed through observations.

Cutting by vertical tools as affected by degree of confinement was studied by Kostritsyn (1956). Cutters were described as thin knives and it was noted that near the
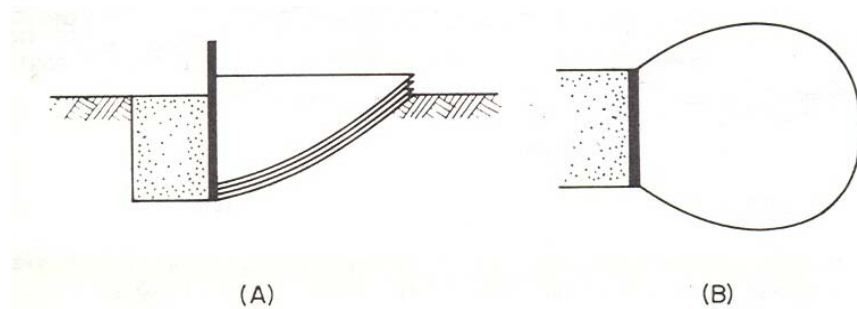
**Figure 2.3 The nature of soil failure caused by a vertical tool in a firm soil:
(A) side view; (B) Plan view (from Gill and Vanden Berg 1968)**

surface soil would rupture or move upward where at deeper depths, the movement of soil is parallel to the direction of the travel of the cutter (Figure 2.4-A). As illustrated in Figure 2.4-B, the draft versus depth graph shows that below the critical depth, in which soil movement is horizontally, this relationship is linear. Based on his studies, Kostritsyn declared that at deeper depths soil confinement causes pure cutting where at shallower depths other types of failure may occur. Finally, it was concluded that a gradual transition from pure cutting to a complex action occurs as the depth of operation of a vertical tool is decreased.

Godwin and Spoor (1977) found that critical depth was smaller in a looser soil. As well, critical depth increased as soil angle of internal friction, tool width, and forward rake angle were increased. A critical depth of 120 mm for a vertical tool without profile as wide as 25.4 mm in a dense soil was suggested.

Dynamic aspects of such straight tools without profile which include shear type processes have been studied by several researchers. According to the studies of Payne and Tanner (1959), Dransfield et al. (1964), Verma (1971), Spoor and Godwin (1978), and Stafford (1979) the following features are valid for this kind of narrow tools. Draft force increases with depth of operation and varies with time as soil blocks are torn up. In non-cohesive soils, draft increases linearly with depth where in a highly cohesive soil this relationship is almost quadratic. The relation between draft and width of tool is linear as well.
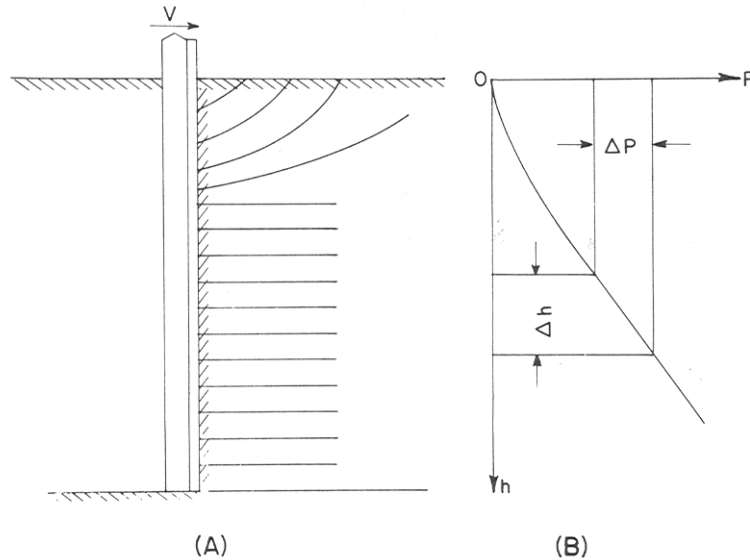
Figure 2.4 (A) Soil movement caused by a thin vertical cutter, (B) relation of cutting force to depth of operation for a vertical cutter (from Gill and Vanden Berg 1968)

Those soil blocks between such a tool and unbroken soil which are completely separated or in the process of being torn up can be treated as rigid bodies, and the following forces may act on them. The gravitational force (weight), an inertia force if the soil block is accelerating or decelerating, a soil-metal friction force and adhesion force if the soil block is adjacent to the tool surface. In addition soil-soil friction forces with adjacent soil or soil blocks, and cohesive forces if part of its surface is a developing failure surface, should be counted as acting forces (Koolen and Kuipers 1983). The researchers also expressed that acceleration force is proportional to the square of the velocity.

2.2.2 Effect of Tool Parameters on Draft Requirement

In a comparison between power requirements of three subsoilers including a conventional, a triplex, and a parabolic subsoiler, the following results were reported by Smith and Williford (1988). In general, draft decreased for all three implements as speed increased except for the highest speed tested which showed a very definite increase in the draft. This increase in draft was most pronounced for the triplex and conventional subsoilers. No attempt was made to explain the soil dynamics of this response; however, the response was consistently observed for all three implements. Therefore, there

21

appears to be an optimum ground speed for which less draft was required to operate the subsoilers for the soil conditions and operating depths used for the test. The researchers believed the shape of subsoiler could have a significant impact on power requirement.

Khalilian et al. (1988) measured draft and energy requirements of several tillage implements used for conservation tillage in coastal plain soils. Their results showed no significant differences in draft requirements (kN/shank) between a subsoiler and a paraplow at the same depth of operation. Draft increased with an increase in tillage depth. The chisel plow required significantly less draft per shank. They reported values of 2.68, 4.45, and 5.00 kN/shank for the chisel, subsoiler and paraplow respectively when ran at 0.25 m of depth and 6.4-7.20 km h^{-1} of speed. At deeper depths, the results changed inversely a bit. At 0.35 m depth of operation and speeds between 6.7 and 7.0 km h^{-1}, values of 6.25 and 6.00 kN/shank were reported for the subsoiler and paraplow respectively.

Research was conducted on the design of subsoilers at the National Tillage Machinery Laboratory in the 1950's (Nichols and Reaves 1958). Although the research indicated a reduction in draft requirement of a subsoiler with a straight shank, the common design of the subsoiler in 1950's and 1960's had either a straight shank or a shank inclined about 10 degrees. Tupper (1974) introduced a specific curved subsoiler shank as parabolic subsoiler in which he reported a reduction in power requirement and 43.4% reduction in wheel slip when compared with conventional subsoiler.

The model introduced by McKyes and Desir (1984) suggested that both the specific draft force per unit soil area and the degree of soil loosening were observed to increase with the relative narrowness of the tillage blades and with the rake angle of the tool.

Field experiments conducted by McKyes and Maswaure (1997) proved that the degree of soil loosening was generally smaller at a rake angle of 60° than at 30° or 90°, and tended to be higher at greater depths of operation. In addition, a larger depth to width ratio generally increased the degree of loosening. Results for the soil studied indicated that the best implement design for low draft, high cutting efficiency, and

superior soil loosening should have a rake angle of about 30° and should be fairly narrow with a depth to width ratio (slenderness) of 2 or more.

2.3   Operational Parameters

In this section, the effects of operational parameters such as depth and speed which influence draft and energy requirements of tillage implements are discussed.

2.3.1   Draft-Depth Relationship

Wolf et al. (1981) reported that draft increased sharply with depth of subsoiling on one soil condition. Reid (1978) obtained an increased in draft of 4.22 kN per row with a subsoiler-bedder when subsoiling depth was increased from 0.30 to 0.410 m in a Tifton sandy loam. Increase in draft requirement with increase in subsoiling depth was also reported by Garner et al. (1987).

Summers et al. (1986) studied the effects of depth and speed on draft requirement of different tillage implements on three different Oklahoma soils. Results showed that draft was linearly proportional to depth for mould board plow, chisel plow, disk, and sweep plow.

Girma (1989) measured applied forces on mould board plow during a tillage operation. At a constant speed of 0.8 m s^{-1}, he reported a polynomial relationship including first and second order of depth between draft requirement and depth of operation for mould board plow.

According to the ASAE standards (1980) a second order polynomial function for draft-depth relationship was published for both chisel plows and field cultivators respectively. Kiss and Bellow (1981) reported the same draft-depth relationship for the cultivator sweeps and spikes as published by ASAE standards.

Glancey et al. (1996) measured draft requirement of different tillage implements. They reported that the draft values for the mouldboard plow, chisel plow, subsoiler, standard chisel, and standard lister were all found to depend primarily on operating depth. Even the effect of speeds below 7.2 km h^{-1} was found to be small when compared with the depth effect.

2.3.2 Soil Acceleration and Draft-Speed Relationship

The relationship between draft and speed has been reported as linear, second-order, polynomial, parabolic and exponential (Rowe and Barnes 1961; Siemens et al. 1965; Stafford 1979; Swick and Perumpral 1989; Gupta and Surendranath 1989; Owen 1989). These differences can be interpreted as a result of the inertia required to accelerate soil, effect of shear rate on soil shear strength and effect of shear rate on soil-metal friction, all of which vary with soil type and condition.

Payne (1956) conducted a series of draft measurement tests using a flat vertical blade, 25 mm wide, in three different soils including clay, clay loam, and sandy loam soils. Increasing speed from 0.2 to 2.7 m s^{-1} resulted in 20% increase in the draft. Data showed a linear relationship between draft and speed for these tests.

In an effort by Wismer and Luth (1972) to distinguish between inertial and non-inertial effects of increasing speed of a tillage tool on pure frictional and pure cohesive soils, inertial effects were not significant on a chisel plow while tested in a sandy silt soil with a maximum speed of 4 m s^{-1}. A linear draft-speed relationship was reported for a 3-m wide chisel implement.

Hendrick and Williams (1973) indicated that there are some reasons that when the speed of a tillage tool passing through the soil increases, the speed of stress wave propagation and the area of plastic deformation decrease. The researchers then discussed about the possibility of approaching a zero plastic deformation as a result of a continuous reduction in stress propagation. They suggested a range of 10 to 12 m s^{-1} for the speed of plastic propagation as the most common range for the agricultural soils.

Stafford (1979) studied the relationship between soil cutting forces and tool speed at different soil water contents. He noticed that soil was behaving totally different below and above the plastic limit. It was reported that below the plastic limit, an increasing draft-speed relationship was predominant, where above the plastic limit a reduction in the rate of increasing draft was occurred. This researcher did not go beyond 5 m s^{-1} of speed.

Linke and Kushwaha (1992) performed some real tests in the field using vertical narrow tools running at speeds up to 18 m s^{-1}. It was concluded that beyond a certain

speed level, draft decreased or remained constant, and the response of the draft to the operating depth was large.

Wheeler and Godwin (1994) conducted some laboratory tests using narrow tillage tools in frictional and cohesive soils running at speeds up to 5.6 m s^{-1}. They reported that draft increased as speed was increased. These researchers (Wheeler and Godwin 1996) used again narrow tools in cohesive field soils at speeds up to 4.2 m s^{-1} and reported the same results.

The manner in which tool speed can influence draft has also received much attention from researchers. Mckibben and reed (1952) reported that the effect of tool speed on draft was also influenced by the clay and moisture content as well as the kind of tillage tool in use. An increase in draft between 20 and 80% was suggested by Rowe and Barnes (1961) as the speed was doubled from 5 to 10 km h^{-1}. They believed that this was the result of having higher shear strength at higher rates of shear, but that the increase was not as great with soils having high clay content. Stafford (1979) showed that the relationship between draft and speed was influenced by soil moisture content and the nature of the soil failure, but at speeds in excess of 18 km h^{-1}, draft was independent of speed. According to the ASAE standards (1980), a linear draft-speed relationship was published for both chisel plows and field cultivators.

Experiments accomplished by Onwualu and Watts (1998) showed that a polynomial best described draft-speed relationship for narrow tillage tools. The polynomial relationship was attributed to the combined effect of inertial forces (square of speed) as the soil slides over the tool and the effect of shearing rate on tool forces (linear).

2.4   Soil-Tool Interaction

Tillage is a process to modify soil properties by pulverization, cutting, inversion, or movement of the soil resulting in improved soil conditions for optimal crop growth and yield (Grisso et al. 1996). This process involves soil from one side and tillage tool from the other side to interact with each other. Forces engaged in the process are of special importance for researchers who are working to model soil failure during tillage

operations. Most theoretical models for predicting dynamic soil-tool interaction are based on the addition of a velocity component to the static wedge approach. For both two dimensional (2-D) and three dimensional (3-D) analyses, this involves equations that describe the acceleration of the wedge from zero to a velocity that enables it to slide up the interface. This is based on an analysis by Soehne (Gill and Vanden Berg 1968) and has been used in different forms for the 2-D analysis (Rowe and Barnes 1961; McKyes 1985) and the 3-D analysis (Owen 1989; Gupta et al. 1989).

Different models based on the wedge approach for soil-tool interaction have been evaluated in the past for narrow blades operating at very slow speeds, the so-called passive case (Plasse et al. 1985; Grisso and perumpral 1985). A comparison of their performance in predicting dynamic soil-tool interaction for both wide and narrow blades has not been done in an integrated manner. Yet such information is required for modeling of soil-tool interaction.

According to McKyes and Ali (1985), there is a traditional variation to Coulomb's strength law as follows:

$$\tau_{max} = C_a + \sigma_n \tan \delta \qquad (2.5)$$

where:

τ_{max} = maximum shear strength along the soil-tool interface

C_a = soil to tool adhesion strength, independent of normal pressure

σ_n = normal pressure acting on the internal shear surface

δ = angle of friction between soil and the tool material

Based on the Equation 2.5, soil-tool interaction force includes soil adhesion and angle of friction between soil and tool surface.

2.4.1 Soil-tool Adhesion

As shown in Equation 2.5, when the shearing process acts between soil and tool surface, a new character as soil-tool adhesion, C_a, appears. This parameter plays the same role in soil-tool interaction as cohesion does in the case of soil-soil interaction. Adhesion of soil increases as the moisture content of soil is increased. However, after

increasing to a certain amount, if moisture content is still increasing, adhesion will decrease The reason for this change is that at the beginning, soil moisture tension increases as moisture content is increased; therefore, adhesion is increased, but at higher soil moisture content, positive pore pressure develops in the soil under load and tension decreases which in turn, results in decreasing of adhesion and of moisture lubrication effect (Nichols 1931).

2.4.2   Soil-tool friction

This kind of friction is developed when soil moves on another material such as tillage tool surface. The coefficient of friction between soil and tool surface predominantly depends on the surface roughness. Angle of friction between soil and tool, sometimes referred to as angle of external friction, for same soil is usually less than angle of internal friction (Koolen and Kuipers 1983). The researchers emphasized, though a tillage tool with a rusted steel surface may have a coefficient of friction as high as soil internal friction. All factors affecting soil internal friction can affect soil-tool friction as well as the type of tillage tool surface.

Primary experiments were conducted by Payne (1956) as soil cutting patterns on blades and required draft for different situations. Flat vertical blades were used in widths of 7.5 and 10 cm in clay and sandy loam soils at different depths of 5 to 22.5 cm. Nichols (1931) found out that the static coefficient of friction of dry sand before movement on steel was 0.26, whereas after movement, this value decreased to an amount of 0.23. This change was explained as the change in soil particle arrangement, position, and water tension.

Researchers have no agreement on the effects of tool speed and moisture content on the value of soil-tool friction angle. Stafford and Tanner (1983b) reported that soil-tool friction angle increased logarithmically with the sliding speed over a wide range of soil moisture content and tool speed when tested in clay and sandy loam soils. In contrast, Payne (1956) expressed that soil-metal friction was independent of tool speed at low normal stresses (Maximum 20 kPa). Nikiforov and Bredun (1965) found a decrease of soil-metal friction angle at speeds of 1-5 m s^{-1} for a moist soil at very low normal stresses up to 25 kPa.

27

The reason for having contradiction on the effect of tool speed on soil friction was explained by Koolen and Kuipers (1983). This was attributed to the fact that there were several methodological problems in determination of friction coefficient as follows. The normal stress causes rearrangement of soil particles and deforms them a little. Therefore, beside the friction force, an additional force for deformation should always be assumed which can overestimate friction coefficient. As well, normal stress can force water out of the pores which in the soil-tool interface this water can reduce friction coefficient. If this water is under suction, it can produce an extra effective stress at the interface. Finally, in a tillage operation, the size of the soil-tool interface area is influenced by tool speed and consequently the amount of normal stress on the soil-tool interface is not equally distributed. Based on above reasons, researchers claim that determination of the effect of speed on friction coefficient satisfactorily is not currently possible. Therefore, friction energy is currently assumed to be independent of speed as a primary approximation.

2.5   Tillage Energy

The world has been facing a crisis in the field of energy in the last decades. The crisis is as serious as many analysts believe that the origin of many conflicts in the world reflects the crisis in the field of energy and resources of energy. In agriculture, although new machinery systems have facilitated production, they have increased the demand for energy. Tillage as one preliminary and basic step for any agricultural production demands huge amount of energy.

In a tillage operation, energy can be expressed in terms of energy per unit area or per volume of disturbed soil (Panwar and Siemens 1972). Since energy requirement per unit volume has the same unit as draft per unit area, it can be shown as the draft requirement to cut a furrow in an exact cross section as expressed by McKyes (1985) and Chancellor (1994). Energy can also be expressed as the rate of energy per depth of operation (Darmora and Pandey 1995). The most important factors in determination of energy requirement of a tillage tool are draft and the amount of disturbed soil. In other words, if those two values are available, energy can easily be calculated as the product

28

of draft and the length of disturbed soil. For a tillage operation, the report of energy requirement should include the depth of operation as well.

Cooper and Gill (1966) illustrated that energy consumed in a tillage operation was a function of both initial and final conditions of soil. This obviously includes soil physical properties such as soil moisture content, soil bulk density as well as soil texture. Gill and Vanden Berg (1968) reported two additional factors including tool shape and manner of tool movement as affecting factors on energy requirement of a tillage tool. The report refers to the tool affecting factors such as tool speed, tool operating depth, tool shape, and tool rake angle. Perdok and Werken (1982) studied energy requirement of different tillage implements at different soil textures (Table 2.1).

Table 2.1 Specific work (kJ m^{-3}) for the main tillage implements in several soil types (from Perdok and Werken 1982)

Implement	Soil Type				
	Sand	Sandy Loam	Silt	Clay Loam	Heavy Clay
Moldboard plow	30 ± 5	40 ± 5	60 ± 8	80 ± 10	120 ± 20
Chisel plow	20 ± 4	27 ± 4	40 ± 6	55 ± 7	80 ± 10
Cultivator	18 ± 3	24 ± 4	36 ± 5	48 ± 6	65 ± 8
Disk harrow	18 ± 3	22 ± 4	30 ± 4	40 ± 5	55 ± 7
Rotary tiller	150 ± 15	75 ± 20	210 ± 25	250 ± 30	320 ± 40
Oscillating harrow	45 ± 8	60 ± 10	88 ± 12	118 ± 15	175 ± 20
Powered harrow	120 ± 10	5 ± 15	165 ± 20	90 ± 25	250 ± 30

The most recent methods of tillage operations and the new tillage implements have been designed to reduce the total energy and time requirements for the tillage operations as well as to provide a better seed bed. These methods include minimum tillage, no tillage, strip tillage, and mulch tillage.

Blumel (1986) expressed that tillage energy can be divided into friction energy, deformation energy, cutting energy, and acceleration energy. It was emphasized that it is very difficult to measure these components separately, and even qualitative examinations are most often difficult. Kushwaha and Linke (1996) published a graph of

tillage energy versus tool speed as a conclusion of all literature that presents the influence of speed on those energy components (Figure 2.5). As shown in Figure 2.5, cutting and deformation energy values drop after a critical speed range, friction energy stays constant, and acceleration energy continues increasing after the critical speed range. The critical range of speed was estimated between 3 and 5 m s^{-1}. Since total tillage energy is the summation of those energy components, it was concluded that the increase in energy requirement above the critical speed range would be less than that below the critical speed range.
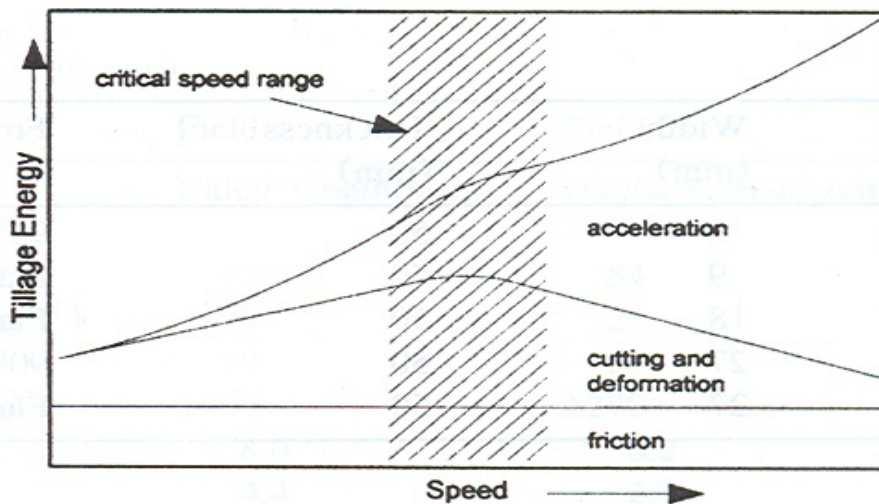
Figure 2.5 Schematic illustration showing the influence of speed on the components of tillage energy (from Kushwaha and Linke 1996)

Panwar and Siemens (1972) related soil moisture content and density to the energy required for pulverizing the soil, and to other soil strength parameters. The results indicated that the energy required to pulverize a soil depended to a large extent on the strength and elastic properties of the soil.

Vetrov and Stanevski (1972) submitted the following equations for energy requirement to cut and separate a chip of soil with a sharp tool.

$$E = \frac{K_e K_v \left[P + \gamma W^2 A_e \dfrac{\sin\alpha\cos\alpha}{\sin(\alpha + \beta)} \right]}{A_e} \tag{2.6}$$

$$K_e = 1 + \frac{V}{V_d} \frac{\sin \alpha}{\sin(\alpha + \beta)} \tag{2.7}$$

$$V_d = \sqrt{\frac{\tau}{\rho}} \tag{2.8}$$

where:

E = tool energy requirement, J

K_e = ratio of mean to maximum cutting force

K_v = coefficient of speed effect

P = quasi-static draft, N

ρ = soil bulk density, kg m^{-3}

V = operating speed, m s^{-1}

V_d = soil disruption speed, m s^{-1}

A_e = average cut area, m^2

α = tool rake angle

β = angle of soil wedge rupture

τ = soil shear strength, N m^{-2}

The relationship between energy and the rate of strain was reported by Niyamapa and Salokhe (1992). Energy requirements to break soil specimens during quasi-static and dynamic triaxial tests were measured. Failure energy per unit volume of a silty loam soil in the quasi-static case was minimal at the lowest water content and rapidly increased with increase in water content. At similar water content, higher bulk density (1.3 Mg m^{-3}) specimens required considerably more energy to fail than lower bulk density ones (1.2 Mg m^{-3}). Failure energy of silty loam and sandy loam soils showed rapid increases with speed up to approximately 5 m s^{-1}, and then decreased.

Michel (1985) reported that a chisel-based system produced equal yields with approximately 40% less fuel and less time for pre-plant tillage operations when working in irrigated sugar beets, dry beans and corn.

Chaplin et al (1988) studied drawbar energy used for tillage operations on loamy sand soils. Their study showed that no-till and ridge plant tillage systems resulted in 84% and 54% drawbar energy saving, respectively. The reduced tillage regime used 62% more drawbar energy than the conventional system commonly practiced in the area.

2.6   Soil-Tool Modeling for Energy Requirement

During the years, Different modeling tools have been implemented to model soil failure during tillage operations. Experimental, empirical, analytical, and numerical modeling methods are different approaches to achieve this goal. Analytical methods have received much attention over last decades from many researchers. Because of the importance of this approach in calculating draft and energy requirements of particularly narrow tillage tools, a fairly extended discussion on analytical models is developed in this chapter. On the other hand, numerical approaches such as Finite Element Method (FEM), Discrete Element Method (DEM), and Artificial Neural Networks (ANN) have been implemented in tillage science as the result of appearance of powerful computers.

To date, there are only few reports on using DEM for tillage studies (Shikanai and Ueno 2002; Khot et al. 2005). This method is one of the numerical analyses in which solid body is treated as aggregate particles. The behaviour of the solid body is estimated from the solution to the equation of motion with respect to each of the particles in the DEM. With this technique, it is possible to treat the phenomenon of soil destruction by agricultural machines. In DEM, dynamic behaviour is described numerically using a time stepping algorithm. The time step is selected such that (1) velocities and acceleration can be assumed constant within the time step, and (2) the time step is indiscriminately small in manner that disturbances cannot propagate from one element further than its immediate neighbour during a single time step. The calculation cycle alternates between force displacement law at the contacts and Newton's second law of motion. The force displacement law is used to calculate the contact forces from relative displacements at contacts. Hryciw et al. (1997) used video tracking and digital image analysis method for experimental validation of DEM simulation for large discontinuous deformation in sandy soil during plowing. Despite some powerful aspects

of DEM in modeling soil-wheel interaction, the number of soil particles which can be handled in DEM simulation is much less than the actual number of particles considered in the laboratory experiments. Jayasuriya (1999) used bigger and narrow soil bins to validate the model for soil-tire interaction in lateratic soil. In addition, it is usually difficult to correlate the test results obtained from subsequent test runs due to the non-uniformity involved during soil bin preparation. As well, literature shows that DEM has not been used for soil tool interaction yet. This can be related to the difficulty of modeling soil failure by DEM during dynamic processes such as tillage operations.

There has also been an attempt to apply Computational Fluid Dynamics (CFD) for soil failure modeling. This method was applied to simulate the soil flow around a simple tool. Simulations used a vertical blade in a rectangular flow domain (Karmakar and Kushwaha 2005a). Soil was treated as a Bingham viscoplastic material in respect to its non-Newtonian rheology. Free-surface simulation of an open channel visco-plastic soil flow indicated soil deformation patterns and the effect of speed on the failure front propagation. Soil deformations, as the flow of a visco-plastic material with yield stress, were observed to possess "plastic flow" and "plug flow" patterns. For a tool speed of 6 m s^{-1}, with a vertical tool of 20 mm thick and 50 mm wide, operating at 100 mm depth, the soil failure front was observed to be 160 mm at a depth of 10 mm below the top soil surface. The critical speed range was found to be 5 to 6.5 m s^{-1}. Soil pressure on the tool surface increased with the tool operating speed. Pressure concentration was the highest at the tool tip; it decreased towards the soil surface and extended over greater area on the tool surface with increase in tool speed (Karmakar and Kushwaha 2005b). Draft was related as a square function of speed. Since this research is the only one found in literature, further investigation would be required to judge about the ability of the method in modeling soil-tool interaction.

Among the numerical approaches, FEM has received more attention and was implemented earlier than the other numerical methods. In addition, literature shows acceptable results obtained from FEM modeling research, however, the results emphasized on the limitations of this method. Therefore, in this section, results of some research pertinent to FEM modeling are presented. These reports will focus on draft and energy affecting factors data resulted from this modeling method.

2.6.1 Analytical Models

Analytical approach is one of the first methods that have been used to predict the interaction between soil and a tillage tool. This approach has been employed by many researchers in the field of soil tillage for about 5 decades. The results of this approach are still valid to some extent and its governing rules are sometimes used in other approaches such as empirical and numerical approaches.

Reece equation (Equation 2.1) formed a basis in analytical approach and has been used by several investigators (Reece, 1965; Hettiaratchi and Reece 1966, 1967; Hettiaratchi et al. 1974). Two-dimensional cases are approximately valid for soil cutting tools with wide blades relative to their depths of operations (width/depth greater than unity). When a cutting tool is not very wide, a large proportion of the cut soil moves sideways (Payne 1956). Since more soil must be moved per unit width of the tool in the 3-D cases compared to the wide blades (2-D), a larger draft is expected for 3-D cases than that of wide blades.

Payne (1956), O'callaghan-Farrelly (1964), Hittiaratchi-Reece (1967), Godwin-Spoor (1977), McKyes-Ali (1977), and Perumpral et al. (1983) are the researchers who have employed a static 3-D soil failure model to investigate soil-tool interaction. In all these models, the effect of travel speed on draft requirement has been ignored.

2.6.1.1 Payne model

By observing the upward displacement of soil ahead of the tillage tool, Payne (1956) assumed a failure zone for tines with a width/depth ratio less than 1:1. Payne and Tanner (1959) found out that in addition to the complexity of the equations, tool geometry such as rake angle, depth, and width can change the shape of the failure zone.

2.6.1.2 O'Callaghan-Farrely model

Based on Payne model and experimental data, O'Callaghan-Farrely (1964) developed a model. Several assumptions were made in this model; (1) A critical depth equal to $0.6 \times$ tine width was assumed; (2) Failure surface above the critical depth was described by a 2-D approach; (3) Two side crescents were neglected; (4) All tines were flat; (5) Rake angle was equal to $90°$; (6) Mass of the soil wedge was neglected; and (7)

Adhesion and external friction between soil and tool surface were not counted. Two equations to calculate draft requirements for shallow and deep tines were developed by the researchers that are not mentioned here. According to Shen and Kushwaha (1998), predictions from those equations are very close to the experimental data except for an underestimation when a very hard soil is encountered. Shen and Kushwaha (1998) expressed that part of shortcomings of this model returns to its assumptions particularly assumptions number 4, 5, and 7 above.

2.6.1.3 Hettiaratchi-Reece model

Hettiaratchi and Reece (1967) developed another model that was similar to the O'Callaghan-Farrely model in some aspects. This model also assumed a critical depth for the operating tool and two traversal failure zones only below the critical depth. In the model, 2-D equations are used to calculate the forward failure forces ahead of a soil-tool interface and 3-D equations for the transverse failure away from the center line of the interface. The equations were used in the same way as for the O'Callaghan-Farrely model except that the mass of soil was counted in this model. According to Grisso and Perumpral (1985), this model overestimated forces for vertical tools $(\alpha = 90°)$, yet the model underestimated inclined tools.

2.6.1.4 Godwin-Spoor model

Godwin and Spoor (1977) suggested a circular shape for the soil failure crescents on the surface and for the sides of a narrow tillage tool to predict the volume of displaced soil by the tool. In this model, r was defined as the total forward distance of soil failure on the surface from the tool face, and soil in front of the tool was analyzed by a 2-D failure region using the N-factors of Hettiaratchi and Reece (1974).

According to Payne and Tanner (1956), the difficulty with such a model was that r changed when the aspect ratio of the blade (d/w) varied and soil strength changed. To solve the problem, Payne and Tanner performed some tests with narrow tillage tools in sandy soils in order to estimate r and s for various rake angles α, slenderness ratios d/w, and soil types. Results showed r changed as the rake angle changed, and a graph was developed to describe the relationship between r/d and the tool angle. According

to Shen and Kushwaha (1998), the determination of the rupture distance r was still difficult.

2.6.1.5 Mckyes-Ali model

Mckyes and Ali (1977) developed an independent analytical model for narrow tools without the need to rely on experimental inputs of soil failure geometry. The model was similar to the Godwin and Spoor model in the shape of the failure zone except that a flat bottom plane for the center wedge was assumed. The straight lines at the bottom of the crescents enabled to define the direction of forces at the bottom of the failure zone.

This model is easier than the Godwin-Spoor model since it does not need prior knowledge of the rupture distance and N-factors are re-evaluated in this model. Moreover, the model uses a technique that increases the magnitude of N factors as the tool becomes narrower. In addition, by setting $w = \infty$, the researchers compared the N-factors with the N-factors used for 2-D models. It was found that for smooth blades, the results were very close, yet for the rough blades with $\alpha > 90° - \phi$, rupture angle and the N-factors were much higher than those for the 2-D soil cutting cases. McKyes (1985) published a set of charts to determine the N-factors for some rake and rupture angles.

2.6.1.6 Grisso et al. model

With a similar shape of the failure zone to that of the Godwin and Spoor and the Mckyes and Ali models, Grisso et al. (1980), Perumpral et al. (1983), developed a model in which side crescents were replaced by two forces acting on the center wedge. Soil weight of the two side crescents was neglected, and side planes of the center wedge were treated as slip planes; therefore, the failure zone of this model included only a center wedge. As in the Mckyes and Ali model, the bottom slip surface was assumed to be straight. As well, the soil in front of the tool was assumed to move upward. This model produced equal values of N_c and N_{ca} as resulted from the previous two models, but N_γ value of the Grisso et al. model was less than one half of the same quantity resulting from the Mckyes and Ali model.

2.6.1.7 Dynamic models

Based on the Mckyes-Ali model, two dynamic soil failure models have been developed in which the effect of tool speed have been accounted. The first model was introduced by Swick-Perumpral (1988) and the second model by Zeng-Yao (1992). The first model had some assumptions which overestimated the size of the side crescents (researchers). Therefore, a new angle of η based on the experimental data was proposed, which was a function of the rupture distance r and the rake angle α.

In the Zeng-Yao dynamic model, the acceleration and strain-rate effects were included. Main difference between this model and the Mckyes-Ali model is that this model needs a prior knowledge of shear strain at failure to determine the position of shear failure boundary (Figure 2.6).
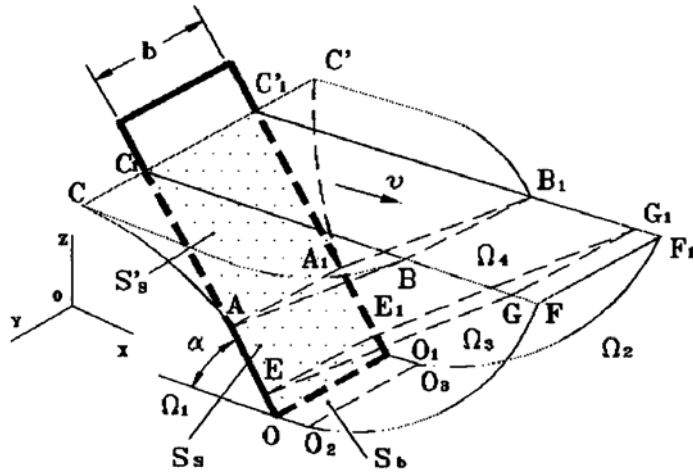
Figure 2.6 Failure zone of the Zeng-Yao model (from Shen and Kushwaha 1998)

Another difference is that total draft of the tool P_x, is divided into five components as shown in Equation 2.10:

$$P_x = P_G \sin\alpha + (P_{SH} + P_A)\cos\beta + P_F \cos\alpha + P_C \qquad (2.9)$$

where:

P_x = total draft of the tool, N

P_G = Compressive force of soil along the blade, N

P_{SH} = side-edge shear force, N

P_A = inertia force of soil in acceleration, N

P_F = frictional force along the cutting blade surface, N

P_C = bottom-edge cutting force, N

2.6.2 Finite Element Method (FEM) Models

Finite element method, which was used for the first time in aviation engineering in the middle of the 20th century, developed by extension in the other branches of science such as Physics, electro-magnetic, Mechanics, and civil engineering. Now, it has become a very powerful tool to solve the problems in those sciences.

Any numerical method of soil failure modeling including FEM has to use a constitutive model to describe the relationship between applied stresses and resultant strains within the soil. Different constitutive models have been developed based on the way that researchers have looked at soil. Linear and nonlinear models have been categorized based on using a linear or nonlinear equation to relate stress and strain within the soil where by using theory of plasticity, soil can be viewed as only elastic, or purely plastic, or both elastic and plastic materials during the loading process. And finally, soil is viewed statically, if time is ignored in calculations, and dynamically if time is considered in modeling. Since many different models for different views of soil have been developed, here only the most common models used in soil tillage studies will be briefly introduced.

The hyperbolic model, which determines the hyperbolic relationship between stress and axial strain, was originally proposed by Kondner and Zelasko (1963) and later Duncan and Chang (1970) modified the model to use in a FEM analysis. Bailey's model was first proposed by Bailey et al. (1984) to predict volumetric strain ε_v under hydrostatic compression. Later, the model was modified to include the effect of shear stress. The Cam clay model was originated at the University of Cambridge, England (Roscoe et al**.** 1958; Schofield and Wroth 1968), and it is one of the simplest elasto-plastic models which is very popular among the soil researchers. A modified version of the Cam clay model by Wroth and Houlsby (1980) shows the relationship between stress

and strain at the normal consolidation line and the swelling line in terms of specific volume and mean normal pressure. The Cap model for the first time was proposed by Drucker et al. (1955) and then it was developed by Dimaggio and Sandler (1971) based on the work accomplished by a research group at MIT (Christian 1966; Tang and Hoeg 1968).

Below, part of research in the area of tillage operations by implementing FEM method has been discussed.

2.6.2.1 Kushwaha and Shen model

Kushwaha and Shen (1995) employed FEM to solve the dynamic equation of interaction between the soil and a tool, which was previously used for the similar cases. By using a two-dimensional FEM, it became possible to predict the draft requirement of a vertical blade on soil. Comparison between the results of soil bin tests and the modeling showed that the predicted draft was very close to the experimental data. It was indicated that the method could work for predicting the forces acting between the soil and any other kinds of tillage tools by some modifications.

2.6.2.2 Rosa and Wulfsohn model

Finite element method was implemented by Rosa and Wulfsohn (1999) to study a constitutive model for high speed tillage by using narrow tillage tools. Two different tools, including a flat and a triangular edged narrow tool, were used for soil bin experiments to test the effect of forward speeds between 0.5 to 10.0 m s^{-1} over a distance of 1 to 3 m. The model's assumptions were: (1) Tool is narrow, rigid, and working in constant depth and velocity; (2) Failure is a 3-D case; (3) Tool deflection is negligible compared to the soil deflection; (4) Soil-tool interface is either totally smooth or totally rough in order to simulate the extreme cases; (5) Soil is assumed an isotropic and homogeneous medium; and (6) Soil particles are ideally assumed lumped masses and gravity effects are negligible compared to the inertial and strain rate effects or the contributed soil stiffness to draft. The results showed an overestimation of 1% at 2.8 m s^{-1} and 25% at 8.4 m s^{-1} for the triangular edged tool, yet the model predicted a correct trend of the draft requirement for the flat (reference) tool. The researchers reported that

the soil model was not completely satisfactory in modeling soil cutting problems, particularly, at failure point. As well, they believed that remoulding the soil, which is common in laboratory tests, could lead to part of the problem during soil modeling in a FEM approach, and further development is needed to have more realistic soil conditions.

2.6.2.3 Chi and Kushwaha model

Chi and Kushwaha (1991) used a non-linear three-dimensional FEM to investigate soil-tool interaction. One of the main goals of this research was the evaluation of the effect of draft requirements of tillage tools on wear and friction losses. Actual tests in the soil bin were conducted to compare with the results of the model. Draft was measured for different rake angles of the tool. Results of both theoretical and experimental methods obviously showed that the draft requirement decreased as the rake angle decreased, but stayed constant for the rake angles less than $45°$. Results were very close, showing only about 0.8% error for a rake angle of 45° and 10.5% error for a rake angle of 90° when comparing the model with the actual test results of the soil bin. Stress on the edge of the tool was very large, and the maximum stress increased as depth was increased; therefore, the outer edges of the tool at the bottom suffered the greatest stress and wear. As well, this stress increased as the rake angle was increased. Since vertical position of the tool required the highest draft, it showed the highest level of the stress.

2.6.2.4 Mouazen and Nemenyi model

To date, only a few studies have focussed on real tillage implements using FEM to investigate the forces interacting between soil and tillage tools. Mouazen and Nemenyi (1999) developed FEM to analyze the reaction of a subsoiler in a non-homogeneous sandy loam soil. In this research, the effect of tool geometry on subsoiler performance, by implementing a subsoiler shank attached to a chisel with different angles and effective cutting widths, was investigated by implementing a 3-dimensional FEM model. Simulation of soil-tool interaction was developed by adopting the Coulomb's law of friction. The FEM model overestimated the measured draft force in a range between 11 to 16.8% for a non-homogeneous and between 15 to 18.4% for a

homogeneous soil for all four different chisel angles when the results were compared to the soil bin test results.

2.6.2.5 Fielke model

Fielke (1999) investigated the effect of cutting edge geometry of a 400 mm wide experimental sweep on horizontal and vertical components of forces. As well, he studied soil failure patterns, and soil movement below the tillage depth using a 2-dimensional FEM. The researcher found out that replacing a sharp cutting edge tool with a blunt one can increase draft requirement up to 80%. In addition, the direction of the vertical force can change from one that acts to pull the tool into the soil to a force that provides tool lift. In this study, soil was represented by a linear elasto-plastic model, and the Mohr-Coulomb theory was employed as the soil failure criterion. Results of the modeling showed the power of FEM to model soil-tool interaction.

2.6.2.6 Plouffe et al. model

Plouffe et al. (1999) employed a 3-dimensional FEM to simulate forces applied on a moldboard plow during an operation. Three plowing depths of 100, 150, and 200 mm and three forward speeds of 0.25, 1, and 2 m s^{-1} were implemented. A cylindrical plow bottom was fixed on a triaxial dynamometer and its movement in both vertical and lateral directions was controlled by two hydraulic cylinders. The type of soil used in the soil bin was a Sainte-Rosalie clay soil (53% clay, 27% silt, 20% sand, and 2.97% organic matter), which is a typical soil for moldboard plowing in Quebec, Canada. Results showed no significant difference between experimental data and the simulated data for the longitudinal forces (F_x), but for the vertical forces (F_z), simulated forces were significantly lower than measured forces for the forward speeds of 0.25 and 2 m s^{-1}. Both results showed an increase in F_y as depth and speed increased.

2.7   Summary

In this chapter, different aspects of soil tillage energy were discussed based on the results of the previous research works. Those researches have mainly addressed soil parameters, tool parameters, and operating parameters related to the draft and energy

requirement of tillage tools. Since the current research deals with high operating speeds of tool, dynamic properties of soil and the affecting factors on those properties have been introduced and discussed. In addition, Soil shear strength parameters were defined and laboratory and in situ measuring devices and methods were introduced. Consequently, mechanics of vertical tools was explained based on the literature as this research has employed a vertical simple tool for the soil bin experiments and then some aspects of energy in tillage operations were presented and discussed.

In the last two sections, most of the static and dynamic analytical models developed to predict applied forces on narrow and wide tillage tools were introduced, and some governing equations, assumptions, and their limitations were broadly discussed. Finally, different stress-strain relationships of agricultural soils to be applied in a FEM modeling were introduced and many research works using FEM to measure soil forces on tillage tools were discussed. Based on the above mentioned summary of literature, the following points can be concluded:

1. Developing a single equation that can predict draft or energy requirement of a particular tool at different soil and operating conditions is not realistic. The reason refers to the non-homogeneity of soil as a complex mixture of solids, air, and water which reacts differently under different ambient conditions and operational situations.

2. Previous models which have been implemented to predict applied forces of tillage tools used several assumptions that make their area of application limited.

3. To manifest dynamic effects of a tillage operation, tool should be run at high speeds. Achieving such speeds faces practical problems and needs special measuring devices which are not always available.

4. Interpreting results of corresponding tests such as high speed triaxial tests on soil makes some difficulties which affect the results. For example, it is difficult to justify having a homogeneous applied load within whole sample of soil at such high rate of loading. As well, it is hard to believe that remoulded soil samples act similar to field soil under loading conditions. The

correction factors to compensate for such differences have not received enough support to date.

5. The influence of each affecting factor, such as moisture, depth, and speed, on draft and energy requirements of tillage tools is to be determined separately. Unfortunately, the interactions between these parameters have limited knowledge of the individual effects since in practice it is difficult to eliminate the effect of other factors.

6. To date, force and energy requirements of different tillage tools have been measured or calculated in total. In literature, there is no reported information on the subdivisions of those total forces or energies in order to know the contribution of each individual factor in total energy requirement.

7. Different types of soil failure patterns such as shear, tension, compression, and plastic flow have been introduced and defined in the literature. However, the soil failure pattern developed by each tillage implement is not clear enough yet. In addition, if some implements develop more than one pattern of failure to the soil, it is required to know the conditions at which those patterns occur.

8. Using Limit Equilibrium Method (LEM) analysis needs in advance an assumption of a failure profile. Since this assumption has changed from one researcher to another one, the results have accordingly changed.

9. In an analytical approach, different layers of soil have been assumed to have uniformity in their mechanical properties, whereas it is not true, particularly, for soils under natural situations such as soils of agricultural fields.

10. Analytical models do not reflect the influence of tool speed on the shape of soil failure pattern although this influence is well known and accepted.

11. To date, only a few number of FEM modeling have been successfully used in prediction of draft requirement of a real tillage tool. At higher speeds of travel, the closeness of the simulated results to the experimental data reduces dramatically. On the other hand, those research accomplished at lower speeds have not been able to investigate dynamic properties of soil. Therefore, FEM

modeling, like other methods, needs improvements although it is known as a powerful modeling tool in many fields of science.

12. To date, no particular FEM software has been introduced to model an agricultural soil under different loading conditions. In addition, employing FEM needs a good knowledge in mathematics and computers. The assumptions involved in the FEM modeling makes its application very complicated and professional. As a conclusion, FEM cannot be implemented in current research to investigate high speed soil-tool interaction.

Summary of the literature proves that in spite of numerous numbers of research in this area, tillage must still be a technique or art more than being a science. Another point is that efforts should focus on finding particular equations for particular soil, tool, and operating conditions. At the same time, efforts should be made to investigate the components of total draft and energy requirements for different tillage operations. This approach will lead to a reduction of energy requirement of a particular tool by optimizing soil, tool, and operating parameters based on the collected information.

Literature showed that there is a lack of experimental data for the vertical narrow tillage tools particularly at high speed of operations. Since new cultivation methods such as no tillage and minimum tillage methods mostly use some kinds of vertical tools, it is very important to collect more force and energy data of these tools. This will facilitate any calculation-based design of tillage tools in the future.

Considering above mentioned problems and shortcomings in the area of tillage, the current research was an effort to collect energy data for vertical narrow tools running at high speeds of operation. It was also to determine different components of total energy, and to submit equations to relate the total energy requirement to the corresponding energy components. This energy model assumed four main energy consuming components for an employed vertical tillage tool. The energy components were: (1) energy requirements associated with soil-tool interactions, (2) energy requirements associated with interactions between tilled and fixed soil masses, (3) energy requirements associated with soil deformation, and (4) energy requirements associated with the acceleration of the tilled soil. A wide range of speeds from 1 to 24 km h^{-1} were investigated to manifest dynamic aspects of soil-tool interaction. Regression

equations were developed to relate energy requirement of each component to the variables of soil moisture content, tool depth, and tool forward speed. The equations were then validated by extra soil bin experiments conducted at same soil and tool but different operational conditions. Based on the experiments, conducted in soil bin facility, the results were analyzed to come up with some empirical relationships.

3.0   MATERIALS AND METHODS

In this chapter, materials and devices employed in the experiments, experimental procedures, and statistical research design are presented. Soil bin experiments are described in two separate categories: low speed and high speed. The main difference between these two refers to the speed of the tillage tool. In low speed experiments, tool was run at 1 and 8 km h^{-1} speeds by using the regular carriage of the soil bin. In high speed experiments, tool was run at 16 and 24 km h^{-1} speeds by using high speed carriage. Although range of speed was different for these two categories, other variables such as soil moisture contents, and tool operating depths were maintained at the same values for the experiments in both categories. Soil type and soil preparation method were also the same for all experiments. In the last section of this chapter, energy model development is discussed.

3.1   Materials and Devices used for Soil Bin Experiments

In this section, different materials and apparatuses used in both low and high speed experiments are described. Except for the subsections 3.1.1 and 3.1.2, which discuss common sections, other subsections of 3.1 describe particular materials and devices employed for the low speed or high speed experiments individually.

3.1.1 Tillage Tool Specifications

To fulfil the objectives of the energy model development and testing, a tillage tool, based upon a rectangular cross section was used. Based on assumed requirements (a flat shape and vertical tool with a d/w ratio not less than 1 and enough thickness to

prevent bending at high speeds), 2 pieces of a steel bar each 25.4 mm thick, 40 mm wide, and 533 mm long were used as the tillage tool. Two similar tools were made to be installed on both carriages of the soil bin. Pieces were straight and rectangular to simplify force calculations, and its width was equal to the minimum operating depth, which was 40 mm, in order to be assumed as a narrow tool. The overall length of 533 mm was so that it could be held in the tool holder and still be inserted into the soil up to depths of 200 mm (Figure 3.1)
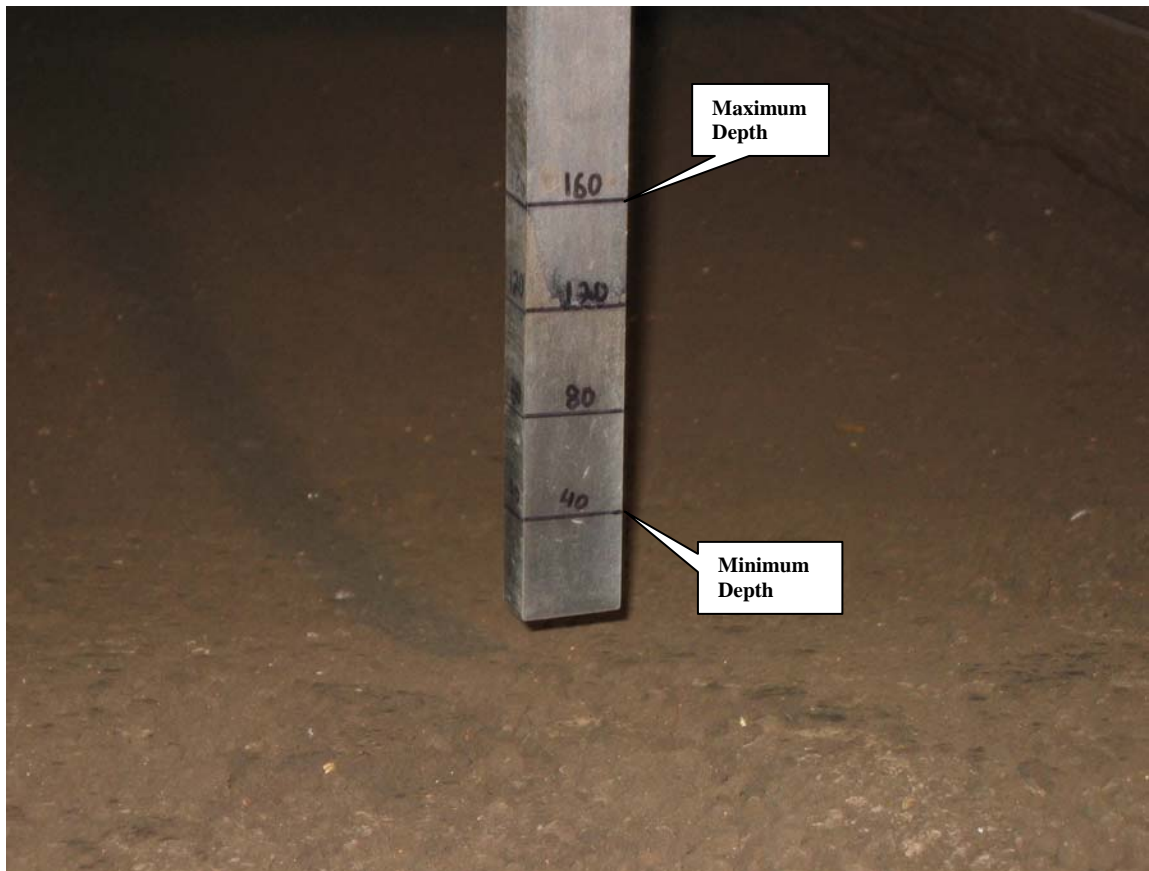
Figure 3.1 Simple tillage tool used for both low and high speed experiments

3.1.2 Soil Bin Facility

The department of Agricultural and Bioresource Engineering at the University of Saskatchewan has an instrumented soil bin which was used for current research. The bin is 1.8 m wide and 12 m long with an effective length of 9 m. About 5.7 m of its length in the middle is designed for instrumental measurement of forces using a data logger

system. The soil bin has a carriage with a tool holder equipped with load cells and other instrumentation to measure forces applied to the tool in horizontal, vertical, and lateral directions. Data collected by the data logger are sent directly to a computer for storage. The soil in the bin is about 0.3 m deep and has a silty clay loam texture (47% sand, 24% silt, and 29% clay).

3.1.3   Low Speed Carriage

The low speed carriage, which is the main carriage of the soil bin, is used to prepare the soil, compact the soil and run any attached tool within the soil. The main frame of the carriage has a cubic shape and is supported by two rails along the sides of the bin through four steel wheels attached to the frame at four corners. A drive chain attached to the frame moves the carriage. An electric motor powers the drive chain and can be used to reverse direction. Different soil preparation devices may be attached to the carriage; a roto-tiller to loose the soil, a sheep foot and a smooth roller to pack the soil, a water sprinkler bar to add water in the soil if necessary.

Tillage tools are attached to the frame with a special holder that enables the tool to be positioned and then fixed in any location across the bin width. The height of the tillage tool is adjustable. Both sheep foot and smooth roller packers were attached to the front side of the frame before operating on the soil (Figure 3.2).

The carriage has a stationary control panel positioned beside the bin to control the carriage movement and the attachments. Functions such as carriage speed, start and stop buttons for the carriage, roto-tiller, and sprinklers are all controlled from this panel.

To measure the resisting force of soil when a tool passes through it, the tool holder is equipped with six load cells which measure forces in three directions. From these six load cells, three are used for vertical forces, two for horizontal or draft forces, and one for lateral forces. The capacity of each load cell is 4453 N, except for the very front one, which is used for vertical forces with a capacity of 8906 N.

A data logger (model AT-MIO-16F-5, National Instruments Corporation, USA) is installed to record force data from the six corresponding load cells.
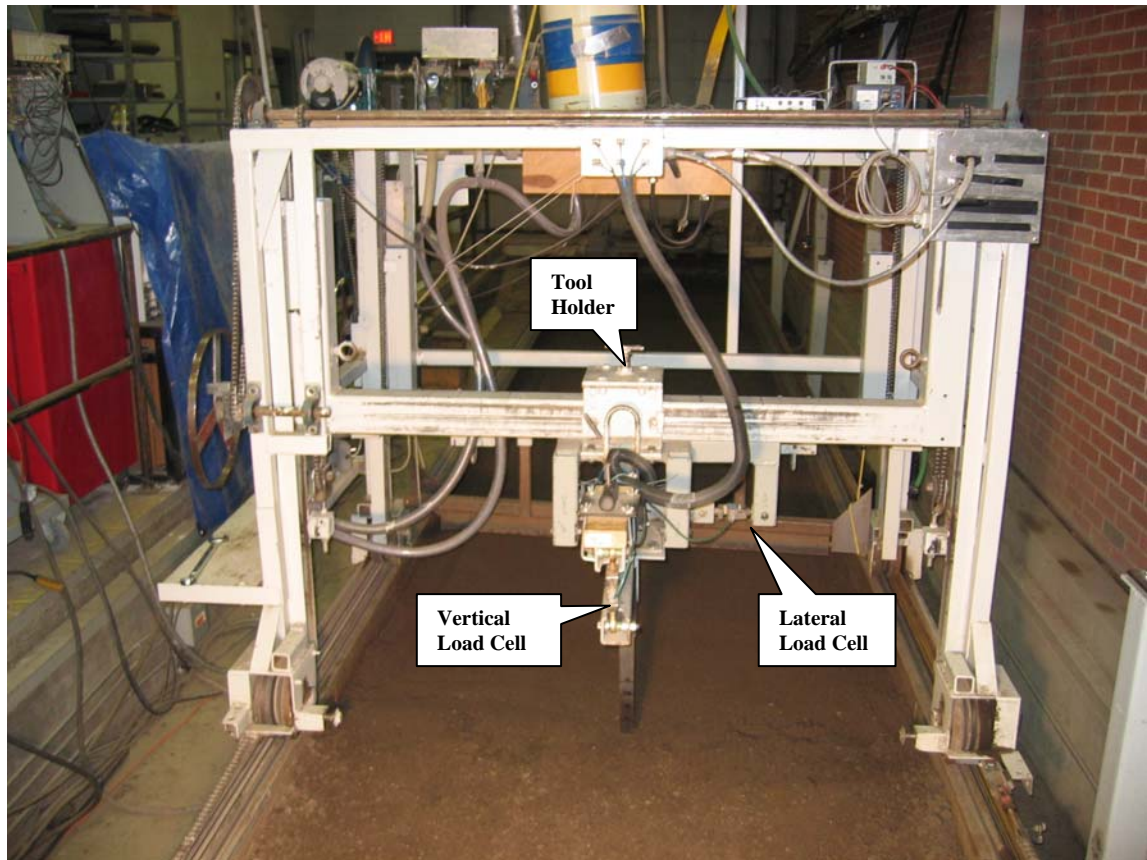
Figure 3.2 Low speed tool carriage

3.1.4 High Speed Carriage

The high speed system is an attachment to the regular soil bin and has its own carriage, data collection system, and drive assembly from that of the low speed system. It consists of a long folding I-beam which is the support of the rail system. A carriage, holding the tillage tool, six load cells, and a data logger, runs along the I-beam on a series of ball bearings. Movement of the carriage is by a chain system powered by a hydraulic motor (Figure 3.3).

The high speed system was designed in 1995 and modified and upgraded after. With the use of a hydraulic jack, the main beam can fold up along the wall when not in use, so the low speed carriage can be operated. The design of the beam allows the tool to be attached in only one place, close to the center line of the bin. Therefore, with this set up, soil can be used once per each soil preparation considering that it cannot move laterally.
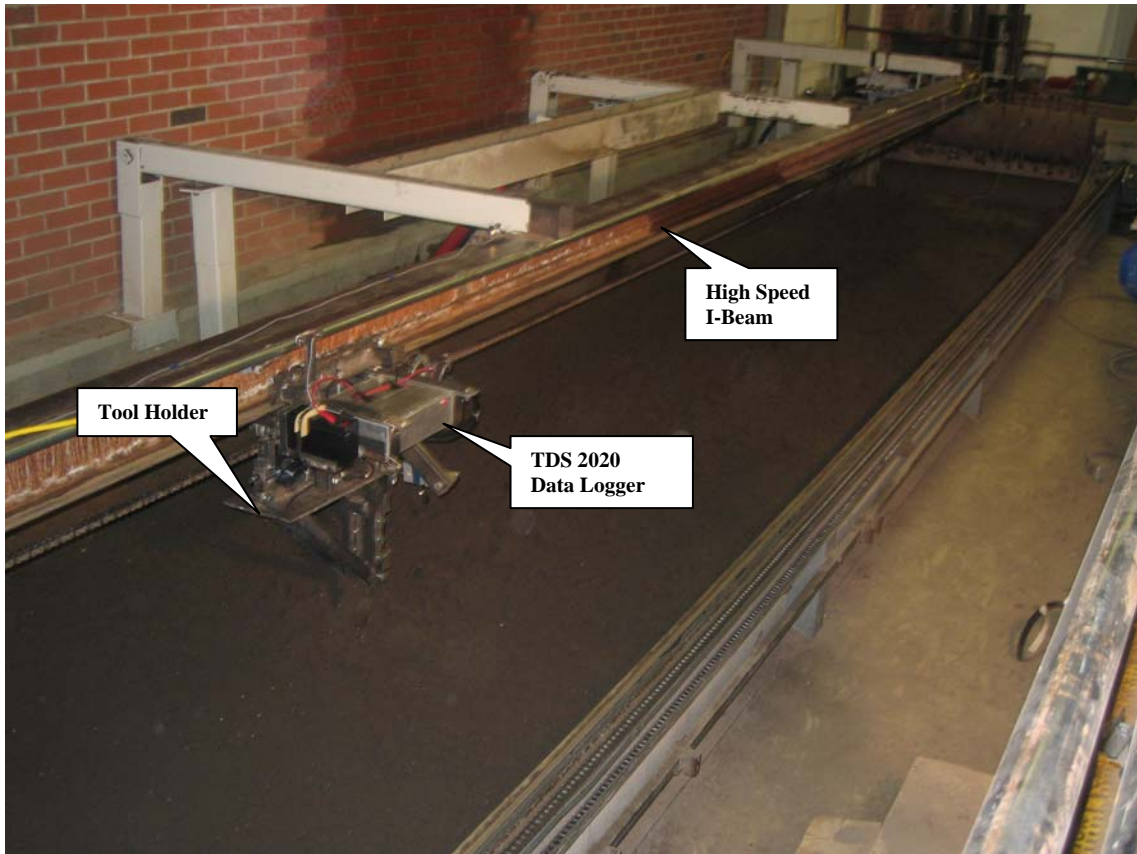
Figure 3.3 I-beam of the high speed carriage

Tool holder and its corresponding parts such as data logger and load cells of the high speed beam are moving along the beam back and forth through a chain conveyor run by a hydraulic motor. The hydraulic motor is fixed on one end of the beam and by turning a chain sprocket can move the chain in one direction, and if the rotation of the hydraulic motor is changed, the holder and data logger start moving in the opposite direction. More details of the hydraulic control unit are provided in Appendix E.

3.1.4.1 Electronic Control Unit

A new electronic control box was designed and fabricated in order to control movement of high speed carriage through switches installed on the beam as well as on the hydraulic system at different modes of movement. As shown in Figure 3.4, there are seven buttons on the box to perform the required tasks. The system allows carriage to go forward at low speed at jogging or high speed modes and to return back at jogging or auto return modes.

On the main beam of the carriage, four switches including two reed switches and two emergency switches are installed to control data collection and prevent any extra movement of the carriage. The distance between two reed switches is exactly 4.54 m, the same as the maximum length of data collection. The end reed switch is supposed to stop the carriage immediately after it is passed by the carriage. If the reed switch cannot act quickly, emergency switch which is installed about 1.2 m beyond the reed switch is designed to stop the carriage. In practice, it was experienced that none of those two switches could stop the carriage at speeds higher than 16 km h^{-1} and shallow depth of 40 mm. Therefore, as a vital rule, it became necessary to use the stop button of the electronic control box at high speeds to stop the carriage regardless of the depth of operation.

Figure 3.4 Electronic control box to control carriage movement

3.1.4.2 On Board Data Logger

One eight-channel data logger model TDS2020 is installed on the carriage to collect force data as the tool is passing through the soil. The logger receives its power from a Panasonic 12-volt lead-acid rechargeable battery, installed on the logger frame. In the front side of the logger (Figure 3.5), there are six ports to connect load cell wires, another port to connect wire from reed switch, one RS 232 port to connect computer to the logger, and one port to connect speed sensor to the logger.

For the current research, a program in the Forth language was written in MS-Dos and was saved on a 133 PC computer used stationary beside the bin as part of data acquisition system. The program offered two mode of data collection to the logger. In the first mode, labelled as "slow mode", the logger collected data for fourteen seconds starting from triggering point at the first reed switch. In the second mode, labelled as "fast mode", the logger collected data for only two seconds. Since low speed experiments were accomplished by another carriage as discussed previously, the only mode used for the current research was the fast mode. A copy of the Forth program is given in Appendix F.
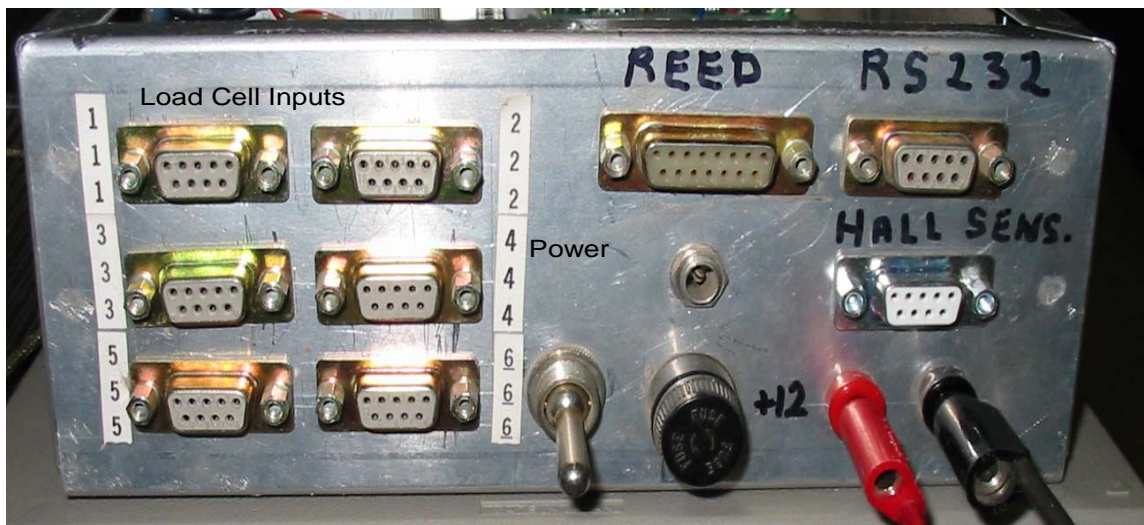
Figure 3.5 Front view of the on-board data logger

Inside the box of the data logger, there are several electronic kits and six signal conditioner as well as seven zeroing pots to set load cell readings when calibration is

required. One red light, labelled on Figure 3.6 as collecting light, was added to the box to indicate the start of data collection when turned on as it passed the reed switch. Since for all high speed experiments it took less than two seconds to pass the other reed switch at the end of the beam, the red light went off always after the carriage was stopped. The real rate of data sampling was 904 samples per second, thus for 1.88 seconds of data 1700 data points were recorded.
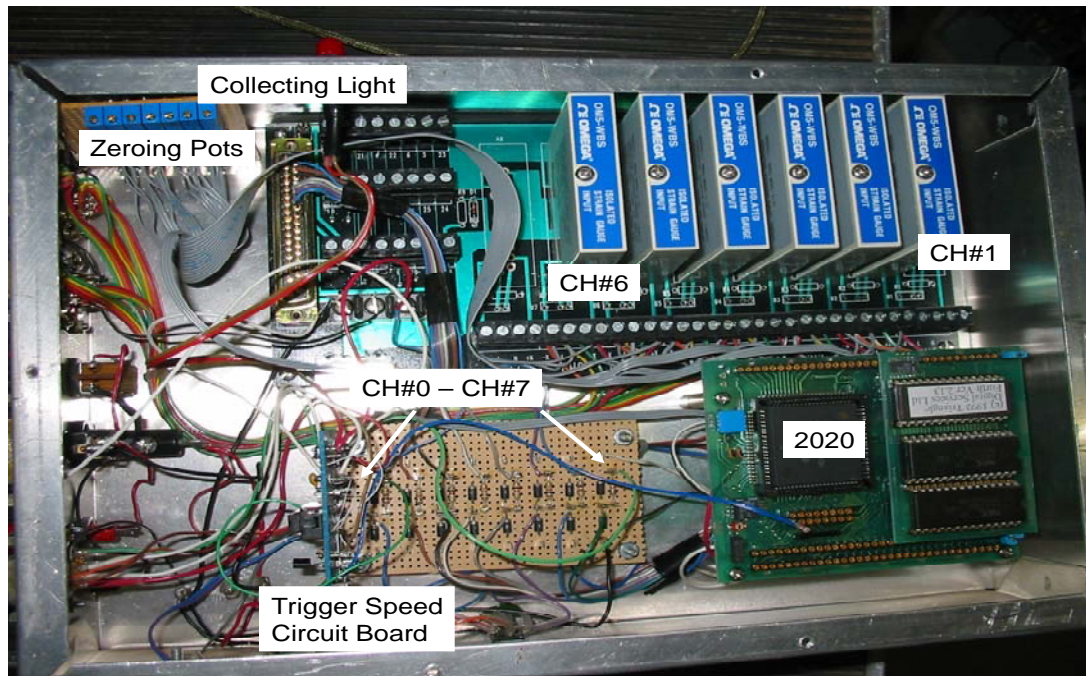
Figure 3.6 A view of inside the logger of high speed carriage

Since tool travel was always over in less than one second, only less than half of the data were collected during tool movement, so more than half of the data points were invalid because they were collected after the tool was stopped. Table 3.1 shows the time required for the tool travel at each tool speed (mode of movement) and the approximate data points which were valid.

3.1.4.3 Load Cells of High Speed Carriage

The tool holder of the high speed carriage includes six load cells to measure resistive forces of the soil in three dimensions when the tool is traveling within the soil. Three of them measure vertical forces, two for horizontal or draft forces and one measures lateral force. All load cells have a force capacity of 4453 N except for the very

Table 3.1 Required time and approximate number of valid data points at each tool speed

Tool speed (km h^{-1})	Required travel Time (s)	Total collected data points	Approximate valid data points
16	0.90	1700	810
24	0.59	1700	531

front vertical one which has a capacity of 8906 N. Figure 3.7 shows a configuration of those load cells installed on the tool holder.
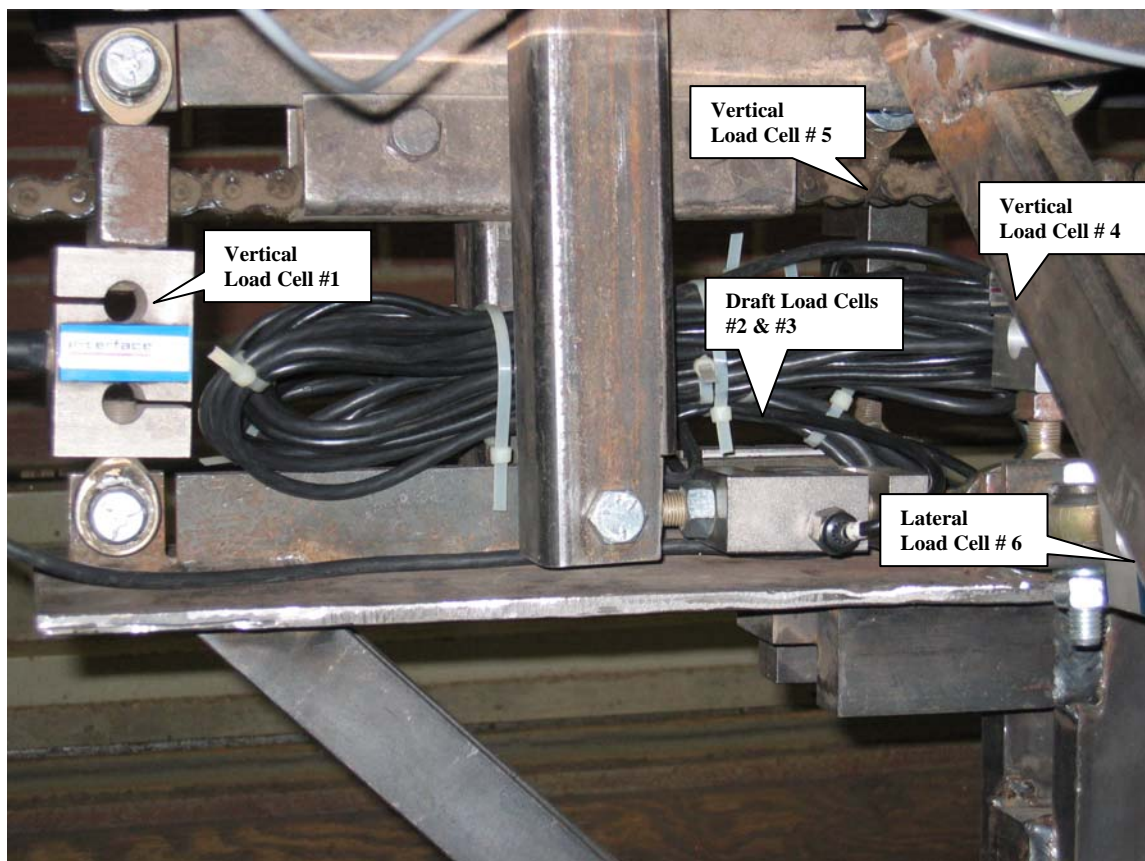
Figure 3.7 Configuration of the load cells installed on the tool holder

3.1.4.4 High Speed Measurement

On the initial design of the high speed beam, an optical sensor installed concentrically with the drive shaft was used to pick up signals to be converted later to

the speed values. Since that system did not match the new modifications, a frictional wheel with a magnetic pick up was employed instead to measure the tool speed.

The frictional wheel consisted of rubber with a diameter of 125 mm which was pressed to the main beam and was attached to the tool holder through a strong arm and with almost zero deflection (Figure 3.8). As shown in Figure 3.8, a chain sprocket with 17 teeth is concentrically welded to the wheel. By turning the wheel, sprocket turns at the same rpm, with each tooth sending a signal to data logger by passing the magnetic sensor installed on the bent part of the arm. Having the diameter of the wheel and the number of the pulses received from the sensor, it was possible to measure forward speed of the tool in different sections of its travel.
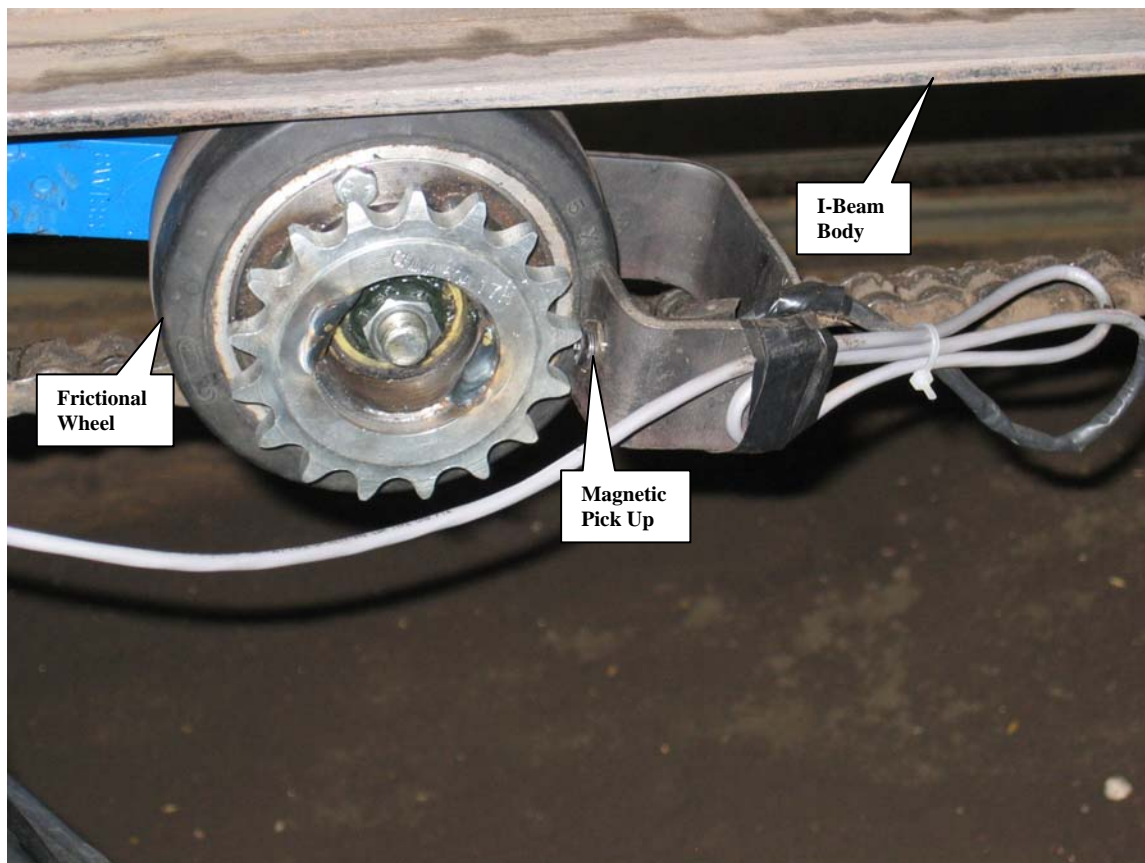
Figure 3.8 Frictional wheel and magnetic pick up attached to the holder to measure the tool speed

3.2   Experimental Design

To analyze the results of the experiments, a completely randomized design (CRD) with two replications was the statistical design with a 2x4x4 factorial treatment design to investigate the interactions between different variable factors. All soil bin experiments were based on variations of three parameters, soil moisture content, tool operating depth, and tool forward speed. Each parameter had different testing levels as shown in Table 3.2.

Based on the above variables and their levels, there were 32 different treatments that with 2 replications made 64 tillage tests in the soil bin.

Table 3.2 Parameters of soil bin experiments and their Testing levels

Moisture content (%)	Code	Operating depth (mm)	Code	Forward speed (km h^{-1})	Code
13-15	M14	40	D4	1	S1
		80	D8	8	S8
19-21	M20	120	D12	16	S16
		160	D16	24	S24

3.2.1   Randomization for Low Speed Experiments

Since the soil bin data were to be processed later in an experimental design analysis, it was necessary to apply randomization to determine the order of doing the experiments. Among three variables of moisture content, operating depth and forward speed, soil moisture content was fixed because changing it for every test was not feasible. Therefore, for 14% moisture content, each treatment which could vary based on only depth and speed, was written on a piece of paper and put in a basket and then the experiments were accomplished in the same order as they were polled out from the basket. The same randomization was applied to the treatments at 20% moisture content, and these experiments were carried out after the experiments at 14% moisture content were completed.

3.2.2   Randomization for High Speed Experiments

Despite low speed experiments, in randomization process of high speed experiments, tool speed had to be a fixed parameter for the safety issues. Since running the tool at 24 km h^{-1} speed had a high risk of breaking down the carriage, it was suggested to initially finish all experiments at 16 km h^{-1} speed then begin to perform 24 km h^{-1} speed tests. As well, changing moisture for each test was not feasible considering time limitations and achievability of same moisture content if the moisture was repeatedly changed. Therefore, depth of operation remained the only variable to randomize high speed tests. In practice, after performing all high speed tests at 20% moisture content and 16 km h^{-1} speed including 8 tests, the soil was left for several days to get dry. At average of 14% moisture content, first, experiments at 16 kmh^{-1} speed and then experiments at 24 km h^{-1} speed, which included a total of 16 tests, were carried out. Finally, soil was sprayed with water again to reach 20% moisture content; at this condition, 8 high speed tests at 24 km h^{-1} speed were carried out.

3.3   Experimental Procedures

In this section, the experimental procedures employed for the soil bin and laboratory tests have been discussed.

3.3.1   Soil Preparation

Preparation of the soil for both high and low speed experiments included four steps. In the first step, water was sprayed by attaching the sprinkler bar to the frame and running the frame on the soil along the bin. If more water was required, the number of passes was increased. In the second step, the roto-tiller was attached to the frame and by cultivating the top soil up to approximately 100 mm depth broke down any soil hard pan as well as mixed dry and wet soil layers. If the initial soil was very dry and needed much water, the water was added in several passes, and after each spraying, one roto-tilling was carried out. In the third step, the soil was levelled. Soil levelling was accomplished by a scraper blade almost as wide as the frame width. In the fourth step, packers were attached to the front side of the frame, to compact the soil. The sheep-foot packer was used to compact subsoil at maximum depth of 100 mm, then the smooth roller packer

was used to compact top soil. It was necessary to use the leveller after using sheep-foot packer since the soil was left disturbed after using that packer and was to be levelled before running the smooth packer.

The number of passes of each packer was based on the initial and final moisture content of the soil and the level of required soil compaction. The criteria for obtaining the same compaction level were soil dry bulk density and soil cone index. Table 3.3 shows the number of passes of each packer at different soil moisture contents.

Table 3.3 Number of passes of each packer on the soil at different moisture contents.

Soil Moisture Content (mass, %)	Passes of Sheep foot packer	Passes of smooth roller packer
13-15	4	6
19-21	2	3

3.3.2 Monitoring of Soil Conditions

The values of soil bulk density were determined at two different ranges of depth. For the range of 0-100 mm depth, the desired soil dry bulk density was 1.15- 1.20 Mg m^{-3} mostly closer to 1.15 Mg m^{-3} whereas for the range of 100-200 mm depth, there was same range of bulk density, but closer to 1.2 Mg m^{-3}. Two soil bulk density samples were taken immediately after each test from the undisturbed soil adjacent to the tool track. A core sampler 71 mm inside diameter and 51 mm high was used to take the samples.

For each test, 6 moisture samples from different parts of the soil were taken, weighed, then dried for 24 hr at $105^{\circ}C$, then weighed again to determine soil moisture content. As shown in Table 3.2, any soil moisture located between 13% and 15% (mass moisture on a dry basis) was accepted as first level of moisture content (14%), and any average moisture located between 19% and 21% was accepted as the second level of moisture content (20%).

For each soil bin experiment, after compaction and before running the tool, soil cone index was measured by a mechanical cone penetrometer. Since the level of compaction by packers was same for all treatments, almost the same cone index values

were achieved for different treatments. For each experiment, soil cone index was measured at 6 points of the bin. Table 3.4 shows an average cone index of the soil at different depths immediately before running the tool.

Table 3.4 Average soil cone index at different depths and moisture contents

Depth (mm)	Average Cone Index at 14% M.C (kPa)	Average Cone Index at 20% M.C (kPa)
0	108.7	112.5
40	318.7	243.5
80	652.0	579.3
120	707.4	712.3
160	845.8	855.4
200	1016.6	1153.9

3.3.3 Soil Bin Experimental Procedure for Low Speed Tests

A total of 16 tests including 8 treatments in 2 replicates at 14% moisture content and then 16 more experiments at 20% moisture content were carried out as low speed experiments. To begin each experiment, after the soil was prepared, carriage was taken about one meter behind the triggering point of collecting data. At this point, the tool was lowered to the soil surface. Soil underneath the tool was dug enough to let the tool come down to desired depth. A long flat piece of wood was used on the undisturbed surface of the soil and beside the tool as the index to measure operating depth from the soil surface. Tool was lowered into the dug hole by turning the control wheel on the frame, and when the measuring tape showed desirable depth adjustment, the wheel was locked at the point.

For low speed experiments, it was possible to use soil for two runs per each soil preparation as the tool holder was able to slide across the bin width. Therefore, it was required to slide tool holder to the appropriate point on the frame and fix it at the point before lowering tool into the soil. In addition, the speed of the carriage was fixed on 1 or 8 km h^{-1} speed based on the existing treatment before running the tool; this was accomplished by increasing the rpm of the electric motor, and was shown by the digital

indicator on the control panel. At this point, the tool was ready to run. When the start button on the control board was pressed, the tool started cutting the soil, and by the time it passed the first triggering point for collecting data, the actual speed was reached. For 1 km h^{-1} forward speed, the automatic stop switch, installed beside the bin, was able to stop the carriage before hitting the end of the bin. In contrast, for 8 km h^{-1} of speed, it was vital for the carriage to be manually stopped by the break button on the board to avoid any collision at the end due to the great inertia of the carriage. When the second switch was passed by the carriage, data collection was completed, and the values of forces and corresponding curves were immediately shown on the screen.

3.3.4   Soil Bin Experimental Procedure for High Speed Tests

All 32 high speed experiments included 16 treatments at 2 replicates which half of them conducted at 14% and the other half at 20% moisture content. For each high speed experiment, after soil preparation, regular carriage was parked at the very end of the bin and then high speed beam was lowered. Tool was returned to the starting point at the opposite end of the beam and close to the hydraulic motor by the jogging mode of the electronic control box. A hole was dug into the soil and underneath the tool and by using a flat piece of wood as a depth index across the bin and beside the tool, it was possible to lower the tool to a desirable depth and to fix it to the holder by the tightening bolts. The starting point was somewhere between the emergency switch and the reed switch. Passing each of those switches resulted either in disabling hydraulic system in running the tool or losing data collection process by the logger (more details of running high speed carriage and collecting data is given in Appendix E).

3.3.5   Calibration Curves of Load Cells

To ensure the accuracy of the measurements, load cells were calibrated in advance of being used for force measurement. For load cells of both low and high speed carriages, dead weight method was used for the calibration. A detailed description of Load cells calibration is available in Appendix D.

3.3.6 Direct Shear Test

Soil physical properties including cohesion, adhesion, internal and external friction angles were measured through the laboratory tests in order to be used later in the energy model. Direct shear test was employed to measure these values of soil shear strength under same moisture and density conditions as applied in the soil bin experiments. The only difference was the shearing rate; where soil in the soil bin experiments was sheared in a varying rate ranging from 1 to 24 km h^{-1} speed, soil in the shear box was continuously sheared at a constant rate of 0.4 mm min^{-1}.

3.3.6.1 Soil Sample Preparation for Direct Shear Test

In the available direct shear apparatus, the amount of dead load was multiplied by 10 through a particular linkage before applying to the soil sample. For example, the linkage was applying a load as much as 500 N to the soil sample if the initial load was 50 N.

Three levels of moisture content with middle points of 14%, 17%, and 20% dry basis were tested, and for 2 replicates, a total of 30 real tests were performed. If the results of 2 replicates for each treatment were not close to each other, more tests were repeated to verify the real values of shearing force for that treatment.

For all tests at three different levels of moisture content, 5 dead loads were applied. Table 3.5 shows dead loads, surface area of the shear box, and corresponding stresses produced by those loads.

As those direct shear tests data were to be applied to the results of the soil bin tests in order to measure draft requirement of the tillage tool, it was necessary to shear the soil at the same bulk density as sheared in the soil bin by the tillage tool. During the soil bin experiments, bulk density of the soil was always maintained in the range

Table 3.5 Applied dead loads and corresponding normal stresses on soil sample in shear tests

Dead load x 10 (N)	Shear box surface area (m^2)	Stress on soil sample (kPa)
100	0.01	10
200	0.01	20
300	0.01	30
400	0.01	40
500	0.01	50

of 1.35-1.40 Mg m^{-3} wet bulk density, or approximately 1.15-1.20 Mg m^{-3} dry bulk density by controlling the number of passes of the packers.

To reach desirable bulk density of the soil at each level of moisture content, it was required to have same amount of soil for each test regardless of its existing moisture content (same amount of dry soil). Also, it was necessary to reach the soil to the desirable bulk density at its existing moisture content. These two tasks must have been accomplished before putting soil sample in direct shear apparatus and applying normal load to it. Therefore, for each test, after putting exact amount of soil in the shear box, by calculations, it was determined that how much volume change was required to achieve desirable bulk density at that particular moisture content. Since the shear box has a fixed surface area, the only dimension to change was the height of the sample. To decrease the height of the sample, soil sample was placed under a piston of a hydraulic jack and a uniform pressure was applied to the whole surface of the soil until the final height was reached. This final height of sample indicated desirable bulk density for the existing moisture content. Figure 3.9 shows a soil sample under pressure of the hydraulic jack, and Figure 3.10 shows the decrease in the height of the soil sample after applying load by the hydraulic jack and reaching desirable bulk density.
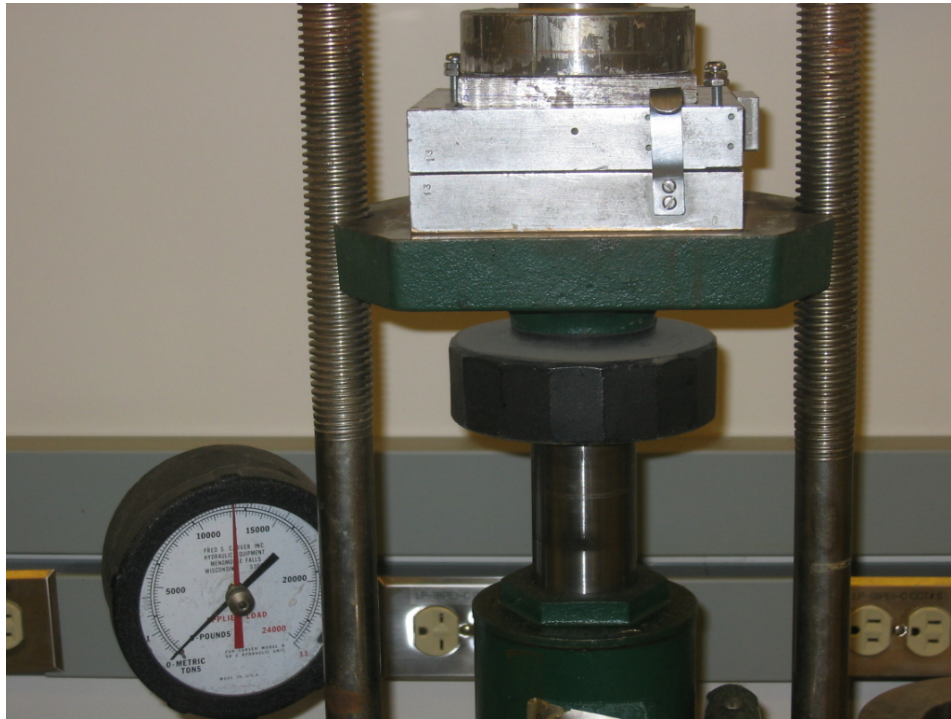
Figure 3.9 Applying load to the soil sample by a hydraulic jack

Figure 3.10 Reduction in height of soil sample after applying load by the hydraulic jack

3.3.6.2 Measurement of Soil Parameters

After pre-compression treatment was carried out, soil sample was ready to put in the direct shear apparatus for the shearing process. Same pre-compression stress was applied to all soil samples used at same level of moisture content before starting direct shear tests. As shown in Table 3.6, the values of pre-compression stress were different for different soil moisture contents. Although at same moisture content, pre-compression values to measure cohesion and internal friction angle were equal to those values to measure adhesion and external friction angle, the change in the sample height after being compressed was different.

For the measurement of cohesion and angle of internal friction, both halves of the shear box accommodated required soil sample. In contrast, to measure adhesion and angle of external friction, lower half of the box was fully occupied by a flat square piece of metal from the same material as the tillage tool, and only the upper half of the box included soil for the test.

Table 3.6 Values of Pre-compression stresses applied to the soil samples at different moisture contents and for different soil parameters

Soil Moisture (db %)	Pre-compression stress for C, ϕ (kPa)	Initial Height (mm)	Final Height (mm)	Pre-compression stress for C_a, δ (kPa)	Initial Height (mm)	Final Height (mm)
13-15	245.2	36.2	27.8	245.2	25.0	19.3
16-18	186.4	36.2	29.2	186.4	25.0	20.1
19-21	122.6	36.2	30.2	122.6	25.0	20.7

3.4   Data Analysis

After the soil bin experiments were carried out, a statistical analysis based on a completely randomized design with a factorial treatment design were carried out in SAS program. From a total of 64 soil bin experiments, 4 of them were not completed because of the power limitations in the hydraulic system. Incomplete experiments included treatments at 160 mm depth and 24 km h^{-1} speed at both 14% and 20% moisture contents for both two replicates. The values of draft requirement for those experiments

were later estimated based on the other data points (discussion on the validity of the estimation of the missing data is presented in section 4.3 in chapter 4). The estimated values along with the other soil bin values were used in the statistical analysis. Different SAS analyses were used for the soil bin experimental values and for the direct shear tests values respectively.

In the first analysis, experimental values of the soil bin experiments were used. The data included energy values at 4 different depths, 4 speeds, 2 moisture contents, and for 2 replicates. These included 64 energy data points that entered SAS program. In conducting the analysis a completely randomized design with 2 replicates was used and the data were analyzed with a factorial analysis of variance to investigate the interactions between different variables. F-test was used for the analyses of whole energy model, different levels of each individual variable, and interactions between different variables. In addition, t-test was used to determine different significant levels of variables by using Least Significant Difference (LSD) method at 5% significant level (Appendix A, Tables A1-A8).

For each parameter of cohesion, adhesion, and soil internal and external friction angles also separate SAS analysis were conducted. For any of these parameters 6 data points including the values of that parameter at 3 levels of moisture content and 2 replicates were used in the corresponding analysis. For each parameter, F-test analyzed data to determine if there was any significant difference in the analysis of variance for that parameter. After that, t-test was conducted for each parameter to determine different significant levels of that parameter by using LSD method at 5% significant level (Appendix A, Tables A.9-A.20).

3.5 Energy Model Development

Results of all soil bin and direct shear tests were used in the development of the proposed energy model. This model consisted of four main energy components; (1) energy requirements associated with soil-tool interactions; (2) energy requirements associated with interactions between tilled and fixed soil masses; (3) energy requirements associated with soil deformation; and (4) energy requirements associated

with the acceleration of the tilled soil. The total energy required by the tillage tool was divided into these four main components based on studies by Blumel (1986) and Kushwaha and Linke (1996). Since the drive system of the tool did not use any tractive device, it was assumed that there was no energy loss by slippage or friction. As well, in this model the effects of interactions between different variables did not produce any new component, but they were taken into account as part of one of the four main components. Energy was defined as the product of force and distance that shows the amount of work done by the tool for soil manipulation during a tillage operation. Since the force required to cultivate one meter of soil ahead of tool was the base of energy calculation in this model, thus the values of draft forces and their corresponding energy values are numerically equal to each other. It is noticeable that researchers have emphasized on draft requirement of tillage tools more than energy requirement considering that the main component of energy is still draft.

In development of this energy model, two basic assumptions were made as follows:

1)   Deformation energy of soil at depths up to 40 mm inclusive is negligible.

2)   Acceleration energy of soil at speeds up to 1 km h^{-1} inclusive is negligible.

3.5.1   Validation of the Basic Assumptions

Validation of these basic assumptions was an important for reliability of the model. First assumption of the model was that deformation energy of soil at depths up to 40 mm was equal to zero. This can be discussed from different aspects. First of all, it should be noted that for such a vertical narrow tool, the amount of translocated soil due to the tool movement is very low. For vertical tools, it was observed (O'Callaghan and Farrelly 1964) that at shallow depth, the tine displaced a chip of soil, slightly wider than the tine face width, immediately in front of it; while for deep operations, a fissure was developed in the soil some distance in front of the tine face and across the path of the tine. The fissure curved backwards on both sides of the tine forming a triangular wedge. In addition, since this is the first 40 mm depth of top soil, that is in contact with the free space, thus easy to be translocated. It should be noted that the cutting energy required to originally cut this top soil was provided by soil-tool energy component. The frictional

66

energy requirement to separate this chip of soil at 40 mm depth was entirely provided by soil-soil energy component. The energy to accelerate this soil body was provided by soil acceleration energy. The only unaccounted part was the weight of this small soil body. Since the amount of the soil was very low, this assumption worked reasonably well for this energy model. The assumption of neglecting the weight of soil wedge in case of narrow tools is common in the literature (O'Callaghan and Farrelly 1964 and Grisso et al. 1980). Validation of this basic assumption from energy point of view will be discussed in section 4.9.8.

The second assumption was that acceleration energy at speeds up to 1 km h^{-1} was equal to zero. First of all, visual aspects of experiments supported the validity of this assumption. It was noticed that the mode of tool movement was periodic. This means that soil at low speeds of tool was compressed ahead of the tool for a while then it was released. This process was very slow and possible to observe at 1 km h^{-1} speed and did not throw much soil around. This assumption has been supported by previous research as well. Experiments conducted by James et al. (1996) on draft requirement of mouldboard plow, chisel plow, subsoiler, standard chisel, and standard lister showed that the effect of speed for all the implements was small below 7.2 km h^{-1} speed. In addition, based on research reported by Schuring and Emori (1964), which was validated later by Godwin and Dogherty (2003), inertial forces for narrow tools below a speed of $\sqrt{5gw}$ in which g and w represent gravitational acceleration and width of tool respectively, were insignificant. In current research, tool width was 40 mm, and the equivalent speed based upon this equation was 5.04 km h^{-1}. Therefore, it is reasonable to accept that 1 km h^{-1} speed did not produce any significant inertial force or energy. Moreover, validation of this basic assumption from energy point of view will be discussed in section 4.9.8.

3.5.2 Soil-Tool Interaction Energy

This energy component supposed to capture all interactions that occur between tool surface and the soil. Soil-tool adhesion and soil-tool friction, the two main components of soil strength against tool movement, are included in soil-tool interaction energy. Soil moisture affects soil-tool energy component as it would affect adhesion and soil-tool friction angle. In addition, surface area of the tool engaged with the soil, or in

other words, depth of operation for a constant tool width, will affect this energy component. Tool speed would not change this energy component because in this energy model, the effect of speed on cutting energy would be part of soil acceleration energy.

The Coulomb's law was employed to calculate soil-tool energy component by using soil bin and direct shear tests data. According to the modified Coulomb's law (Equation 3.1), adhesion and soil-tool friction would contribute to this component of energy.

$$S_{cutting} = C_a A_{tool} + N \tan \delta \qquad (3.1)$$

where:

$S_{cutting}$ = soil cutting force, N

C_a = soil-tool adhesion, Pa

A_{tool} = tool surface area engaged with soil, m^2

N = normal force applied on the tool surface, N

δ = soil-tool friction angle

First of all, adhesion and soil-metal friction angle were measured through direct shear tests. Second, for soil-metal friction force, two values were required according to the above equation. These two are normal force applied on the tool surface during tillage and soil-metal friction angle. Since a vertical narrow tool was employed in the soil bin experiments, normal load on the tool surface was equal to the draft requirement of the tool, which was measured by soil bin instrumentation. Soil-metal friction angle was also measured through direct shear tests. Having these values substituted in the Equation 4.1, the corresponding value of soil-tool interaction draft was calculated. The value of soil-tool interaction draft multiplied by one meter of tilled soil gave equivalent soil-tool energy requirement.

It is considerable that the contribution of adhesion multiplied by tool surface area, which represents the adhesive part of Coulomb's equation, is minor. It is because of a very small surface area of the tool which makes the value of their multiplication negligible. Therefore, the frictional part of the Coulomb's equation makes up almost

total value of soil-tool component. Although friction angle and soil shear strength are affected by tool speed, but their effects on tool energy requirement is taken into account as part of soil acceleration energy component.

3.5.3 Soil-soil Interaction Energy

In current energy model, soil-soil energy component accounts for interactions that take place in the interface of soil particles. Therefore, it includes cohesion and soil internal friction. Since moisture content affects these two parameters, soil-soil energy component is correspondingly affected by soil moisture content.

Soil-soil interaction energy is assumed as not affected by change in depth of operation because of three reasons. First, undisturbed soil body adjacent to the wedge of soil in front of the tool is not necessarily in contact with the tool. Therefore, it is not necessarily affected by the tool depth. For such a vertical narrow tool as employed in this research, a wedge of soil is the only soil in contact with the tool surface (Gill and Vanden Berg 1968; McKyes 1985). To clarify this point, it is noticeable that when a vertical tool having a plane surface moves within a moist soil as the soil in current experiments, soil particles are compressed to each other by the tool, and they do not slide on each other. From time to time, a block of compacted soil slides up on the tool surface at its interface with the tool, and after passing edges of tool surface, it is left both sides of the tool or returned into the tool furrow. Therefore, no sensible movement between soil particles is manifested in such tool and soil conditions, and consequently no extra soil-soil energy is consumed as a result of an increased depth. Considering the concept of critical depth of soil for vertical narrow tools (Zelenin 1950; Kostritsyn 1956 and McKyes 1985), soil in front of the tool can be divided into two sections as above and below critical depth. Above the critical depth, soil at appreciable soil moisture content is compressed up to a certain point then sled on the tool surface upward and released. Therefore, this part of soil displacement is directly related to the soil-tool interaction energy (Godwin and Spoor 1977). Below the critical depth, the soil moves in horizontal and sideway directions and builds up a wall of compressed soil both sides of the moving tool. Therefore, it changes the force only on tool surface which is taken into

account as part of soil-tool interaction energy (Godwin and Spoor 1977), but has nothing related to the soil-soil interaction energy.

The second reason explaining that why soil-soil interaction energy is not affected by tool depth returns to the reality that two main forces are concerned with regard to the adjacent soil body to the wedge of soil in front of the tool. These two are frictional and gravitational forces. Frictional forces are accounted as cohesion and internal friction, and this is why soil-soil energy value changes at different moisture contents. On the other hand, in this energy model, Gravitational forces are taken into account as part of deformation energy, and this is why deformation energy component is affected by depth of operation, but soil-soil component is not.

The third reason comes from the effectiveness of the soil gravitational forces on total force. It should be noted that even if the surface area of the soil wedge is entered as part of the value of soil-soil energy, its value when is multiplied by cohesion value (based on Coulomb's equation) will contribute minor effect of total value of this energy component. In addition, since friction force between soil wedge and undisturbed adjacent soil body builds the main part of soil-soil energy, it is considerable that the friction force between these two soil bodies is neither affected by apparent contact area of the bodies nor by the normal force (Gill and Vanden Berg 1968). Since depth of operation represent contact area thus, soil-soil energy component is not affected by depth of operation.

Similar to soil-tool interaction energy, this energy component is also assumed not to change by tool forward speed. This is reasonable because soil-soil energy value was determined at a speed in which inertia effect was negligible. Soil-soil interaction was previously presented in Coulomb's law as Equation 2.4 although the equation was expressed in stress components. If written in force components, it would need the following terms to be measured.

Soil shear force includes two terms of soil cohesion and soil-soil friction force. To measure soil-soil friction force, applied force on soil rupture plane and angle of internal friction should be measured. A series of direct shear tests would provide cohesion values to be used in the equation. Measurement of normal force applied on the soil rupture plane needed knowing the shape and the features of the rupture plane, which

was practically impossible (Hettiaratchi 1993). Therefore, an indirect method was employed to calculate soil-soil interaction force and consequently soil-soil energy component for this model.

Considering the basic assumptions, for each level of moisture content, where operating depth and forward speed were very low (1 km h^{-1} speed and 40 mm depth), the only energies contributing in total energy of the tool were soil-tool and soil-soil interaction energies. Soil-tool interaction energy was measured based on Equation 4.1 as discussed above. To measure soil-soil interaction energy, the difference between total energy of the tool in each experiment, obtained from soil bin instrumentation, and the amount of soil-tool interaction energy was the amount of soil-soil interaction energy. Same values of soil-soil interaction energy were exactly accounted to the different levels of operating depth and forward speed, but not for different moisture contents. Soil-soil interaction energy was supposed to change only at different levels of moisture content, but maintained a constant value when the depth or speed was changed.

3.5.4 Soil Deformation Energy

When a tool moves within the soil, cut soil will be translocated by the moving tool. Deformation energy component is standing to show the energy consumed for this soil translocation. Based upon the soil conditions and tool features, translocated soil may be taken to the soil surface then released, piled up on undisturbed soil, turned down and manipulated, or thrown away from the tool moving line. In the current model, regardless of what would happen to the soil after cutting, deformation energy will present the energy which has been consumed to translocate the soil from its origin of the rest. The weight of the translocated soil is one important affecting factor on soil deformation energy. Also, this is the one major difference between soil deformation and soil-soil interaction energies. In this energy model, it is assumed that soil-soil interaction energy is not responsible for the weight of the translocated soil.

It is assumed that moisture content variations would change the value of this component. The reason is that any change in moisture would change cohesion and angle of internal friction which both affect the interlocking forces between particles. Consequently, it would affect the amount of soil that undergoes deformation and thereby

71

energy consumption. The value of deformation component is also affected by depth of operation since at deeper depths of operation tool engages more amount of soil ahead to be translocated and thus, demands more energy. In contrast, tool forward speed would not influence this energy component. Deformation energy component keeps a constant value at different forward speeds. The reason is the energy required to throw extra soil at higher speeds compared to lower speeds is assumed as part of soil acceleration energy in this model. It is also important to know that the first basic assumption of having zero deformation energy at operating depths up to 40 mm is valid only for the employed tool and its specifications in this research. It may not be valid for other tools configurations.

To measure soil deformation energy in this model, after measuring soil-tool and soil-soil interaction energies at lowest depth and speed levels, deformation energy was measured as following. When the depth of operation was increased, more energy would be required. Since at low speeds there was no acceleration energy involved yet, the difference between the total tool energy and the summation of soil-tool and soil-soil interaction energies gave the soil deformation energy value. When the depth of operation was increased again, soil deformation energy was accordingly increased. This energy component was achieved new values at different moisture contents and different depths, but not at different forward speeds. Therefore, same values of deformation energy were used at different levels of forward speed. For example, same values of deformation energy were applied to the first, second, third, and fourth levels of forward speed.

3.5.5 Soil Acceleration Energy

In the current model, the soil acceleration energy component is the only component responsible for any resistive energy consuming event manifested due to the increase in tool forward speed. Therefore, some effects that in other models may be entitled as part of soil-tool, soil-soil, or deformation energy components, in the current model are exclusively part of soil acceleration energy component.

Soil moisture content affects acceleration energy by changing soil compressibility level and the compressing energy required to press soil particles to each other before they can be released. The change in rate of soil shearing due to increased speed is also affected by soil moisture content. The effect of speed on soil cohesion,

adhesion, and friction angles is also affected by soil moisture content. Acceleration energy is also affected by tool operating depth, which determines whether the soil should come up to the ground surface, or be compressed in the direction of movement (based on the critical depth level). In this way, Depth of operation affects the energy requirement to accelerate the soil. Evidently, this component of energy is dominantly influenced by tool forward speed.

The basic assumption of having zero acceleration energy at low speeds up to 1 km h^{-1} provided an opportunity to calculate soil deformation energy at different operating depths. When tool forward speed was increased up to its second level, new acceleration effects became significant. However, at this level of speed, same deformation energy value was applied as for the first level of speed. Therefore, the value of soil acceleration energy was calculated as the difference between the total energy of the tool and the summation of soil-tool interaction, soil-soil interaction, and soil deformation energies. Acceleration energy component was changed with changing moisture content, depth of operation, and tool forward speed.

As a summary of entire energy model, the following equation shows the relationship between the total energy requirement of the tool and the four main components of tillage energy. In addition, the equation summarizes the affecting parameters of each energy component.

Total energy= Soil-Tool Interactions Energy (= f (moisture content, depth)) +

                Soil-Soil Interactions Energy (= f (moisture content)) +

                Soil Deformation Energy (= f (moisture content, depth)) +

                Soil acceleration Energy (= f (moisture content, depth, speed))

4.0   RESULTS AND DISCUSSION

In this chapter, experimental determinations of energy components along with an example of data set up in the model are described in the first section. Estimating missing data, draft-depth and draft-speed relationships are discussed in the next three sections of this chapter. Energy components versus depth and discussion on this relationship based on experimental results are presented in sections 4.5 and 4.6. Energy components versus speed and implementing soil mechanics to justify this relationship are discussed in sections 4.7 and 4.8. Discussion on regression equations of different energy components of the current model through statistical analyses and validation of those equations are in section 4.9 of the chapter. Results of statistical analysis of experimental design and results and discussion on direct shear tests and cone index measurements are in sections 4.10 through 4.12.

4.1   Experimental Determination of Energy Components

In this section, the procedure employed to set up the four main energy components in the proposed energy model is discussed. Energy data in Table 4.1 represent the soil bin experimental data at an average moisture content of 14% and different depths and tool speeds. The values of each energy component are portions of total energy, and the summation of those four components is equal to the total energy requirement of the tool for each particular treatment. The following discussion explains the details of data set up in the energy model based on the experimental data presented in Table 4.1.

Table 4.1 Data set up of energy components in the energy model at 14% moisture content

1	2	3	4	5	6	7	8
Depth (mm)	Speed (km/h)	Tool Area (m^2)	Total Energy (J)	Soil-tool Energy (J)	Soil-soil Energy (J)	Deformation Energy (J)	Acceleration Energy (J)
40	1	0.0016	44.90	30.93	13.97	0.00	0.00
80	1	0.0032	345.80	225.45	13.97	106.38	0.00
120	1	0.0048	774.40	501.56	13.97	258.87	0.00
160	1	0.0064	923.70	599.20	13.97	310.53	0.00
40	8	0.0016	136.22	30.93	13.97	0.00	91.32
80	8	0.0032	416.99	225.45	13.97	106.38	71.20
120	8	0.0048	850.32	501.56	13.97	258.87	75.92
160	8	0.0064	1509.70	599.20	13.97	310.53	586.00
40	16	0.0016	300.30	30.93	13.97	0.00	255.36
80	16	0.0032	830.90	225.45	13.97	106.38	485.10
120	16	0.0048	1329.80	501.56	13.97	258.87	555.44
160	16	0.0064	2346.70	599.20	13.97	310.53	1423.00
40	24	0.0016	1184.80	30.93	13.97	0.00	1139.92
80	24	0.0032	2107.90	225.45	13.97	106.38	1762.10
120	24	0.0048	2419.90	501.56	13.97	258.87	1645.54
160	24	0.0064	3083.70	599.20	13.97	310.53	2160.00

Since draft times one meter of distance gives the energy value, this energy value for each treatment has the same numerical value as the corresponding draft requirement of the tool for that treatment. Soil-tool energy in column five has been calculated based on Coulomb's law at 1 km h^{-1} speed. Same values of soil-tool energy have been repeated for higher speeds of operation. Column six presents a single value for soil-soil energy

and it has been calculated in the very first top row of the table in absence of deformation and acceleration energies as the difference between the total energy and soil-tool energy value. Since moisture content has not changed, same value of soil-soil energy has been repeated for the rest of the table.

Column seven shows values of deformation energy. In the first row, its value is zero because of the assumption of having negligible deformation energy at 40 mm depth. Therefore, it can be seen that this zero value for deformation energy has been repeated at several other places in Table 4.1 in which depth is 40 mm. At 80 mm depth, deformation energy has been calculated as the difference between the total energy and the summation of soil-tool and soil-soil energies. Its values have been calculated in the absence of acceleration energy (at 1 km h^{-1} speed), and have been exactly repeated at higher speeds.

In column eight, values of acceleration energy are presented. Its value at 1 km h^{-1} is zero as acceleration energy at this speed is negligible. At 40 mm depth and 8 km h^{-1} speed, all other energy components have already been determined. The only undetermined energy component at this stage is acceleration energy component. Therefore, the difference between the total energy requirement and the summation of soil-tool, soil-soil, and deformation energies will give the amount of acceleration energy. This is the only energy component in this model whose value is always changing. As shown in Table 4.1, acceleration energy value changes with depth and speed; and even at 20% moisture content, acceleration energy resulted in different values, so it is also affected by moisture content.

4.1.1 An Example of Energy Components Determination

The following example explains how the energy components were calculated. In the first row of data, total energy is equal to 44.90 J. This is numerically equal to the draft requirement of the tool at 14% moisture content, 40 mm depth, and 1 km h^{-1} speed. This value was obtained through soil bin experiments. When multiplied by 1 meter of cultivated soil, the same value of energy requirement is calculated. Since the model assumes only soil-tool and soil-soil interaction energies to be applicable at this depth and speed, the total energy is divided between these two components as following:

Soil-tool energy=

$$(C_a A_{tool}) + (draft \times \tan \delta) = (1400 \times 0.0016) + (44.90 \times 0.639) = 30.93J \quad (4.1)$$

where:

C_a = 1400 Pa

A_{tool} = (tool width $\times$ tool depth) = (0.04m $\times$ 0.04m) = 0.0016 m^2

Draft = 44.90 N

$\delta = 32.6^\circ$

Soil-soil energy = total energy – soil-tool energy = 44.90-30.93=13.97 J   (4.2)

In the second row of Table 4.1, a new component as deformation energy appears since the depth of operation is increased. Total energy is 345.80 which will be divided into three components as follows: (1) soil-tool energy is again calculated based on Equation 3.1. (2) Soil-soil energy keeps same value as 13.97 J. (3) Soil deformation energy is calculated as below:

Soil deformation energy = Total energy – (soil-tool energy + soil-soil energy)

$$= 345.80 - (225.45 + 13.97) = 106.38 \text{ J} \quad (4.3)$$

In the fifth row of Table 4.1, soil acceleration energy appears as the speed of tool increases to 8 km h^{-1}. Total energy shown for this row is 136.22 J. From this total energy, 28.69 J goes for soil-tool interaction energy as was calculated in Equation 4.1. Since depth and moisture are the same as the first row of the table, this energy component keeps a similar value. Soil-soil interaction energy also keeps a same value of 13.97 J as the moisture content has not changed yet. Soil deformation energy is zero at 40 mm depth based upon the first assumption of this energy model. The last component in this row is soil acceleration energy which was calculated as:

Soil acceleration energy = Total energy – (soil-tool energy + soil-soil energy +

soil deformation energy)

$$= 136.22 - (30.93 + 13.97 + 0) = 91.32 \text{ J} \qquad (4.4)$$

The same method was employed to determine the values of energy components for other treatments as their values are shown in Table 4.1.

4.2   Estimating Missing Data

As mentioned in Chapter 3, draft measurement of 4 soil bin tests were not completed due to the lack of power requirement. Therefore, draft requirements for those data points were later estimated based on the draft values of the other treatments. To estimate those missing data, two approaches were tried. In the first approach, named as depth approach, draft data versus corresponding depths of operation at 24 km h^{-1} speed for each moisture level were separately plotted (Figure 4.1).
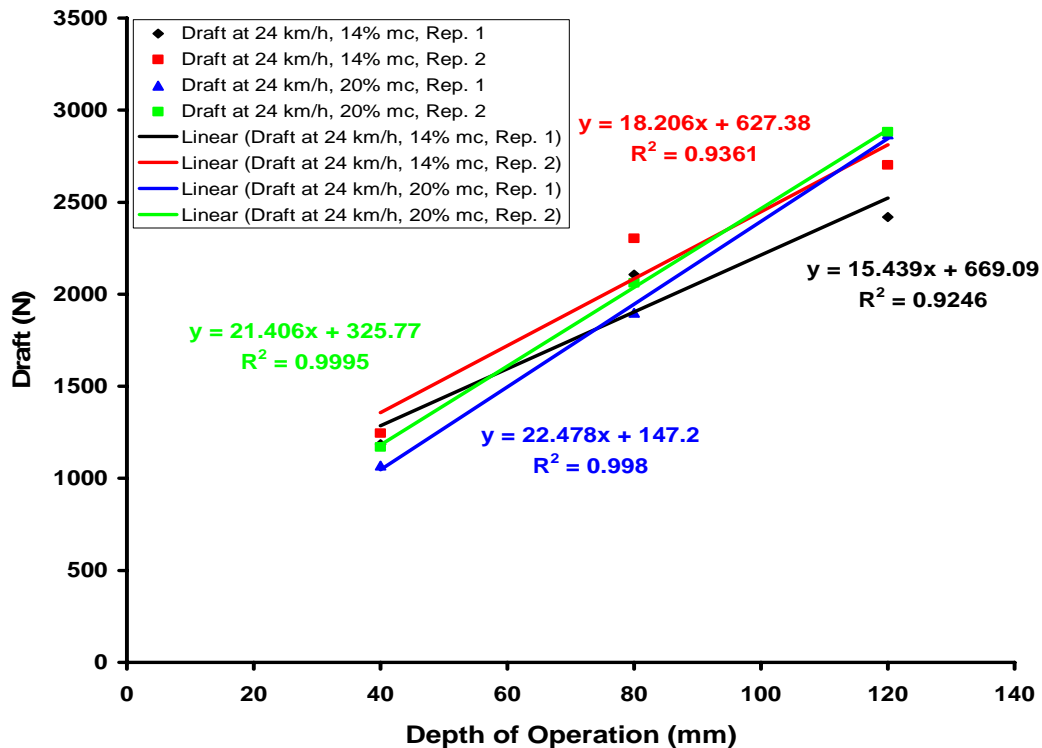
Figure 4.1 Prediction of draft missing data by extrapolating draft-depth relationship at 24 km h^{-1} speed

Equations of the best fit lines to these data were used to estimate the missing draft data.

In the second approach, named as speed approach, draft data versus their corresponding speed at 160 mm depth were separately plotted for each level of moisture content as presented in Figure 4.2. Although both approaches gave very close estimation of missing data to each other, the second approach (speed approach) was employed because this approach generally showed a higher R^2 for the relationship between the corresponding data points. Equations of the best fit lines to these data, which were linear, were used to estimate the values of the missing data. Figure 4.2 shows the resultant equations used to estimate each value based on the extrapolation method.
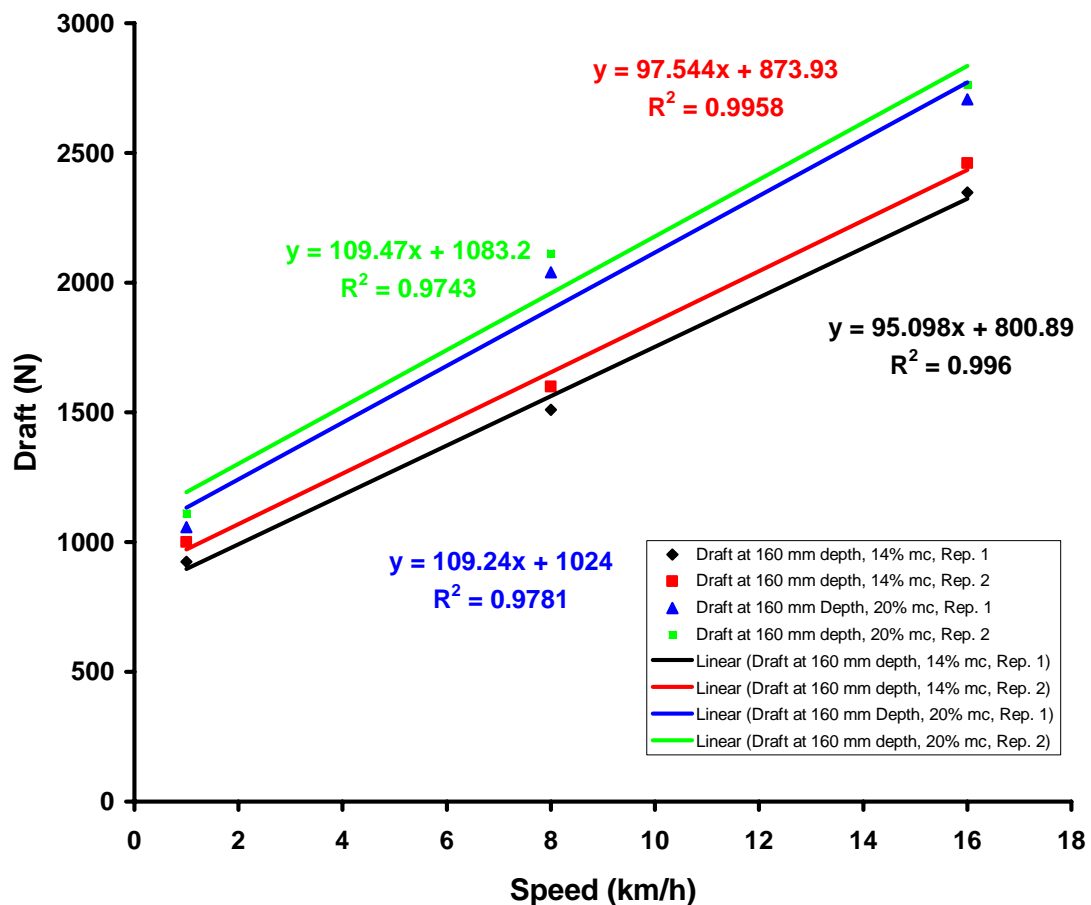
Figure 4.2 Prediction of draft missing data by extrapolating draft-speed relationship at 160 mm depth

In Table 4.2, In the column of treatment, M_{14}, D_{16} and S_{24} represent moisture content in percentage dry basis, depth in mm, and speed in km h^{-1} respectively.

Table 4.2 Estimating equations of missing values of draft

Treatment (replicate)	Estimated Value (N)	Linear Equation	R^2
$M_{14}D_{16}S_{24}(1)$	3083.70	D=95.098S+800.89	0.996
$M_{14}D_{16}S_{24}(2)$	3215.50	D=97.554S+873.93	0.995
$M_{20}D_{16}S_{24}(1)$	3605.30	D=109.24S+1024	0.978
$M_{20}D_{16}S_{24}(2)$	3710.48	D=109.47S+1083.2	0.974

D: Draft in Newton   S: Speed in km/h

To validate the extrapolation method and corresponding estimated values, experimental draft values of same tool and soil conditions at 160 mm depth and speeds between 16 and 24 km h^{-1} were applied to the predicting equations in Table 4.2. The closeness between the estimated and experimental draft data assured the predictability of the equations. Table 4.3 shows the experimental data and their corresponding estimated data calculated based on the equations in Table 4.2.

Table 4.3 Validation of draft predicting equations

Treatment	Speed (km h^{-1})	Experimental Draft (N)	Estimated Draft (N)	Error (%)
$M_{14}D_{16}S_{18}$	18	2774.9	2634.8	5.0
$M_{14}D_{16}S_{21}$	21	3141.5	2927.4	6.8
$M_{20}D_{16}S_{18}$	18	2990.3	2737.7	9.2

As shown in Table 4.3, draft predicting equations are able to closely give an estimation of tool draft for the extrapolated span of data.

4.3   Draft – Depth Relationship

To determine the relationship between draft and operating depth for the existing tool, the values of draft and depth at each level of speed were plotted against each other. Logarithms of both draft and corresponding depth have been used to plot the values. Table 4.4 presents a power relationship in the resultant equations at 14% moisture content. Similar equations for logarithmic draft-depth relationship at different forward speeds and 20% moisture content have been derived as shown in Table 4.5.

Table 4.4 Predicting equations of draft – depth relationship at %14 moisture content and valid between 40 and 160 mm depths

Speed (km h^{-1})	Replicate	Draft-Depth Relationship at 14% Moisture Content	R^2
1	1	$D=0.013d^{2.2584}$	0.9598
1	2	$D=0.0121d^{2.2826}$	0.9663
8	1	$D=0.2306d^{1.722}$	0.9981
8	2	$D=0.1806d^{1.7819}$	0.9962
16	1	$D=1.4461d^{1.4445}$	0.9944
16	2	$D=1.8484d^{1.4036}$	0.9946
24	1	$D=103.72d^{0.6685}$	0.9793
24	2	$D=107.27d^{0.6773}$	0.9735

D: Draft in Newton   d: Depth in mm

As it can be seen, predicting equations of draft-depth relationship at both 14% and 20% moisture contents show good correlation between draft and depth of operation for the tool. Values of R^2 are very close to 1 which indicates data points are fairly well fitted to their corresponding equations. Evidently, same relationships between total energy requirement and operating depths can be drawn for the current tool.

Glancey et al. (1996) measured draft of different tillage tools at different soil, tool and operational conditions. They reported that log-log relationship best described draft-depth relationship at any given depth for the chisel plow, mouldboard plow and subsoiler compared to linear and semi-log relationships.

Table 4.5 Predicting equations of draft – depth relationship at 20% moisture content and valid between 40 and 160 mm depths

Speed (km h^{-1})	Replicate	Draft-Depth Relationship at 20% Moisture Content	R^2
1	1	$D=0.443d^{1.5675}$	0.9691
1	2	$D=0.4084d^{1.596}$	0.9686
8	1	$D=3.7253d^{1.2274}$	0.9900
8	2	$D=4.3934d^{1.2022}$	0.9860
16	1	$D=20.365d^{0.9395}$	0.9436
16	2	$D=29.884d^{0.866}$	0.9125
24	1	$D=40.25d^{0.8863}$	0.9982
24	2	$D=54.648d^{0.8296}$	0.9998

D: Draft in Newton   d: Depth in mm

4.4   Draft - Speed Relationship

Another important relationship is between speed and draft of the tool at different depths of operation. As in the previous case, logarithms of both values have been used. Table 4.6 presents this relationship at 14% moisture content of soil. For 20% moisture content, draft–speed relationship at different depths of operation has been shown in Table 4.7.

Table 4.6 Predicting equations of draft – speed relationship at 14% moisture content and valid between 8 and 24 km h^{-1} speeds

Depth (km h^{-1})	Replicate	Draft-Speed Relationship at 14% Moisture Content	R^2
40	1	$D=2.3808S^{1.8797}$	0.9103
40	2	$D=2.1143S^{1.9446}$	0.9387
80	1	$D=19.955S^{1.4232}$	0.9454
80	2	$D=15.473S^{1.5258}$	0.9401
120	1	$D=119.53S^{0.9189}$	0.9465
120	2	$D=121.17S^{0.9468}$	0.9402
160	1	$D=390.95S^{0.6486}$	0.9998
160	2	$D=426.74S^{0.6342}$	0.9997

D: Draft in Newton   S: Speed in km/h

Table 4.7 Predicting equations of draft – speed relationship at 20% moisture content and valid between 8 and 24 km h^{-1} speeds

Depth (km h^{-1})	Replicate	Draft-Speed Relationship at 20% Moisture Content	R^2
40	1	$D=46.599S^{0.9861}$	1.000
40	2	$D=49.859S^{0.9986}$	0.9980
80	1	$D=129.94S^{0.8115}$	0.9085
80	2	$D=118.83S^{0.8605}$	0.8943
120	1	$D=274.49S^{0.7137}$	0.9304
120	2	$D=329.5S^{0.6599}$	0.9313
160	1	$D=698.07S^{0.5067}$	0.9764
160	2	$D=733.13S^{0.499}$	0.9688

D: Draft in Newton   S: Speed in km/h

Equations in Table 4.6 and Table 4.7 show power relationships between the draft and speed for the current tool at both levels of moisture content. Closeness of the R^2 values to 1 indicates good fitness of the equations to their corresponding data. Since for

the current tool, draft and energy requirements are numerically equal to each other, same relationships between total energy and forward speed of tool are applicable.

4.5　Energy Components versus Depth

In the previous section, the trend of total draft and energy requirements of the tool with depth were discussed. In this section, trends of different components of total energy with depth are discussed.

The trend of change in energy components due to the change in depth of operation at each level of forward speed and for both levels of moisture content are discussed in this section. Two different approaches have been used to have a better presentation of this relationship. In the first approach (absolute approach), actual values of the energy components have been used. In the second approach (relative approach), instead of actual values, the values of the energy components as percentages of the total energy requirement of the tool have been plotted versus different depths of operation.

4.5.1　Energy-Depth Relationship at 14 Percent Moisture Content (Absolute Approach)

When the actual values of energy components at 14% moisture content and different forward speeds are compared to each other, the following trends as shown in Figure 4.3 are presented.

1.　Absolute value of soil-tool energy increases as depth of operation increases, but the rate of this increase is same at different forward speeds.

2.　Soil-soil energy keeps a constant value at different depths and forward speeds.

3.　Deformation energy increases with increasing depth, but its increase is same for different forward speeds.

4.　Acceleration energy shows two different trends as follows. First, at 8 km h^{-1} speed, it decreases from 40 to 80 mm depth then increases at 120 and 160 mm depth. Second, at 16 and 24 km h^{-1} speed, acceleration energy has an increasing trend with depth with only one exception, a decrease at 120 mm depth and 24 km h^{-1} speed. It is possible that this happened as a result of passing a critical depth.
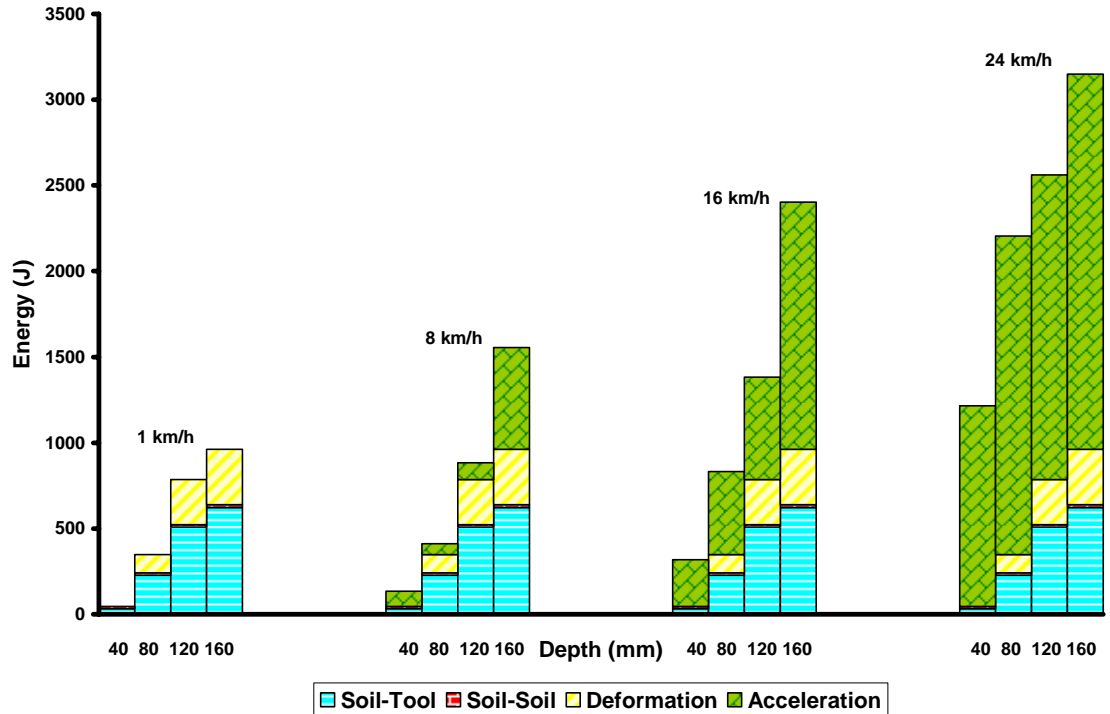
Figure 4.3 Energy-depth relationship at 14% moisture content and different forward speeds (absolute values)

Therefore, it was possible that soil acceleration energy was higher at 80 mm depth where the tool was working above the critical depth, and it decreased at 120 mm depth where the tool was working below the critical depth, but trend in general is increasing.

4.5.2 Energy-depth Relationship at 14 Percent Moisture Content (Relative Approach)

As shown in Figure 4.4, the following trends of energy components with depth can be seen.

1. At 1 km h^{-1} speed and different depths of operation, soil-tool interaction component has the highest percentage among the other components with almost a constant value of 68.8% of the total energy requirement.

2. At 8 km h^{-1} speed, soil-tool interaction still has the highest percentage except for the depth of 40 mm.

3. Soil-tool interaction energy has an increasing trend with increasing depth up to 120 mm depth then decreases at 160 mm depth.

4. Soil-soil interaction energy has a decreasing trend as the depth of operation increases for all operating speeds with a maximum value of 31.19% at 1 km h^{-1} speed and 40 mm depth and a minimum value of 0.45% at 24 km h^{-1} speed and 160 mm depth.

5. Deformation energy has an increasing trend as depth increases up to 120 mm depth and then decreases, or stays almost constant at 160 mm depth for the speeds of 1 and 24 km h^{-1}. It has a maximum value of 33.68% of the total energy at 1 km h^{-1} speed and 160 mm depth and a minimum value of 4.86% at 24 km h^{-1} speed and 80 mm depth.
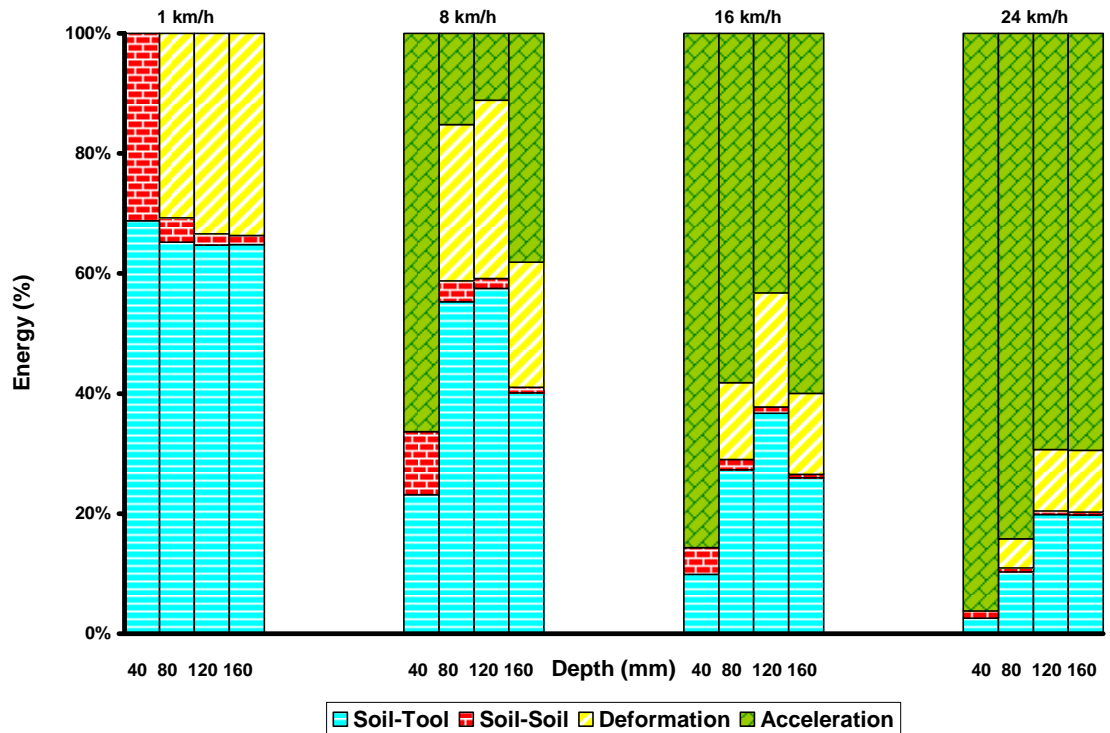
Figure 4.4 Energy-depth relationship at 14% moisture content and different forward speeds (relative values)

6. Acceleration energy has a decreasing trend up to 120 mm depth as the depth increases then it increases at 160 mm depth. Yet, its value at 160 mm depth is less than that of 40 mm depth for all the forward speeds. It reaches a maximum value of 96.24% at 24 km h^{-1} and 40 mm depth and a minimum value of 11.17% at 8 km h^{-1} speed and 120 mm depth.

4.5.3 Energy-Depth Relationship at 20 Percent Moisture Content (Absolute Approach)

In this section, absolute values of energy components against depths of operations at 20% moisture content and different forward speeds are presented. Figure 4.5 shows the following trends:

1. Soil-tool energy has an increasing trend with depth of operation, but this trend stays same at different forward speeds;

2. Soil-soil energy at this level of moisture content keeps a constant value at different depths of operation;

3. Deformation energy has an increasing trend with depth, but this trend is same for different forward speeds; and

4. Acceleration energy has an increasing trend as the depth of operation increases with only one exception at 80 mm depth and 16 km h^{-1} speed.
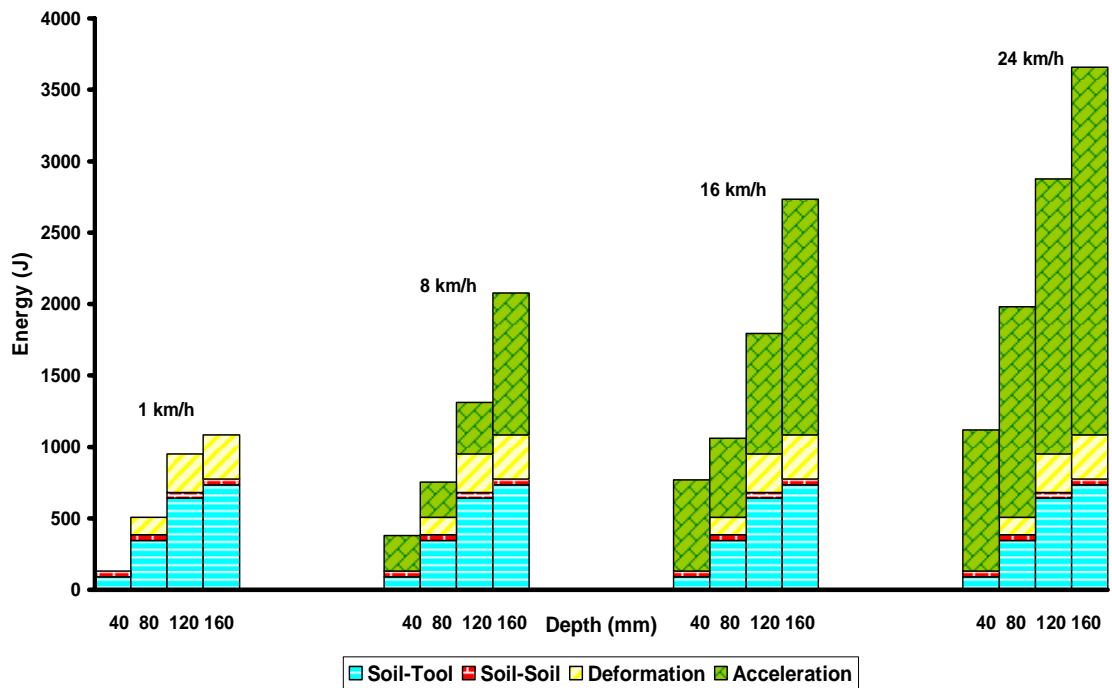
Figure 4.5 Energy-depth relationship at 20% moisture content and different forward speeds (absolute values)

4.5.4 Energy-Depth Relationship at 20 Percent Moisture Content (Relative Approach)

As shown in Figure 4.6, the following trends of energy components with depth can be seen.

1. Soil-tool energy component increases as depth of operation increases up to 120 mm depth then it decreases at 160 mm depth. The trend is consistent with all forward speeds except for 1 km h^{-1} in which soil-tool energy keeps almost a constant value at different depths of operation including 160 mm. This energy component reaches its
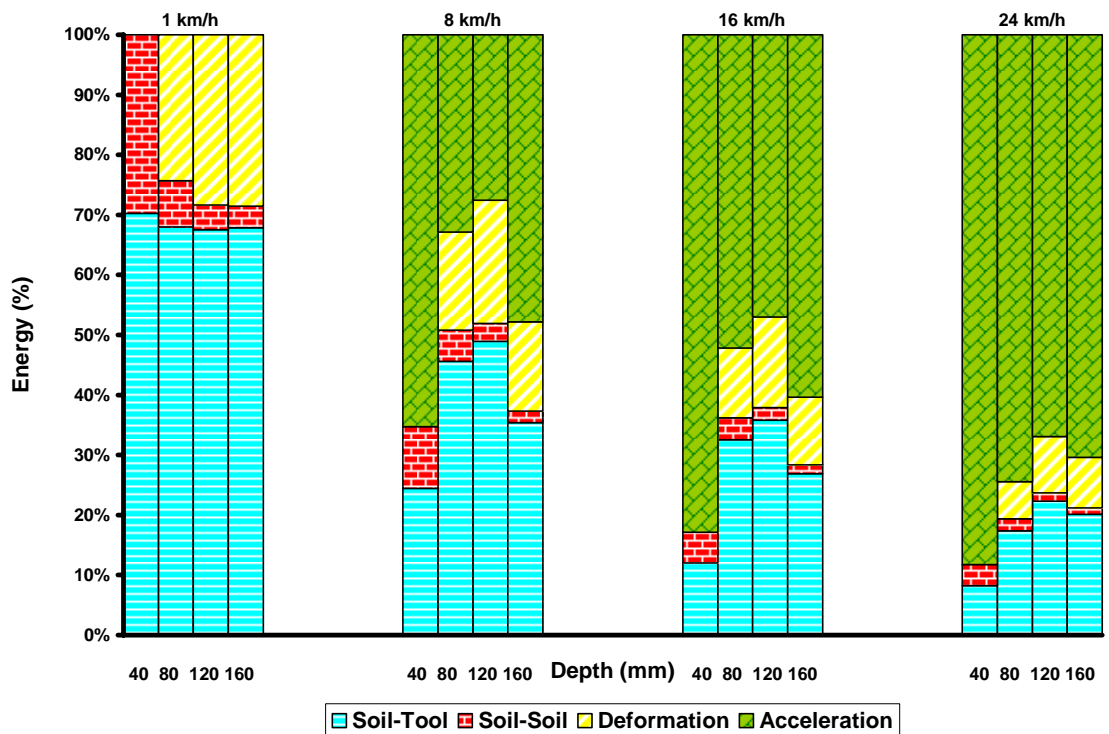
Figure 4.6 Energy-depth relationship at 20% moisture content and different forward speeds (relative values)

maximum value of 70.24% at 1 km h^{-1} and 40 mm depth and has a minimum value of 8.24% at 24 km h^{-1} and 40 mm depth.

2. Soil-soil energy has a decreasing trend as operating depth increases. The trend is consistent with all speeds without any exception. The maximum value of 29.77% for soil-soil energy is achieved at 1 km h^{-1} and 40 mm depth where the minimum value of 1.07% for it occurs at 24 km h^{-1} and 160 mm depth.

3. Deformation energy has an increasing trend up to 120 mm depth then its value decreases at 160 mm depth of operation. This trend is valid for all speeds except for 1 km h^{-1} in which deformation energy increases even at 160 mm depth which can be a result of the absence of soil acceleration energy component at this speed. The component shows a maximum value of 28.55% at 1 km h^{-1} and 160 mm depth and a minimum value of 6.22% at 24 km h^{-1} and 80 mm depth.

4. Acceleration energy has a decreasing trend up to 120 mm depth as depth increases then it increases at 160 mm depth. This trend is valid for all operating depths. The component reaches a maximum value of 88.27% at 24 km h^{-1} and 40 mm depth where its minimum value of 27.56% is achieved at 8 km h^{-1} and 120 mm depth.

4.6 Discussion on Results of Energy-Depth Relationship

As explained earlier in the model development section, two basic assumptions including having negligible deformation energy at depths up to 40 mm and negligible acceleration energy at speeds up to 1 km h^{-1} have been made for development of this energy model. Considering these assumptions, minor inclinations from the major trends of each energy component of the model, discussed in section 4.5, should be ignored particularly inclinations occurred at 40 mm depth and 1 km h^{-1} speed as these are facilitating assumptions and may be not perfectly precise.

Soil-soil energy which results from interaction between soil particles during soil movement is a function of only soil moisture content. Consequently, at 20% moisture content, its actual value (Figure 4.5) shows a higher value when compared to 14% moisture content. On the other hand, as a percentage of total energy (Figure 4.6), soil-soil energy value continuously drops at higher depths. This shows that soil-soil energy comparatively has the minimum effect on total energy among the other components. This feature makes its contribution as a percentage of total energy maximal in absence of other components at 40 mm depth and 1 km h^{-1} speed and makes its value minimal in presence of the other components at maximum depth and speed (160 mm depth and 24 km h^{-1} speed).

Soil-tool energy is calculated based on Coulomb's law which was explained in details in model development section (3.5.2). In Figure 4.4 and Figure 4.6, relative values of soil-tool energy at 1 km h^{-1} speed do not follow its existing trend for the other speeds. A combination of some inclinations from major trends of the model due to those basic assumptions, and the possibility of an overestimation of this energy component by the Coulomb's low can justify this kind of fluctuations of the component from the major trend of the model.

Soil-tool energy based on its previous definition is a function of soil-tool adhesion, surface area of tool engaged with soil, and soil-tool friction angle. Therefore, it has to change with moisture which affects soil adhesion and friction angle as well as with depth which increases the surface area of tool engaged with the soil. As it can be seen, none of these factors are affected by tool forward speed as the calculations corresponding to this energy component were carried out in a static situation. Therefore, soil-tool energy stays constant at different speeds. Comparing two levels of moisture content shows that soil-tool energy reaches higher values at 20% moisture content. It can be explained that at higher moisture contents, soil compressibility level increases. Hillel (1982) expressed that as the soil wetness increases the moisture weakens the inter-particle bonds causing swelling and reducing internal friction that makes the soil more workable and compactable. Therefore, during tool movement, the tool has to compress more soil ahead before the soil can leave the line of movement. A more compressed soil at higher moisture content needs more energy to be cut and sled on the tool surface which in turn results in a higher value for soil-tool energy at 20% compared to 14% moisture content. For this reason, it seems that Coulomb's law gives a very close estimation of this energy component to the reality. A reduction of its contribution to total energy after 120 mm depth indicates that the effect of deformation energy overcomes this effect although its actual value continues to increase even after 120 mm depth.

At both levels of moisture content, actual values of deformation energy (Figure 4.3 and Figure 4.5) increase with depth, but as percentages of total energy (Figure 4.4 and Figure 4.6), they increase up to 120 mm depth then start a decreasing trend Considering the increasing effect of speed, it can be concluded that acceleration effect

overcomes deformation effect after 120 mm depth of operation. Same trend appears for soil-tool energy. Since it is a function of moisture content and operating depth, at both levels of moisture content, it increases with depth. Although its actual value continues increasing with depth, but as a percentage of total energy, its relative value drops after 120 mm depth. Similarly, this can be explained as the effect of deformation effect that overcomes soil-tool energy effect beyond 120 mm depth.

Deformation energy is a function of soil moisture content and depth of operation. Although its absolute value increases with depth, but as a percentage of total energy, its value drops beyond 120 mm depth. The reason is that the effect of acceleration energy at maximum depth of 160 mm overcomes deformation energy. In addition, absolute values of deformation energy increase as moisture content of soil is increased, but this relationship has a decreasing trend with depth of operation. For instance, if the average values of deformation energy at 20% and 14% moisture contents are compared to each other, there is 15% difference at 80 mm depth, about 1% difference at 120 mm depth, and almost no difference at 160 mm depth of operation. Perhaps the best reason to justify this trend is that with such a vertical tool, soil at the very bottom depth of operation is not coming up to the ground surface. In support the idea, literature shows (Kostritsyn 1956) such a soil used in this research is more likely to be compressed in the direction of the movement than coming up to the surface. Since deformation energy is not contributing for the energy increased due to the soil compression, its value trends to a constant at 160 mm depth regardless of soil moisture content. The energy component which is accountable for compressing soil within soil body in this energy model is soil-tool energy which is increased for operation at higher depths, with higher moisture content (20% moisture content) if speed effect is neglected. In contrast, at higher speeds, acceleration energy is accountable for any extra energy resulting from compressing soil ahead of the tool. This includes soil compressing energy at 8, 16 and 24 km h^{-1} speed.

4.7   Energy Components versus Speed

The trend of change in each energy component due to the change in tool forward speed at each level of operating depth and for both levels of moisture content is

discussed in this section. Similar to the energy-depth relationship, two different approaches have been used here to show this relationship. In the first approach (absolute approach), absolute values of energy components have been used. In the second approach (relative approach), energy components, as percentages of total energy requirement of the tool, have been plotted against different speed values.

4.7.1   Energy-Speed Relationship at 14 Percent Moisture Content (Absolute Approach)

Figure 4.7 shows a comparison between actual values of different energy components versus tool speed at different levels of depth for the current energy model. The trends are as follows:

1.   At each depth of operation, soil-soil, soil-tool, and deformation energies have constant values for all forward speeds. Although they are constant, yet, their magnitudes
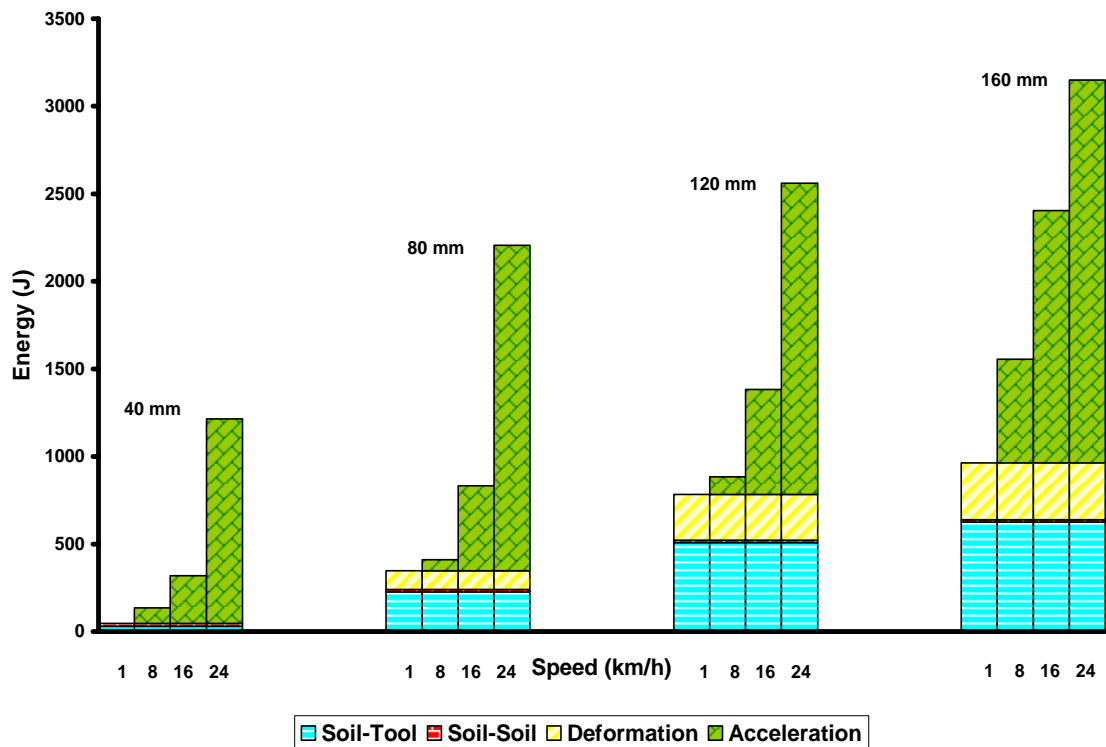
Figure 4.7 Energy-speed relationship at 14% moisture content and different operating depths (absolute values)

change at different depths in cases of soil-tool and deformation components and stay constant with depth in case of soil-soil component; and

2. Acceleration energy shows different values at same level of speed but at different depths of operation. This component resulted to a maximum value at 24 km h^{-1} speed and 160 mm depth and a minimum at 8 km h^{-1} speed and 80 mm depth.

4.7.2 Energy-speed Relationship at 14 Percent Moisture Content (Relative Approach)

As shown in Figure 4.8, the following trends of energy components with speed can be observed:

1. Soil- tool energy has a decreasing trend as forward speed increases at different depths of operation. It has a maximum value of 68.8% at 1 km h^{-1} speed and 40 mm depth and a minimum value of 2.6 % at 24 km h^{-1} speed and 40 mm depth.
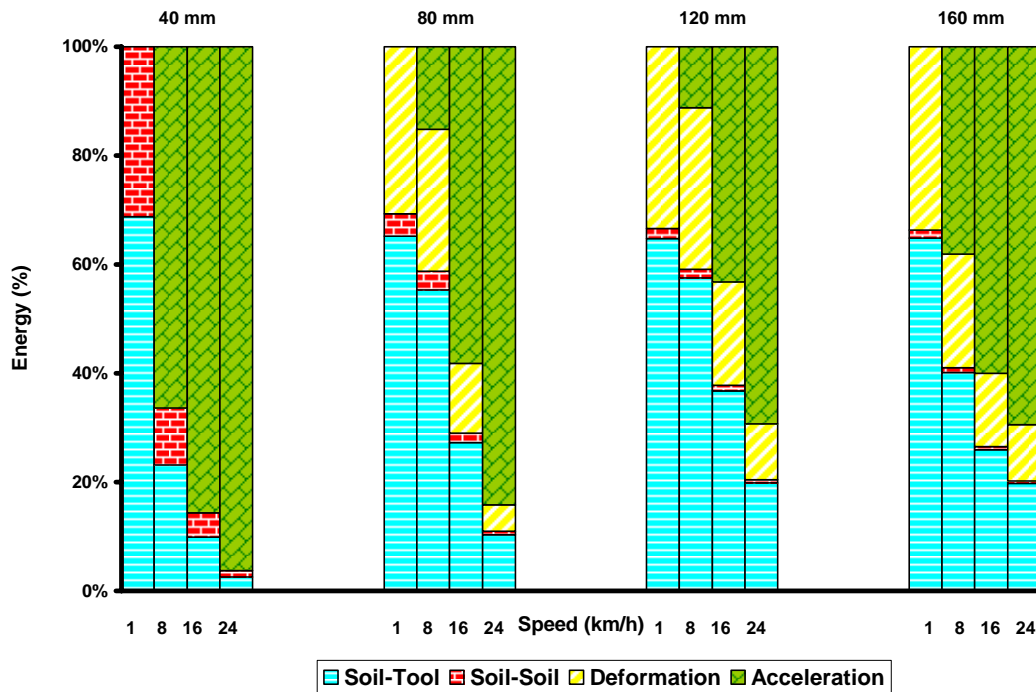
Figure 4.8 Energy-speed relationship at 14% moisture content and different operating depths (relative values)

2. Soil-soil energy has a decreasing trend as forward speed increased at different depths of operation. It reached a maximum of 31.19% at 1 km h^{-1} speed and 40 mm depth and a minimum of 0.45% at 24 km h^{-1} speed and at 160 mm depth.

3. Deformation energy has a decreasing trend as forward speed increased at different depths of operation. It achieved a maximum of 33.68% at 1 km h^{-1} speed and 160 mm depth and a minimum of 4.86% at 24 km h^{-1} speed and 80 mm depth.

4. Acceleration energy has an increasing trend with speed at different depths of operation. Maximum value achieved by this energy component reduced at 120 mm depth and then increased at 160 mm depth again. It has a maximum value of 96.24% at 24 km h^{-1} speed and 40 mm depth and a minimum value of 11.17% at 8 km h^{-1} speed and 120 mm depth.

4.7.3 Energy-Speed Relationship at 20 Percent Moisture Content (Absolute Approach)

Absolute values of energy components at 20% moisture content and different depths show the following trends presented (Figure 4.9).
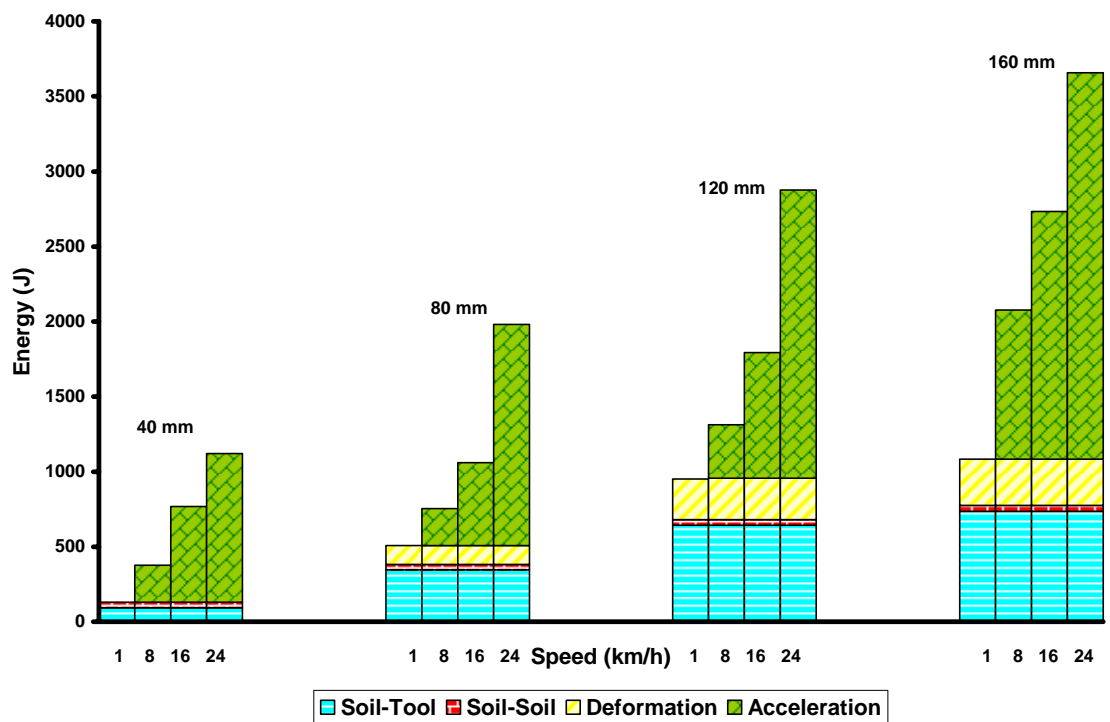
Figure 4.9 Energy-speed relationship at 20% moisture content and different operating depths (absolute values)

1. At each depth of operation, soil-soil, soil-tool, and deformation energies have constant values for all forward speeds. These constant values increased with depth in

cases of soil-tool and deformation components. For soil-soil energy, its value remained constant for all speeds and at different depths of operation.

2. Acceleration energy showed different values at each level of depth but different speeds of operation. This component achieved a maximum value at 24 km h^{-1} and 160 mm depth and a minimum value at 8 km h^{-1} and 40 mm depth.

4.7.4 Energy-Speed Relationship at 20 Percent Moisture Content (Relative Approach)

At 20% moisture content, different energy components are showing the following trends as shown in Figure 4.10.
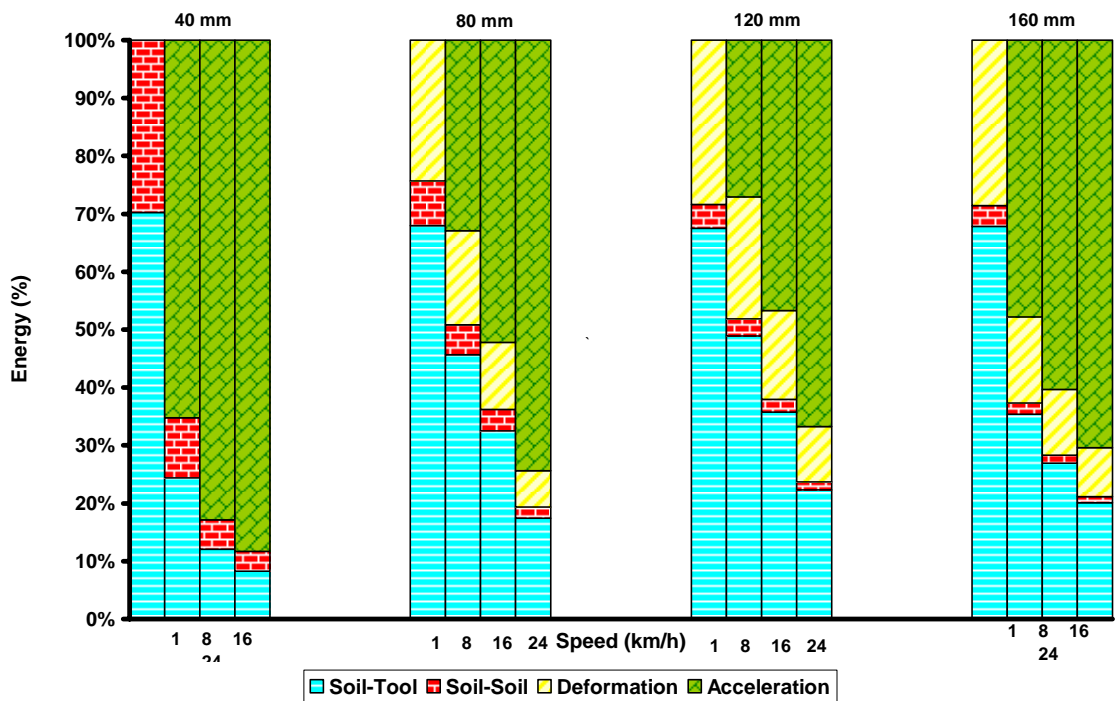
Figure 4.10 Energy-speed relationship at 20% moisture content and different operating depths (relative values)

1. Soil-tool has a continuous decreasing trend as forward speed increased for all different depths of operation. Maximum value of 70.24% occurred at 1 km h^{-1} speed and 40 mm depth whereas minimum of 8.24% occurred at 24 km h^{-1} speed and 40 mm depth.

2. Soil-soil energy has a decreasing trend as forward speed increased for all different depths of operation. It reached a maximum of 29.77% at 1 km h^{-1} speed and 40 mm depth and a minimum of 1.07% at 24 km h^{-1} speed and 160 mm depth.

3. Deformation energy showed a decreasing trend as forward speed increased for all different depths of operation. It had a maximum value of 28.55% at 1 km h^{-1} and 160 mm depth and a minimum of 6.22% at 24 km h^{-1} speed and 80 mm depth.

4. Acceleration energy had a dominantly increasing trend as forward speed increased for all different depths of operation. In spite of the fact, the maximum value achieved at each depth level decreased at higher depths up to 120 mm depth and then increased at 160 mm depth again. Maximum value of acceleration energy was 88.27% which occurred at 24 km h^{-1} speed and 40 mm depth and its minimum value was 27.08% at 8 km h^{-1} speed and 120 mm depth.

4.8   Discussion on Results of Energy-Speed Relationship

Data presented in Section 4.8 are the same data as presented in Section 4.6. The only difference between these two sections is that in the former section, data were arranged and viewed in an order of increasing depth at fixed speeds; where in the latter section, same data are arranged based on an increasing speed at fixed depths. By viewing data from this point of view, it was possible to see speed effect in the absence of depth effect; in other words, to see acceleration effect in absence of any new deformation effect. Therefore, part of discussion on energy-depth relationship is applicable and related to this section which is not repeated here again. In addition to different trends presented on the plots in Section 4.8, the following discussion is important as well.

At both 14% and 20% moisture contents, actual values of acceleration energy increased with increasing depth at each speed which indicated increasing inertial forces related to the new mass of soil. This new mass of soil is resulted when the tool goes deeper in the soil, and it can multiply the effect of depth at higher speeds. Although the weight of translocated soil is counted as part of soil deformation energy, any extra energy used to move this weight of soil at higher speeds would be part of acceleration

energy. On the other hand, acceleration energy increased with increasing speed at each depth. This effect can be interpreted as changing in shear force value due to the changing in shear rate in soils with appreciable amounts of clay content. Since soil used for current experiments had about 29% clay content, thus would be acceptable a change in soil shearing rate due to the change in tool speed.

Although the actual value of soil acceleration energy in energy-depth relationship plots (Figure 4.3 and Figure 4.5) increased with increasing depth, its contribution as percentage of total energy requirement (Figure 4.4 and Figure 4.6) is decreasing up to120 mm depth then starts rising after 120 mm depth. It shows that among both depth and speed effects on energy requirement, depth effect is predominant somehow up to 120 mm depth and then acceleration effect overcomes depth effect for current soil and tool conditions. Considering this point and the trends of other energy components indicated that 120 mm depth plays a key role in current experiments; it is a depth where the trend of most components generally change and can be noticed as a critical point.

4.9   Development of Regression Equations for the Energy Components

In this section, regression equations for the energy components are developed and discussed. Specific equations for the four main components of the model including soil-tool energy, soil-soil energy, soil deformation energy, and soil acceleration energy are developed separately. In development of each regression equation data of both replicates for that energy component have been used.

4.9.1   Regression Equation for Soil-tool Energy Component

In the current energy model, soil-tool energy component is a function of soil moisture content and tool operating depth. Therefore, values of soil-tool energy at both moisture levels and different operating depths were entered in a SAS analysis to develop a regression equation. The predictors and coefficients are presented in Table 4.8. Therefore, the general form of the equation to calculate soil-tool energy component, based upon the values in Table 4.8, would be as shown in Equation 4.5.

Table 4.8 Coefficients of regression equation for soil-tool energy

Predictor	Applicable Coefficient
Intercept	-463.72
Moisture Content (%)	10.57
Depth (mm)	7.87
Moisture * Depth (% * mm)	0.07
Depth ** 2 (mm)^2	-0.02

* Multiplication   ** Exponent

$$\text{Soil-tool energy (J)} = -463.72 + (10.57 * M.C.) + (7.87 * Depth) + \qquad (4.5)$$
$$(0.07 * M.C. * Depth) + (-0.02 * Depth ** 2)$$

When the values of soil-tool energy predicted by the above equation were compared with the experimental data, there was a very good fit of the data as illustrated in Figure 4.11. As shown in this figure, at each level of moisture content and operating depth, experimental values of both replicates have been compared to the values of soil-tool energy predicted by the regression equation.
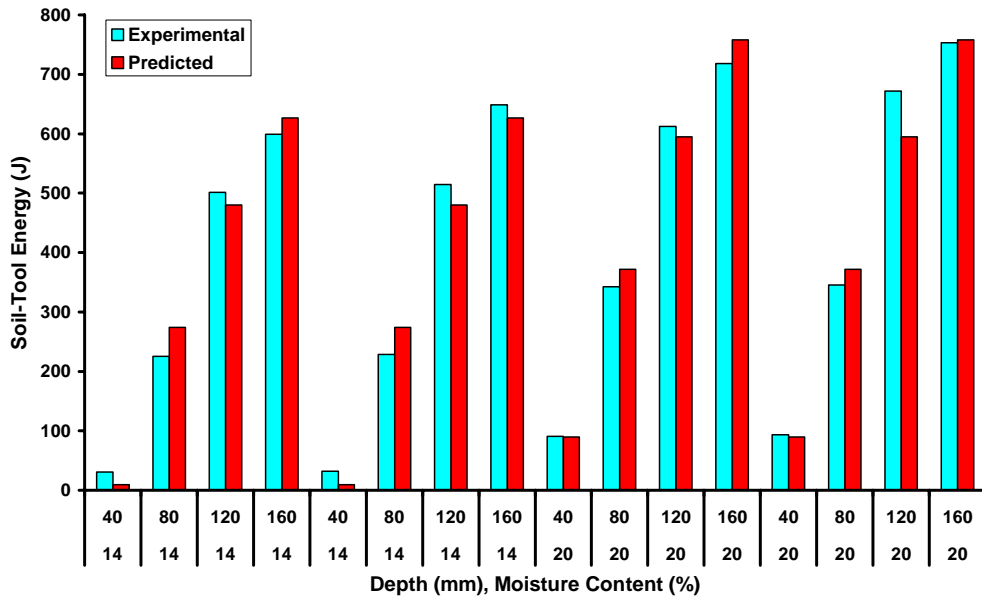
Figure 4.11 Comparison between experimental and predicted data of soil-tool interaction energy

4.9.2 Regression Equation for Soil-soil Energy Component

This component of energy is the function of a single variable of soil moisture content. Therefore, two values were obtained (one value per each level of moisture content) at each replicate. Table 4.9 shows the coefficients of regression equation built up based on soil-soil values at both replicates 1 and 2.

Table 4.9 Coefficients of regression equation for soil-soil energy

Predictor	Applicable Coefficient
Intercept	-43.58
Moisture Content (%)	4.13

The general form of the equation to calculate soil-soil energy component, based upon the values in Table 4.9, would be as shown in Equation 4.6.

$$\text{Soil-soil energy (J)} = -43.58 + (4.13 * M.C.) \tag{4.6}$$

By comparison the experimental values of soil-soil energy with the predicted values, resulted from the regression model, a very good fit of data was achieved as shown in Figure 4.12.

Table B.2 (Appendix B) shows the difference between the predicted and experimental data for soil-soil energy values in percentage. As well, the results of regression analysis for this energy component are presented in Table C.2 (Appendix C).
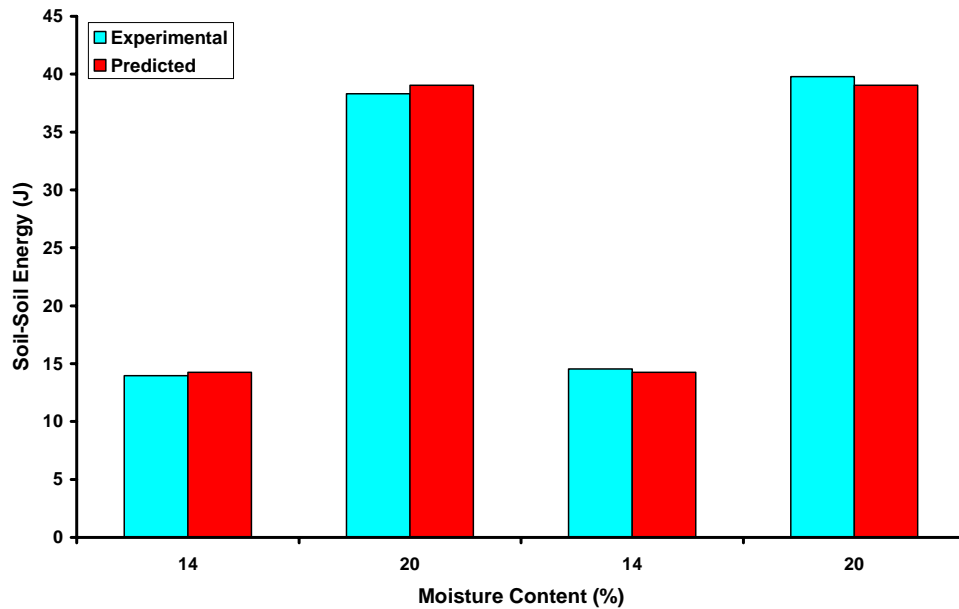
Figure 4.12 Comparison between experimental and predicted data of soil-soil interaction energy

4.9.3 Regression Equation for Soil Deformation Energy Component

Deformation energy was defined as a function of soil moisture content and tool operating depth. Therefore, to develop a regression equation, values of soil deformation component of replicates 1 and 2 were included in a SAS analysis. Since deformation energy at 40 mm depth was assumed to be zero in current model, this value was not included in the regression model. Table 4.10 shows the predictors and their corresponding coefficients for the equation.

Table 4.10 Coefficients of regression equation for deformation energy

Predictor	Applicable Coefficient
Intercept	-625.51
Moisture Content (%)	8.12
Depth (mm)	11.11
Moisture * Depth (% * mm)	-0.06
Depth ** 2 (mm)^2	-0.03

* Multiplication   ** Exponent

Therefore, the general form of the equation to calculate soil deformation energy component, based upon the values in Table 4.10, would be as shown in Equation 4.7.

Soil deformation energy (J) = -625.51 + (8.12 * M.C.) + (11.11 * Depth) +   (4.7)
(-0.06 * M.C. * Depth) + (-0.03 * Depth ** 2)

Deformation energy data were then fitted to the regression model. As shown in Figure 4.13, a good agreement between the predicted data and data of both replicates was achieved.
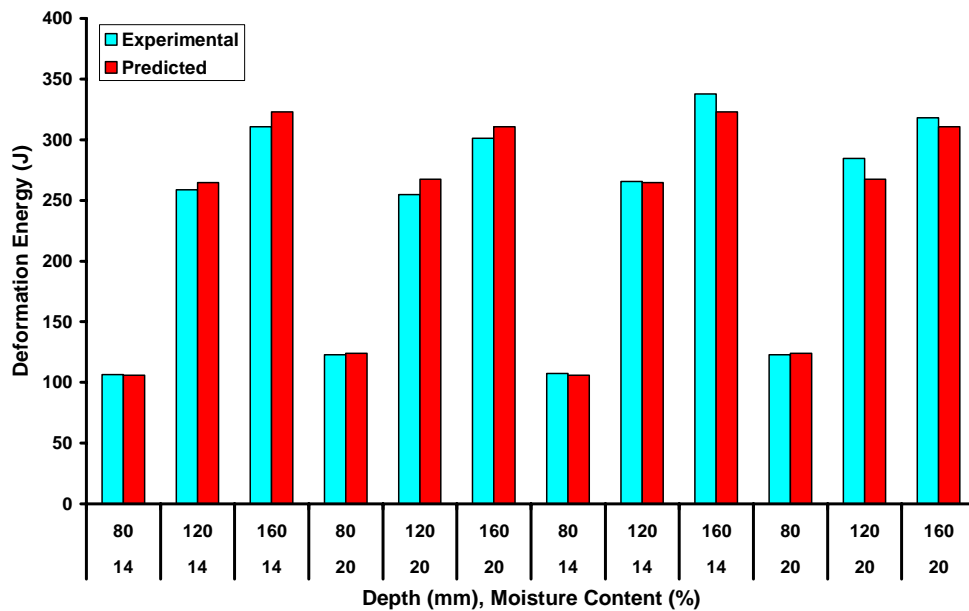
Figure 4.13 Comparison between experimental and predicted data of soil deformation energy

Table B.3 (Appendix B) presents the difference between the predicted and experimental data for deformation energy in percentage, and Table C.3 (Appendix C) shows the results of regression analysis in SAS for this energy component.

4.9.4   Regression Equation for Acceleration Energy Component - First Approach

Soil acceleration energy is a function of those three variables of soil moisture content, tool operating depth, and tool forward speed. It was found difficult to obtain a single equation to cover all variations of the three variables thoroughly. Therefore, different approaches were used to achieve better fit of data to the regression equation. In

the first approach, all soil acceleration energy values of both replicates 1 and 2 at different moisture contents, depths, and speeds were included in a SAS analysis to obtain a regression equation. Predictors indicated in the SAS analysis and the resultant coefficients are as presented in Table 4.11.

Table 4.11 Coefficients of regression equation for acceleration energy-all speeds

Predictor	Applicable Coefficient
Intercept	-928.51
Moisture Content (%)	90.12
Depth (mm)	-7.20
Speed (km h^{-1})	48.34
Moisture * Depth (% * mm)	-0.21
Moisture * Speed (% * km h^{-1})	-6.41
Depth * Speed (mm * km h^{-1})	-0.30
Moisture * Depth * Speed (% * mm * km h^{-1})	0.04
Depth ** 2 (mm)^2	0.07
Speed ** 2 (km h^{-1})^2	3.60

* Multiplication   ** Exponent

Since in this energy model, acceleration energy at 1 km h^{-1} speed was equal to zero, this value was not entered in the SAS analysis. This elimination included all acceleration energy values at different depths and moisture contents calculated at 1 km h^{-1} speed. The general form of the equation to calculate soil acceleration energy component, based upon the values in Table 4.11, would be as shown in Equation 4.8.

$$\text{Soil acceleration energy (J)} = -928.51 + (90.12 * M.C.) + (-7.20 * Depth) \quad (4.8)$$
$$+ (48.34 * Speed) + (-0.21 * M.C. * Depth) +$$
$$(-6.41 * M.C. * Speed) + (-0.30 * Depth * Speed)$$
$$+ (0.04 * M.C. * Depth * Speed) + (0.07 * Depth$$
$$** 2) + (3.60 * Speed ** 2)$$

When experimental values of acceleration energy were compared to the predicted values, resulted from the regression equation, a good fit of data for both replicates was obtained. To have a better presentation, the comparison has been shown in Figure 4.14 and Figure 4.15 for each level of moisture content separately.
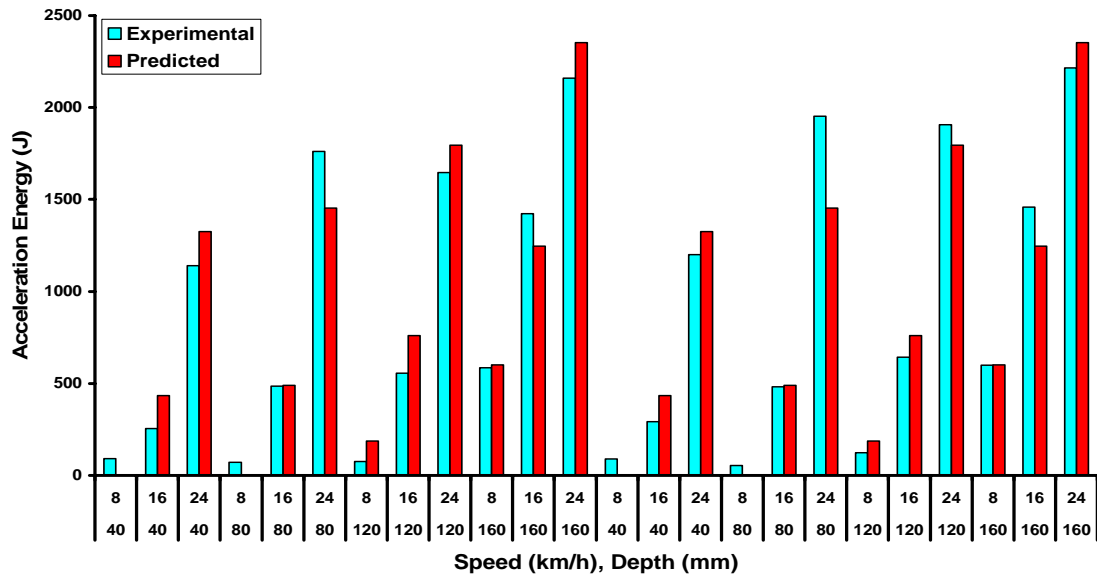
Figure 4.14 Comparison between experimental and predicted soil cceleration energy data at 14% moisture content (speeds of 8, 16, 24 km h^{-1})
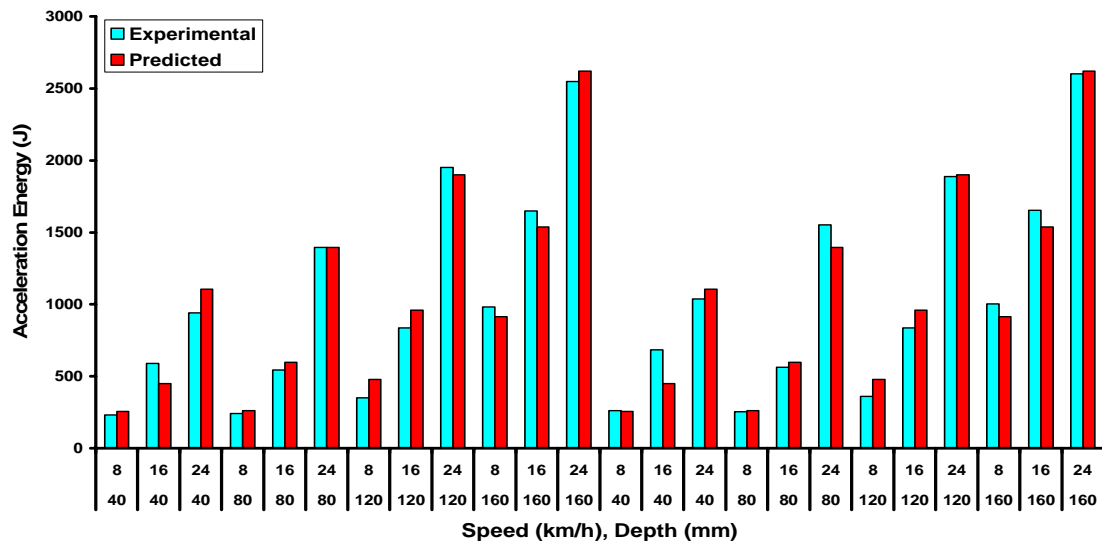
Figure 4.15 Comparison between experimental and predicted soil cceleration energy data at 20% moisture content (speeds of 8, 16, 24 km h^{-1})

The difference between the predicted and experimental values in percentage, are given in Table B.4 (Appendix B). Results of regression analysis are presented in Table C.4 (Appendix C) as well. In the current approach, although the equation has the advantage of covering all experimental data points, it is not completely satisfactory. The reason is that there is at least on negative predicted value and also a few predicted values have a large difference with their corresponding experimental values. Therefore, other approaches were tried to introduce a better fit of data.

4.9.5 Regression Equation for Acceleration Energy Component - 2nd Approach

In this second approach, instead of having one equation for entire acceleration energy values, it was decided to develop two separate regression analyses including one analysis for soil acceleration energy data at 16 and 24 km h^{-1} speeds and the other one for only energy data at 8 km h^{-1} speed. As mentioned before, acceleration energy at 1 km h^{-1} speed was equal to zero in this model, and it is not participated in this SAS analysis. When energy data of 16 and 24 km h^{-1} speeds were entered in the SAS analysis, the following coefficients for the presented predictors in Table 4.12 were resulted to build up the regression equation.

Table 4.12 Coefficients of regression equation for acceleration energy – speeds of 16 and 24 km h^{-1}

Predictor	Applicable Coefficient
Intercept	-1298.45
Moisture Content (%)	157.14
Moisture * Depth (% * mm)	-0.44
Moisture * Speed (% * km h^{-1})	-9.32
Depth * Speed (mm * km h^{-1})	-0.53
Moisture * Depth * Speed (% * mm * km h^{-1})	0.04
Depth ** 2 (mm)^2	0.06
Speed ** 2 (km h^{-1})^2	6.29

* Multiplication   ** Exponent

The general form of the equation to calculate soil acceleration energy component, based upon the values in Table 4.12, would be as shown in Equation 4.9.

Soil acceleration energy (J) = -1298.45 + (157.14 * M.C.) +   (4.9)

$$(-0.44 * M.C. * Depth) + (-9.32 * M.C. * Speed) +$$
$$(-0.53 * Depth * Speed) + (0.04 * M.C. * Depth *$$
$$Speed) + (0.06 * Depth ** 2) + (6.29 * Speed ** 2)$$

This regression equation was satisfactorily fitted to the experimental values of acceleration energy at 16 and 24 km h^{-1} speeds. The regression equation could give positive predicted values for the acceleration energy in a reasonable agreement with the experimental data. Figure 4.16 shows a comparison between the experimental and predicted data of both replicates for acceleration data values at 16 and 24 km h^{-1} speeds.

The difference between the predicted values for acceleration energy and experimental values in percentage is given in Table B.5 (Appendix B), and results of regression analysis in Table C.5 (Appendix C).
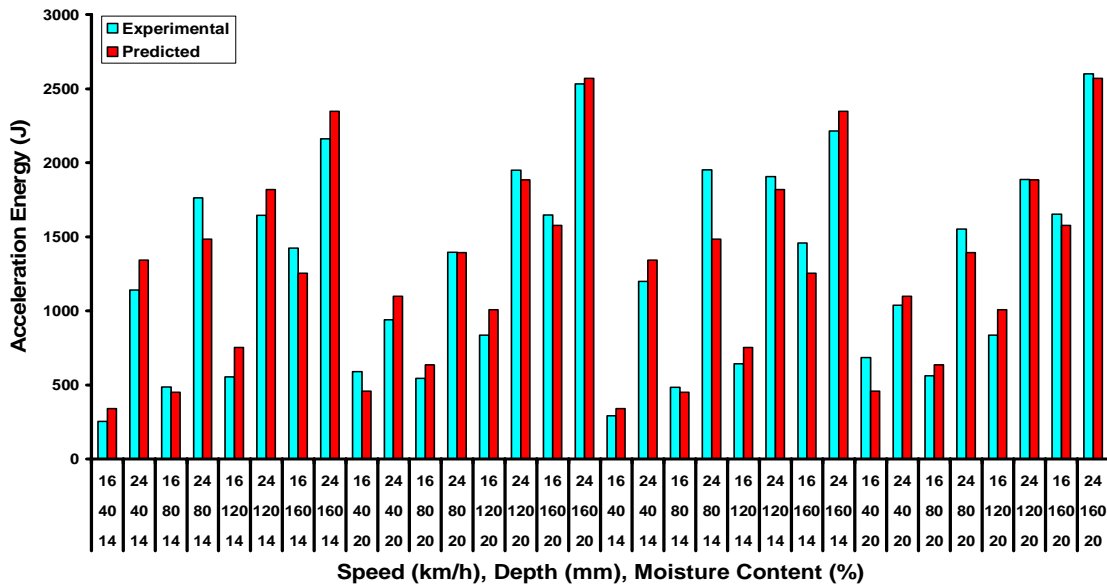
Figure 4.16 Comparison between experimental and predicted soil acceleration energy data at 16 and 24 km h^{-1} speeds

The second approach for the acceleration energy values at 8 kmh^{-1} speed resulted in another regression equation. Table 4.13 presents the predictors and their corresponding coefficients for this regression equation. The general form of the equation

Table 4.13 Coefficients of regression equation for acceleration energy – 8 km h^{-1} speed

Predictor	Applicable Coefficient
Intercept	432.29
Moisture Content (%)	8.25
Depth (mm)	-18.87
Moisture * Depth (% * mm)	0.33
Depth ** 2 (mm)^2	0.09

* Multiplication   ** Exponent

to calculate soil acceleration energy component, based upon the values in Table 4.13, would be as shown in Equation 4.10.

$$\text{Soil acceleration energy (J)} = 432.29 + (8.25 * \text{M.C.}) + \qquad (4.10)$$
$$(-18.87 * \text{Depth}) + (0.33 * \text{M.C.} * \text{Depth}) +$$
$$(0.09 * \text{Depth} ** 2)$$

A comparison between the predicted data by this regression equation and experimental data of both replicates are shown in Figure 4.17. The difference between the predicted values and experimental values in percentage which shows the power of the fit is given in Table B.6 (Appendix B), and results of the regression analysis are given in Table C.6 (Appendix C).

The current regression equation provided a better fit of the acceleration energy data at 8 km h^{-1} speed compared to the regression equation provided by the first approach. However, it still has some unsatisfactory predictions that require searching for a third approach for the energy data at 8 km h^{-1} speed.
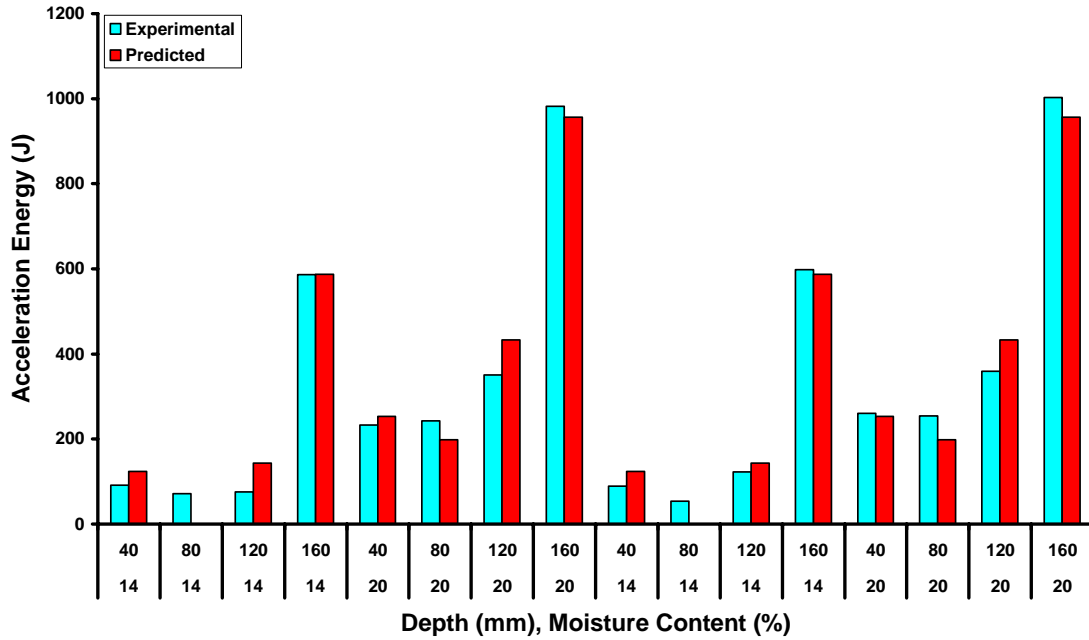
Figure 4.17 Comparison between experimental and predicted soil acceleration energy data at 8 km h^{-1} speed

4.9.6 Regression Equation for Acceleration Energy Component - 3rd Approach for 8 km h^{-1} Speed (Exponential Approach)

In this approach, instead of using first and second order of the variables in developing a regression equation, first order of moisture and exponential of depth have been used. Since only one level of speed (8 km h^{-1}) was under investigation, speed was not entered in SAS analysis as a variable. Coefficients for the predictors used in this regression equation are shown in Table 4.14. The general form of the equation to

Table 4.14 Coefficients of regression equation for acceleration energy – 8 km h^{-1} speed (exponential approach)

Predictor	Applicable Coefficient
Intercept	-380.74
Moisture Content (%)	33.20
EXP (Depth) (mm)	1.30E-68
Moisture * EXP (Depth) (% * mm)	1.09E-68

* Multiplication   EXP: Exponential   E: Exponent

calculate soil acceleration energy component, based upon the values in Table 4.14, would be as shown in Equation 4.11.

Soil acceleration energy (J) = -380.74 + (33.20 * M.C.) + ((1.30E-68 *   (4.11)

EXP (Depth)) + ((1.09E-68 * M.C. * EXP (Depth)

By using the exponential of depth data in this approach a much better fit of data was achieved. Figure 4.18 shows a comparison between the predicted values of this regression equation and the experimental data of both replicates for the acceleration energy at 8 km h^{-1} speed. The difference between the predicted and experimental data of this energy component at 8 km h^{-1} speed in percentage is shown in Table B.7 (Appendix B), and results on regression analysis are given in Table C.7 (Appendix C).
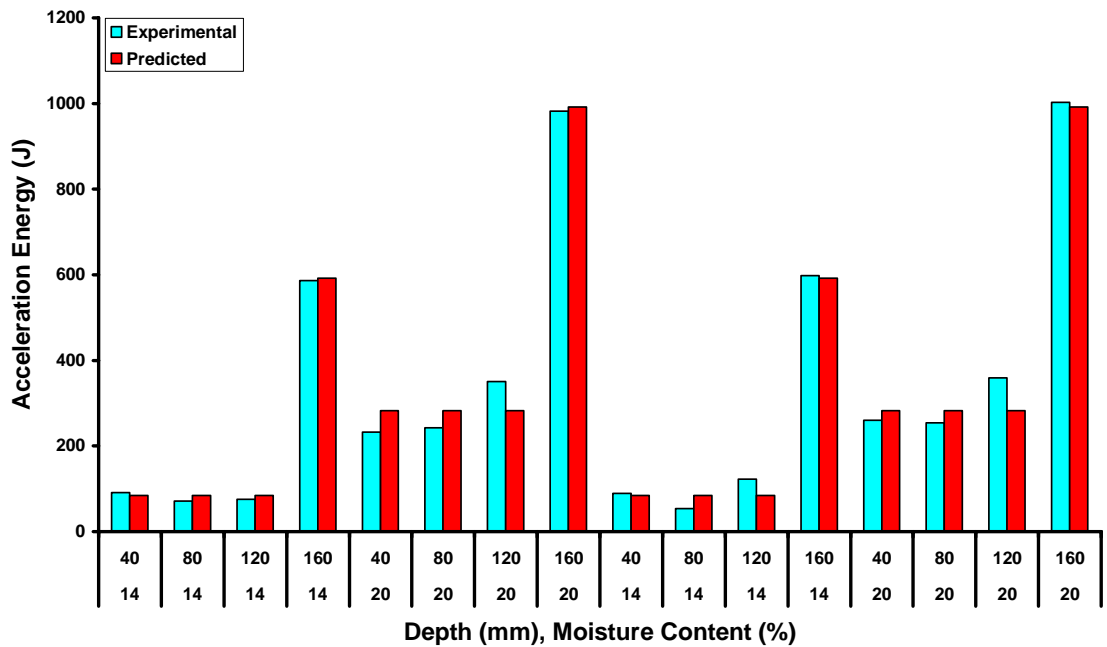
Figure 4.18 Comparison between experimental and predicted data of acceleration energy at 8 km h^{-1} speed (exponential approach)

4.9.7 Discussion on the Validity of Regression Equations

For the development of each regression equation, different combinations of the variables and for each variable, different kinds of relationship with that energy component such as linear, quadratic, and exponential were implemented using the SAS analyses to achieve the best regression equations. Therefore, regression equations

developed in the previous sections are the best fitted equations to the experimental values of the energy components.

Coefficients of all regression equations show that the first order of moisture content with a value greater than unity is best fitted to those equations. Further work showed that either eliminating or increasing order of moisture predictors, when entering experimental data in SAS analysis, both were not appropriate for these energy components. Moisture content was the only variable that had an increasing effect on all energy components. This relationship in general is in agreement with the results of many research works such as Wells and Treesuwan (1977), Ali-Hassan and McKyes (1983), Ayers (1980), and Stafford (1979). These researchers found peak cohesive values and friction angle values occurred at intermediate moisture contents for cohesive soils when density was held constant or with a minor change. Since soil used in current research included 29% clay which could be categorized as a cohesive soil, it was believed that increasing soil-tool, soil-soil, and deformation energy values as affected by moisture increase was mostly because of increase in cohesive and frictional forces. In addition, in the case of acceleration energy, it was believed that by increasing moisture content, soil compressibility particularly at higher speeds would increase which would result in a higher acceleration energy value.

Depth of operation is an affecting factor on three energy components including soil-tool, deformation, and acceleration energy components. Looking at coefficients of soil-tool and deformation energy components shows that their relationships with tool depth included a first as well as a second order of depth (Table 4.8 and Table 4.10). For acceleration energy, where all speeds have been included in the regression equation (Table 4.11), the relationship included first and second order of depth. In contrast, if only two higher levels of speed were used in the regression model (Table 4.12), the relationship between acceleration energy and depth included only the second order of depth, and there was no coefficient for the first order of depth in such equations. Only when the exponential values of speed at 8 km h^{-1} speed have been used for the regression equation (Table 4.14) neither of the first nor the second order relationships occurred. Although employed tool in current research was not a common tillage tool that similar reports could be found in the literature in order to compare the results, but still

some research supported a quadratic relationship. Girma (1989) worked on measurement and prediction of forces on plough bodies. A regression equation was developed that equals draft requirement of the plough body with the summation of a constant, a first order, and a second order of depth of operation. As well, studies by Payne and Tanner (1959), Dransfield et al. (1964), Verma (1971), Spoor and Godwin (1978), and Stafford (1979) on narrow tools showed that draft increased with depth of operation and varied with time as soil blocks were torn up. In non-cohesive soils, draft increased linearly with depth where in a highly cohesive soil this relationship was almost quadratic. Since in this research, moisture content was changing in a wide range and soil was a cohesive soil, it is reasonable to have both linear and quadratic relationships. Energy of the tool has also the same relationships with the above variables as the tool energy is mainly draft multiplied by one meter of soil rupture. Therefore, same recommendations can be made for the energy values as made for the tool draft values.

In the third approach, exponential of the depth data have been used in the regression model. Although, no literature was found to strongly support this relationship, it was to explore the exponential relation. In addition, the range of speed which could influence depth effect was not in the common range of operation in which most researchers have worked. This could influence depth effect excessively, and could change this relationship at higher speeds from quadratic to an exponential relationship.

The speed variable in current energy model was entered only in some of the regression equations of energy component (Table 4.11 and Table 4.12). When experimental data of speed at 8, 16, and 24 km h^{-1} speeds were used in the regression equation, the relationship between acceleration energy and speed values resulted in both linear and quadratic relationships (Table 4.11). In contrast, when experimental data of speed at only 16 and 24 km h^{-1} speeds were used in the regression equation, only quadratic relationship was obtained (Table 4.12). This evidently showed that for the existing tool and soil conditions, 8 km h^{-1} speed was in a range of a liner relationship. On the other hand, 16 and 24 km h^{-1} speeds resulted in a quadratic relationship. Therefore, by eliminating the values of acceleration energy at 8 km h^{-1} speed from the regression equation, linear relationship was automatically eliminated.

Review of literature supports results of regression analysis for soil acceleration energy component in general. Results reported by Koolen and Kuipers (1983), McKibben and Reed (1952), Kepner et al. (1972), Girma (1989) and Onwualu and Watts (1998) showed same relationship between tool speed and draft. Also, draft predicting equation given at ASAE standards (2001) presents a general equation including both linear and quadratic relationships for different tillage implements.

Regression equations developed for different energy components included an intercept with a negative sign. Considering that zero intercept was included in the SAS analyses, the negative sign, which meant negative energy, represented the resistive energy of soil against failure even at zero moisture content, depth, or speed. This resistive energy was interpreted as the resistance of soil against failure due to the soil strength parameters , and in particular, soil cohesion and soil internal friction angle. Ayers (1987) developed regression equations to predict cohesion and friction angle based of soil moisture content and bulk density that included negative intercept at zero moisture and bulk density. In addition, regression equations developed by Garner et al (1987) to predict draft requirement of subsoiler indicated a negative intercept at zero depth of operation. Moreover, research carried out by Stafford and Tanner (1982) and Girma (1989) support the existence of a negative intercept in regression equations if soil cohesion and friction angle are involved.

By looking at data of Table B.5, Appendix B, it is evident that the only unreasonable differences between predicted and experimental data occur at 8 km h^{-1} speed and 14% moisture content regardless of the depth of operation. It is noticeable that this table presents all acceleration energy data being utilized in the regression equation. As mentioned before, eliminating data of 8 km h^{-1} speed and developing two separate equations for different ranges of speed eliminated the problem almost completely (data of Table B.6 and Table B.7). This evidently showed that the inherent difference between acceleration energy requirements at two ranges of speed would not be expressed by any single regression equation to account for all data points of acceleration energy perfectly. This is why specific equations for each range of speed were determined.

4.9.8 Validation of Energy Components

In this section, validation of energy components resulted from this model development is verified. In the first step, validations of the two basic assumptions from energy point of view are discussed. The first assumption of the model was that deformation energy of soil at depths up to 40 mm was equal to zero. From energy point of view, it was noticed that at 14% moisture content, total energy requirement was approximately 45 J. Based on the other experimental data of this model, an average, of 30% of this energy which was 13.5 J at 40 mm depth should go for the deformation component. Compared to the deformation energy at maximum depth, it was only about 4% of it and compared to the maximum of total energy at maximum depth, it was only about 0.43% of that value which in both cases was close to a negligible value. Since at 20% moisture content, values of deformation energy did not increase much, but total energy requirement values were significantly increased, thus, total error was more decreased.

The second assumption was that acceleration energy at speeds up to 1 km h^{-1} was equal to zero. From energy point of view, if the whole energy requirement of the tool which was about 45 J at 14% moisture content was assumed to be acceleration energy, comparing it with more than 3000 J as entire energy requirement, it was about only 1.45% of that total energy and practically negligible. Even at 20% moisture content, it would not make any error more that 3% of total energy.

In validation of different energy components, the results of experiments carried out in the same soil and tool conditions have been developed in the energy model. The resultant values of each energy component have been compared with similar values predicted by their corresponding regression equations. As shown in Table 4.15, experimental and predicted values of different energy components have been compared to each other. The last column presents their difference in percentage. Considering that regression equations were developed at 14% and 20% moisture contents, the difference between experimental and predicted values at 17% moisture content, which is a new moisture level other than those experimental levels, show a promising accuracy in the predictability of the developed equations.

112

Table 4.15 Comparison between experimental and predicted data of different energy components at different moisture contents, depths, and speeds

M.C. (%)	Depth (mm)	Speed (km h⁻¹)	Energy Component	Experimental (J)	Predicted (J)	Difference (%)
17	40	1	soil-tool	86.05	49.28	42.7
17	80	8	soil-tool	260.58	323.07	23.9
17	160	1	soil-tool	695.34	692.19	0.4
17	160	8	soil-tool	695.34	692.19	0.4
17	40	1	soil-soil	31.28	26.65	14.8
17	160	1	deformation	253.84	316.87	24.8
17	160	8	deformation	253.84	316.87	24.8
17	40	8	acceleration	165.19	184.65	10.5
17	160	8	acceleration	843.66	792.15	6.5
14	160	18	acceleration	1812.60	1479.22	22.5
14	160	21	acceleration	2179.24	1882.90	15.7
20	160	18	acceleration	1906.15	1763.61	8.1

Those experimental values at 17% moisture content in Table 4.15 were carried out at low speeds of 1 and 8 km h⁻¹. In contrast, the last three rows in Table 4.15 show the comparison between experimental and predicted values of high speeds runs at 14% and 20% moisture contents. These values resulted from experiments other than experiments of regular replications, but carried out in the same soil bin facility with the same soil and tool. As shown in the table, there is a good agreement with an acceptable difference between the two sets of data. Overall, data in Table 4.15 are the closest data to the experimental data of this research to be used to validate the regression equations developed in the research

Another useful aspect of validation of the model could be the comparison between the ratio of each energy component to the total energy requirement of the tool and the same ratio resulted from similar research works. Unfortunately, to date, there is no report on any attempt to separate the effect of each energy component, or even to clearly determine different energy components in a tillage operation. The only data that may be useful are those that show the change in draft or energy requirement due to the change in soil moisture content, tool depth, or tool speed.

ASAE standards (2001), accepted as an international reference, provides general equations to estimate draft requirement of different types of implements at different working conditions. At this stage, the equation of draft prediction developed for narrow tillage tools was employed to test the validity of energy data arrangement in the current model. Particularly, validity of deformation and acceleration energies components were tested by this predicting equation (Equation 4.12).

$$D = F_i(A + B(S) + C(S)^2)WT \qquad (4.12)$$

where:

D = implement draft, N

F = a dimensionless soil texture adjustment parameter

i = 1 for fine, 2 for medium, and 3 for coarse textured soils

A, B, and C = machine-specific parameters

S = field speed, km/h

W = machine width, m

T = tillage depth, cm

Table 4.16 shows trend of deformation energy increase at constant speed that has been compared for both experimental and predicted values by Equation 4.12. Each value in columns 5 and 6 shows the increase ratio of draft requirement (in experimental data named as deformation energy) as the depth of operation increases from 80 mm depth. Considering that the equation provided by the ASAE standards gives an estimation of real data with up to 50% variation from the real data, due to different soil and tool conditions, the trends are in a reasonable agreement, particularly at 20% moisture content.

Table 4.16 Comparison between experimental and ASAE predicted trends of deformation energy increase

1	2	3	4	5	6	
Moisture Content (%)	Depth (mm)	Experimental Deformation Data (J)	ASAE Data (J)	Increase Ratio from 80 mm (Experimental Data)	Increase Ratio from 80 mm (ASAE Data)	
14	80	106.4	63.8	-	-	
14	120	258.9	95.7	2.4	1.5	
14	160	310.5	127.6	2.9	2.0	*
20	80	122.8	63.8	-	-	
20	120	254.8	95.7	2.1	1.5	*
20	160	301.3	127.6	2.5	2.0	*

* Acceptable correlation between the increase ratios of Exp. and ASAE data.

It is important to notice that although real predicted draft values by the ASAE equation are not close to the experimental deformation values, yet, the increase ratio from 80 mm depth for the two sets of data at columns 5 and 6 can be logically compared to each other. Comparisons in Table 4.16 show that contribution of deformation energy in current model has a reasonable experimental support at different moisture contents.

Table 4.17 presents the comparison between the draft increase ratio from 8 km h^{-1} speed (in experimental data named as acceleration energy increase) due to the increase of speed in both experimental and predicted data at constant operating depths. Considering different soil and tool governing conditions and approximation in the ASAE predicting equation up to 50%, there is a good correlation between the two sets of data.

4.10   Results of Statistical Analysis of Experimental Design

Data were analyzed in SAS as a completely randomized design (CRD) with a factorial treatment design. In Appendix A, Table A.1 shows analysis of variance for the model, and Table A.2 presents analysis of variance for different interactions between the variables. Probability (P) values of those tables indicate that there are significant

Table 4.17 Comparison between experimental and ASAE predicted trends of acceleration energy increase

Moisture Content (%)	Depth (mm)	Speed (km h^{-1})	Experimental Acceleration Data (J)	ASAE Data (J)	Increase Ratio from 8 km h^{-1} (Exp. Data)	Increase Ratio from 8 km h^{-1} (ASAE Data)	
14	40	8	91.3	47.8	-	-	
14	40	16	255.4	96.1	2.8	2.0	*
14	40	24	1139.9	176.8	12.5	3.7	
14	80	8	71.2	95.5	-	-	
14	80	16	485.1	192.3	6.8	2.0	
14	80	24	1762.1	353.6	24.7	3.7	
14	120	8	75.9	143.3	-	-	
14	120	16	555.4	288.5	7.3	2.0	
14	120	24	1645.5	530.4	21.7	3.7	
14	160	8	586.0	191.1	-	-	
14	160	16	1423.0	384.6	2.4	2.0	*
14	160	24	2160.0	707.2	3.7	3.7	*
20	40	8	233.0	47.8	-	-	
20	40	16	589.0	96.1	2.5	2.0	*
20	40	24	940.3	176.8	4.0	3.7	*
20	80	8	242.3	95.5	-	-	
20	80	16	543.3	192.3	2.2	2.0	*
20	80	24	1395.5	353.6	5.8	3.7	
20	120	8	359.4	143.3	-	-	
20	120	16	836.9	288.5	2.3	2.0	*
20	120	24	1887.1	530.4	5.3	3.7	*
20	160	8	1002.6	191.1	-	-	
20	160	16	1652.4	384.6	1.6	2.0	*
20	160	24	2600.0	707.2	2.6	3.7	*

* Acceptable correlation between the increase ratios of Exp. and ASAE data.

differences between different levels of soil moisture content, tool operating depth, and tool forward speed as well as the interactions between different levels of those variables at 95% confidence level.

Table A.3 and Table A.4 show that there is a significant difference between energy requirements at different levels of moisture content and t-test has recognized two significant groups for moisture content. Table A.5 and Table A.6 show that different levels of operating depth require significantly different energy, and t-test has shown four different groups for different depths. Finally, Table A.7 and Table A.8 indicate that t-test has resulted in four different levels of forward speed with significantly different energy requirements.

4.10.1 Discussion on Results of SAS Analysis of Energy Model Variables

According to the information of Table A.1, degrees of freedom for the error term are 32 which is very acceptable and makes results of analysis reliable. R^2 is 0.99 which is very high, and it shows good correlation between experimental data. Coefficient of variation (CV) between data points is 4.97 which in soil and tillage studies is very acceptable. F value of the model compared to its P value is very high, which is good sign of significant differences in the energy model.

Values in Table A.2, which show the details of differences in the model, indicate that forward speed, operating depth, and moisture content have the most significant effects on the energy requirement of the tool respectively. In addition, among the interactions between the variables, interactions between depth-speed, moisture-speed, moisture-depth, and moisture-depth-speed have the most significant effects on the energy requirement respectively. Also, t-tests for different variables show that different levels of variables have their own independent effect on energy requirement.

4.11   Results and Discussion of Direct Shear Tests

Table 4.18 shows raw data of four soil parameters measured in direct shear tests at two replicates.

117

Table 4.18 Values of soil mechanical parameters resulted from direct shear tests

Moisture Content (%db)	Rep.	Internal Friction Angle (ϕ)	Cohesion (kPa) (C)	External Friction Angle (δ)	Adhesion (kPa) (C_a)
13-15	1	35.3	10.2	32.6	1.4
13-15	2	32.7	12.3	33.8	0.38
16-18	1	36.3	6.2	34.9	3.4
16-18	2	36.7	5.7	34.5	3.9
19-21	1	35.6	5.3	33.3	3.8
19-21	2	35.3	6.0	32.7	4.1

When all tests in three levels of moisture content were carried out, final values of those soil parameters were analyzed in SAS program. Table A.9 and Table A.10 show the results of analysis of variance and t-test for the cohesion values. In addition, Table A.11 presents the effect of different levels of soil moisture content on soil cohesion. It shows that cohesion of soil at 14% moisture content is significantly different from soil cohesion at 20% moisture content. Also 14% has the highest effect on soil cohesion among the 3 levels of moisture content. Moreover, cohesion values at 17% and 20% are not significantly different.

The effect of moisture content on soil cohesion, in agreement with current results, has been studied by several researchers. Stafford (1979), Ayers (1980), and Ali-Hassan and McKyes (1983) found peak cohesive values occurred at intermediate moisture contents for cohesive soils. Stafford and Tanner (1983a) reported a logarithmic relationship between soil cohesion and moisture content. Mulqueen et al. (1977) have shown the significant influence of density and moisture content on the cohesion of remoulded soils.

Table A.12 and Table A.13 show the results of analysis of variance and t-test for the values of adhesion at different levels of moisture content. Table A.14 indicates that 20% moisture content has a higher effect on the value of soil-tool adhesion compared to

14% moisture content. However, similar to the case of cohesion, there is no significant difference between the effects of 20% and 17% moisture contents on adhesion value.

Plasse et al. (1985) reported a series of measurements on narrow blades working at different soil types. The values of soil-tool adhesion showed an increase as soil moisture content was increased for both clay and sandy clay soils. The values of adhesion reported at an approximate moisture content of 21% for a sandy clay soil are very close to what was measured at 20% moisture content in current research.

Table A.15 and Table A.16 present the results of analysis of variance and t-test for the values of soil angle of internal friction. Moreover, Table A.17 shows t grouping for those values. According to this table, there is no significant difference between the effects of different soil moisture contents on the value of angle of internal friction. Research conducted by Smith (1964), Camp and Gill (1969), Wells and Treesuwan (1977), Stafford and Tanner (1983), Ali-Hassan et al. (1983), and Ayers (1987) showed the significant effect of moisture content on the value of soil internal friction angle. However, comparing those reported results with the results of the current research, it can be concluded that the range of moisture content employed in this research was not wide enough to influence the effect of moisture content.

Table A.18 and Table A.19 show the results of analysis of variance and t-test for the values of soil external friction angle. In addition, Table A.20 presents the results of t-grouping for the effects of different soil moisture contents on the value on soil external friction angle. The table shows that there is no significant difference between the effects of different levels of soil moisture contents on the value of soil external friction angle.

Unfortunately, there is not any common expression in the literature regarding the effect of soil moisture content on the value of soil-tool friction angle. Research results reported by Plasse et al. (1985) and Aluko and Seig (2000) indicated this confusion. The values of soil-tool friction angle measured by those researchers at different moisture contents do not show any particular relation between the value of soil-metal friction and soil moisture content. In addition, even if there existed literature, still it could not be developed because of a narrow range of moisture content employed for the current research.

Among four parameters measured during direct shear tests only adhesion and soil-tool friction values were used in developing current model. These two values, as explained earlier, were employed to calculate the values of soil-tool interaction energy in the model by entering values in the Coulomb's equation (Equation 4.1). The value of adhesion, particularly after being multiplied by the surface area of tool engaged in the soil was very minor. In contrast, the effect of soil-tool friction angle when entering in the Coulomb's equation was significant. Since tangent of the friction angle is multiplied by the draft requirement of the tool in the Coulomb's equation, an increase as much as 5 degrees in the friction angle can increase soil-tool energy component at least as much as 20%. Therefore, it can be concluded that the value of soil-tool energy component was almost completely determined by the frictional aspects whereas the adhesive aspects had a very minor effect on this energy component. Considering that pre-compression treatment changed soil bulk density, and that the literature shows the effect of bulk density on soil-tool friction angle, it can be concluded that applying pre-compression treatment was necessary for the direct shear tests. Without this treatment, the results of direct shear tests would be considerably different from the reality.

4.12   Results and Discussion on Soil Cone Index Values

As depth of operation increased, soil cone index was increased for both levels of moisture content. Figure 4.19 shows increase in cone index versus depth of operation in the soil profile at 14% and 20% moisture contents. Comparing the trends of increase at both moisture contents indicates that the values of cone index at each measuring point for the two moisture contents are very close to each other. The maximum difference in cone index values occurred at 40 mm depth. At this depth, cone index at 14% moisture content is about 30% more than that of 20% moisture content. The difference between cone index values at other depths is about 10% or less which is very acceptable considering the non-homogeneity of soil medium.
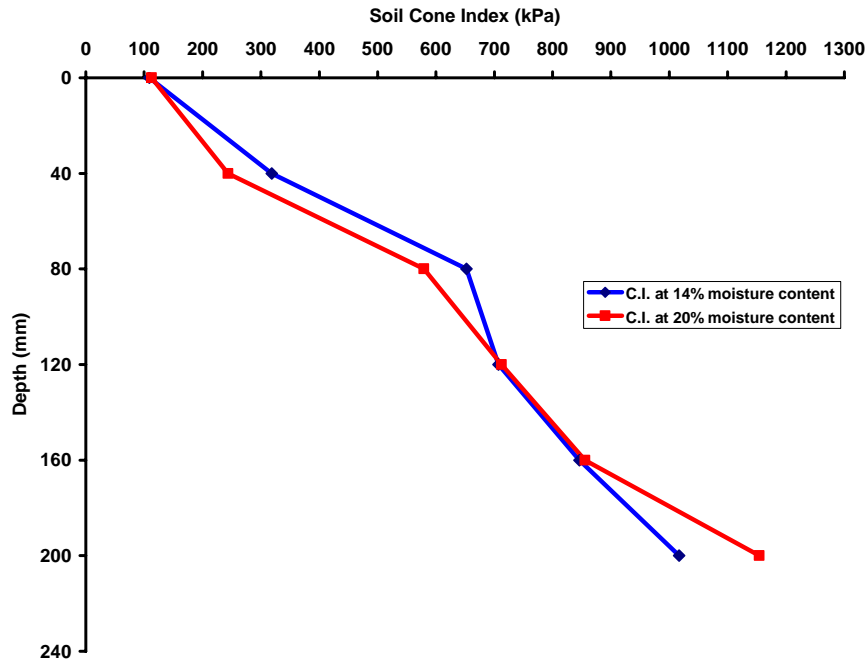
Figure 4.19 Trend of increase in soil cone index versus depth at 14% and 20% moisture contents

The excessive cone index at 40 mm depth and 14% moisture content can be explained as the extra effect of the packers on the top soil. Although the number of passes of each packer was determined by preliminary tests, yet at some moisture contents, it was very difficult to reach same values of cone index. However, having the same dry bulk density at different moisture contents for each depth beside those close values of cone index can guarantee a soil medium with almost same mechanical properties for different tillage treatments in current research.

5.0 SUMMARY, CONCLUSIONS, AND SUGGESTIONS FOR FUTURE RESEARCH

5.1 Summary

Energy requirement of tillage implements has received much attention from researchers through numerous studies carried out in last decades. Despite this attention, a lack of knowledge of agricultural soil mechanics from one side and limitations in developing real tests and collecting experimental data at desirable conditions from the other side have slowed down any new development in this area. One area in tillage energy studies that has too much room to improve yet is the area of extending the knowledge on different energy consuming components in a tillage operation. This improvement would help to optimize energy requirement through optimizing the influencing parameters on those energy components.

Another non-investigated area in tillage energy is pertinent to soil dynamics during tillage operations. Although theory in this area is much, unfortunately, experimental data that can be relied on are very little. The problem comes from the reality that to manifest soil dynamics effects, it is required to run tillage tools at high speeds. This is not possible in most cases as it encounters several practical problems. In addition, high technology instrumentations are required to measure and record desirable data at high speeds. Both tasks (running tool and measuring data at high speeds) are practically hard to do. Finally, the non-homogeneous nature of soil makes research more complicated and prevents researchers from developing a general rule based on the experimental data for most situations.

Current research was planned to investigate energy requirement of tillage tools at high speeds of operation. Two specific objectives were aimed in this study: (1) Developing a mathematical model for the total energy requirement of a tillage tool by evaluating energy requirements for four specified components. (2) Validating the model by experimental data from tests in a soil bin. To achieve these objectives, two things were required. First, a theory was required to be proven and second, an experimental procedure to be carried out. As the theory, it was assumed that energy requirement of a tillage tool includes four main components: (1) energy requirements associated with soil-tool interactions; (2) energy requirements associated with interactions between tilled and fixed soil masses; (3) energy requirements associated with soil deformation; and (4) energy requirements associated with the acceleration of the tilled soil. To investigate the validity of this theory, a set of soil bin experiments were designed. Three variables considered in soil bin experiments were: (1) soil moisture content (2) tool operating depth and (3) tool forward speed. Other factors that could influence energy requirement such as soil texture, soil compaction, tool shape, and tool rake angle were kept constant during soil bin experiments in order to investigate the pure effects of only those three variables. Moisture content in 2 levels, operating depth in 4 levels, and operating speed in 4 levels were considered in a factorial test based on a completely randomized design with two replicates. A narrow vertical tool with a flat shape was fabricated for the experiments to facilitate force calculations.

In this energy model development, both theory and experiments were implemented. Coulomb's equation was directly used to measure soil-tool interaction energy although the values applied to the equation came directly from either direct shear or soil bin tests. In soil bin experiments, high speeds of operation were achieved and very accurate measurements were carried out. Although lack of power did not allow few tests be completed, the equivalent values for those tests were later substituted, based on the other experimental values, and were included in the statistical analysis.

5.2   Conclusions

- Predicting equations of draft-depth relationship at both 14% and 20% moisture contents showed good correlation between draft and depth of operation for the tool.

- Soil-soil energy comparatively had the minimum effect on total energy among the other components. This feature made its contribution as a percentage of total energy maximal in absence of other components at 40 mm depth and 1 km h^{-1} speed and made its value minimal in presence of the other components at maximum depth and speed (160 mm depth and 24 km h^{-1} speed).

- Comparing two levels of moisture content showed that soil-tool energy reached higher values at 20% moisture content. It can be explained in this way that at higher moisture contents, soil compressibility level increased. During tool movement, tool had to compress more soil ahead before the soil could leave the line of movement. A more compressed soil at higher moisture content required more energy to cut and sled on the tool surface which in turn resulted in a higher value for soil-tool energy at 20% moisture compared to that at 14% moisture. A reduction in the relative value of this energy component after 120 mm depth indicated that the effect of deformation energy overcame soil-tool effect beyond 120 mm depth although its actual value continued to increase even after 120 mm depth.

- At both levels of moisture content, actual values of deformation energy increased with depth, but their relative values increased up to 120 mm depth then started decreasing trend. Considering the increasing effect of speed, it can be concluded that soil acceleration effect overcame soil deformation effect after 120 mm depth of operation.

- At both 14% and 20% moisture contents, actual values of acceleration energy increased with increasing depth at each speed which indicated increasing inertia forces related to the new mass of soil. This new mass of soil is resulted when tool was operating deeper in the soil, and it would multiply the effect of depth at

higher speeds. Although weight of translocated soil was accounted as part of soil deformation energy, but any extra energy spent to move this weight of soil at higher speeds was part of acceleration energy. On the other hand, acceleration energy increased with increasing speed at each depth. This effect can be attributed to changes in shear force value due to change in shear rate in soils with appreciable amounts of clay content.

- Coefficients of all regression equations showed that the first order of moisture content with a value greater than unity was best fitted to those equations.

- Depth of operation was an influencing factor on three energy components including soil-tool, deformation, and acceleration energy components.

- For acceleration energy, where all speeds were included in the regression equation, the energy-depth relationship included first and second order of depth. In contrast, if only two higher levels of speed were included in the regression model, the relationship between acceleration energy and depth included only the second order of depth, and there was no coefficient for the first order of depth in such equations.

- When experimental data of speed at 8, 16, and 24 km h^{-1} speeds were included in the regression equation, the relationship between acceleration energy and speed values resulted in both linear and quadratic relationships. It was concluded from the results that for the existing tool and soil conditions, 8 km h^{-1} speed was in a range of a liner relationship. On the other hand, 16 and 24 km h^{-1} speeds resulted in a quadratic relationship.

- Experimental data obtained from the same soil and tool but carried out at different operational conditions were used to validate energy components. Results of statistical analyses showed good agreement between predicted and experimental data for all regression equations developed. In addition, this research provided real experimental data of high speed tillage that can be used for future research.

5.3 Suggestions for Future Research

In this section, suggestions to conduct and improve future research are given in three parts: high speed soil bin facility, soil bin experiments, and energy components.

5.3.1 High Speed Soil Bin Facility

- High speed facility demands more power to enable running tools at higher speeds. This can be done by increasing the power of hydraulic motor.

- Stop and safety switches in high speed facility do not act as quickly as required when running tools at high speeds, so a manual stop is currently vital for both facility and operator. These switches should be replaced by some quick response switches.

- A double action hydraulic jack should be replaced with the existing single action jack to facilitate and safe raising and lowering down of the high speed beam. As well manual operation of the jack should be replaced with a power-assisted system.

5.3.2 Soil Bin Experiments

- Since soil preparation has a key effect on all soil bin experiments results, it is necessary to have such soil preparation devices to satisfy the expectations. Current packers of soil do not prepare soil properly. If maximum operating depth goes beyond 100 mm, then sheep-foot packer does not reach that depth. As well, there should be a guaranteed method of spraying water to the soil to ensure homogeneous wetness within all layers of the soil. Entire water spraying system does not meet this goal perfectly.

- In current research, two replications were planned for each soil bin experiments. As supported by many studies, increasing the number of replications would strengthen the results. For similar research, at least three replications are strongly recommended.

5.3.3 Energy Components

- This research was a starting point for investigations in energy components, so it had several short comings. For future research, using different shapes of tool and different rake angles is suggested.

- If same research with same energy components and same assumptions, but different tillage tools is repeated in the future, then the validity of the assumptions in current research would be better realized. The assumption of having zero deformation energy at 40 mm depth needs to be further investigated, particularly, if the shape or rake angle of the tool is different from vertical.

- Introducing any experimental method which can provide the pure effects of tool operating depth and tool forward speed would be a tail for the current research and a big step towards optimizing tillage energy.

REFERENCES

Ali-Hassan, O.S. and E. McKyes. 1983. Modelling of soil mechanical properties to soil moisture conditions. ASAE Paper No. 83-1053, ASAE, St. Joseph, MI 49085.

Aluko, O.B. and D.A. Seig, 2000. An experimental investigation of the characteristics of and conditions for brittle fracture in two-dimentional soil cutting. *Soil & Tillage Research 57: 143-157.*

American Society of Agricultural Engineers Yearbook. 1980. Standard ASAE D230. 2: 243. St. Joseph, MI: ASAE.

ASAE Standards, 48th edition. 2001. ASAE S313.3 FEB99. Soil cone penetrometer: 847. St. Joseph, MI: ASAE.

Ayers, P.D. 1987. Moisture and density effects on soil shear strength parameters for coarse grained soils. *Transactions of the ASAE* 30(5): 1282-1287.

Ayers, P.D., J.V. Perumpral. 1982. Moisture and density effect on cone index. *Transactions of the ASAE* 25(5): 1169-1172.

Azyamova, E.N. 1963. Studies of dynamics of deformation of soil. Trudy (TSNIIMESKH) Minsk 1:131-139. (Translated by W.R. Gill, National Tillage Machinery Laboratory, USDA-ARS, Auburn, AL).

Bailey, A.C., T.A. Nichols, C.E. Johnson. 1988. Soil Stress State Determination Under Wheel Loads. *Transactions of the ASAE* 31(5): 1309-1314.

Baily, A.C., C.E. Johnson and R.L. Schafer. 1984. Hydrostatic compaction of agricultural soils. *Transactions of the ASAE* 27(4): 925-955.

Bicki, T.J. and J.C. Siemens. 1991. Crop response to wheel traffic soil compaction. *Transactions of the ASAE* 34 (3): 909-913.

Blumel, K. 1986. Messungen an Einer Ackerfrase in der Bodenrinne unter besonderer Berucksichtigung der auftretenden Krafte (Measurements on a rotary tiller in the soil bin in special consideration of the acting forces). Research Report Agricultural Engineering No. 129 of Max-Eyth Society, University of Hohenheim, Germany.

Burt, E.C., R.K. Wood, and A.C. Baily. 1992. Some comparisons of average to peak soil-tire contact pressures. *Transactions of the ASAE* 35 (2): 401-405.

Camp, D.R. and W.R. Gill. 1969. The effect of drying on soil strength parameters. *Soil Science Society of America Proceedings*, 13(5): 641-644.

Chancellor, W.J. 1994. Soil physical properties. In *Advances in Soil Dynamics*. Ed. P.D. Hansen ASAE Monograph, 12, 21-254. St. Joseph, MI: ASAE.

Chancellor, W.J. and S.K. Upadhyaya. 1994. Effects of stability mechanisms during triaxial tests of cylindrical soil samples on stress ratio vs. stain ratio relations. In *Proceedings of the 2nd International Conference in Soil Dynamics*, Silsoe, Bedford, 1-17.

Chaplin, J. C. Jenane and M. Lueders. 1988. Drawbar energy use for tillage operations on loamy sand. *Transactions of the ASAE* 31(6): 1692-1692.

Chen, W.F. 1987. *Evaluation of Constitutive Models in Soil Mechanics*. Rotterdam, Netherlands: A.A. Balkema Publishers.

Chi, L. and R.L. Kushwaha. 1991. Three-dimensional, finite element interaction between soil and simple tillage tool. *Transactions of the ASAE* 34(2): 361-366.

Chi, L., S. Tessier, E. Mckyes and C. Lague. 1993. Modeling mechanical behavior of agricultural soils. *Transactions of the ASAE* 36(6): 1563-1570.

Christian, J.T. 1966. Plain strain deformation analysis of soil. Contact Report No. 3-129, Report 3, Contract DA-22-079-eng-471. Cambridge, MA: Department of Civil Engineering, MIT.

Darmora, D.P. and K.P. Pandey. 1995. Evaluation of performance of furrow openers of combined seed and fertilizer drills. Soil & Tillage Research 34: 127-139.

Dimaggio, F.L. and I.S. Sandler. 1971. Material model for granular soil. *Journal of the Engineering Mechanics Division, American Society of Civil Engineers* 93(3): 935-950.

Dransfield, P., S.T. Willat and A.H. Willis. 1964. Soil-to-implement reaction experienced with simple tines at various angles of attack. *Journal of Agricultural Engineering Research* 9(3): 220-224.

Drucker, D.C., R.E. Gibson and D.J. Hankwe. 1955. Soil mechanics and work-hardening theory of plasticity. In *Proceedings of the American Society of Civil Engineers* Vol. 81, Paper 798, 1-14.

Duncan, J.M. and C.Y. chang. 1970. Nonlinear analysis of stress and strain in soils. Journal of Soil Mechanics and Foundations Division, *American Society of Civil Engineers* 89 (SM5):1629-1653.

Durairaj, C.D. and V.J.F. Kumar. 1999. A discrete analytical procedure for predicting soil failure patterns and reactions of bent leg ploughs. *Soil & Tillage Research* 50: 33-45.

Ellison, W.D. 1947. Soil erosion studies-part II. *Agricultural Engineering* 28:197-201.

Erbach, D.C., J.G. Benjamin, RM. Cruser, M. A. Elamin, S. Mukhtar and C. H. Choi. 1992. Soil and corn response to tillage with para plow. *Transactions of the ASAE* 35(5): 1347-1354.

Fielke, J.M. 1999. Finite element modelling of the interaction of the cutting edge of tillage implements with soil. *Journal of Agricultural Engineering Research* 74: 91-101
Flenniken, J.M., R.E. Hefner and J.A. Weber. 1977. Dynamic soil strength parameters from unconfined compression tests. *Transactions of the ASAE* 20: 21-29.

Flenniken, J.M., R.E. Hefner and J.A. Weber. 1977. Dynamic soil strength parameters from unconfined compression tests. *Transactions of the ASAE* 20: 21-29.

Fornstrom, K.J., R.D. Brazee and W.H. Johnson. 1970. Tillage-tool interaction with a bounded, artificial soil. *Transactions of the ASAE*: 409-416.

Fredlund, D.G. and H. Rahardjo. 1993. *Soil Mechanics for unsaturated Soils*. Toronto, ON. John Wiley & sons Inc.

Garner, T.H., W.R. Raynolds, H.H. Miles, J.W. Davis, D. Wolf and U.M. Peiper. 1987. Energy requirement for subsoiling coastal plain soils. *Transactions of the ASAE* 30(2): 343-349.

Gill, W.R. and G.E. Vanden Berg. 1968. *Soil Dynamics in Tillage and Traction*. USDA-ARS Agricultural Handbook No. 316. U.S., Washington DC 20402: Government Printing Office.

Girma, G. 1989. Measurement and prediction of forces on plough bodies-1. Measurement of forces and soil dynamic parameters. Land and Water Use, eds., Dodd & Grace, ISBN, 1539-1546. 906191 980 0, Balkema, Rotherdam.

Glancey, J.L., S.K. Upadhyaya, W.J. Chancellor and J.W. Rumsey. 1996. Prediction of agricultural implement draft using an instrumented analog tillage tool. *Soil & Tillage Research* 37: 47-65.

Godwin, R.J. and G. Spoor. 1977. Soil failure with narrow tines. *Journal of Agricultural Engineering Research* 22(4): 213-228.

Godwin, R.J. and M.J. O'Dogherty. 2003. Integrated soil tillage force prediction models. In Proceedings of the 9th European Conference of the ISTVS, 2-21. Har2-21.per Adams, UK, September 8th to 11th, 2003,

Govers, G., K. Vandaele, P.J.J. Desmet and J. Poesen. 1994. Characterizing soil tillage as a geomorphological process. *In proceedings 13th International conference. "Soil Tillage for Crop Production of the Environment"*. J. P. Schjonning, S. A. Mikkelsen, K. B. Madsen. ISTRO. 269-274.

Grisso, R.D. and J.V. Perumpral. 1985. Review of models for predicting performance of narrow tillage tool. *Transactions of the ASAE* 28(4): 1062-1067.

Grisso, R.D., J.V. Perumpral and C.S. Desai. 1980. A soil-tool interaction model for narrow tillage tools. ASAE Paper 80-1518, ASAE, St. Joseph, MI 49085.

Grisso, R.D., M. Yasin and M.F. Kocher. 1996. Tillage implement force operating in silty clay loam. *Transactions of the ASAE* 39(6): 1977-1983.

Gupta, C.P. and T. Surendranath. 1989. Stress field in soil owing to tillage tool interaction. *Soil & Tillage Research* 13: 123-149.

Gupta, S.C., A. Hadas, W.B. Voorhees, D. Wolf, W.E. Larson and P.P. Sharma. 1990. Development of guides on the susceptibility of soils to excessive compaction. University of Minnesota BARD Report. St. Paul.

Hakansson, I. and H. Petelkau. 1991. Benefits of reduced vehicles weight. In *Soil Compaction in Crop Production*, ed. B.D. Soane and C. Vanouwerkerk, Amsterdam, Netherland: Elsevier.

Hall, C.W. and W.C. Olsen. 1992. *The Literature of Agricultural Engineering*. Cornell University Press, Ithaca and London.

Hendrick, J.G. and R.G. William. 1973. Soil reaction to high speed cutting. *Transaction of the ASAE* 16(3): 401-403.

Hettiaratchi D.R.B. 1993. The development of a powered low draught tine cultivator. *Soil & Tillage Research* 28(1993): 159-177.

Hettiaratchi, D.R.P. and A.R. Reece. 1967. Symmetrical three-dimensional soil failure. *Journal of Terramechanics* 4(3): 45-67.

Hettiaratchi, D.R.P. and A.R. Reece. 1974. The calculation of passive soil resistance. *Geotechnique* 24(3): 289-310.

Hettiaratchi, D.P., B.D. Witney and A.R. Reece. 1966. The calculation of passive pressure in two dimensional soil failure. *Journal of Agricultural Engineering Research* 11(2): 89-107.

Hillel, D. 1980. *Fundamentals of Soil Physics, 1ˢᵗ edition*. New York, NY: Academic Press, Inc.

Hryciw, R. D., S. A. Raschke, A. M. Ghalib, D. A. Horner and J. F. Peters. 1997. Videotracking for experimental validation of discrete element simulations of large discontinuous deformations. *Computer and Geotechnique* . 21(3): 235-253.

Hunt, D. 2001. *Farm Power and Machinery Management*, 10th edition. Iowa. Lowa State University Press.

Janzen, D.C. 1990. An industry response to concerns in agriculture. ASAE paper No. 90-1074. St. Joseph, MI: ASAE.

Jayasuriya, H.P.W. 1999. Modeling soil-tire interactions in lateratic soil. Unpublished PhD diss. (AE-99-1) Bangkok, Thailand.: Asian Institute of Technology, Department of Agricultural Systems and Engineering.

Johnson, C.E., R.D. Grisso, T.A. Nichols and A.C. Bailey. 1987. Shear measurement for agricultural soils-A review. *Transactions of the ASAE* 30(4): 935-938.

Johnson, C.E., L.L. Jensen, R.L. Schafer and A.C. Baily. 1978. Some soil tool analogs. ASAE Paper No. 77-1054, ASAE, St. Joseph, MI 49085.

Karmakar, S. and R. L. Kushwaha. 2005a. Simulation of soil deformation around a tillage tool using computational fluid dynamics. *Transactions of the ASAE* 48(3): 923-932.

Karmakar, S. and R. L. Kushwaha. 2005b. CFD Simulation of soil forces on a flat tillage tool. ASABE paper No. 051160. St Joseph, ASABE.

Katsygin, V.V. 1964. Relation of draft of agricultural machines to operation speeds. *Voprosy Sel'skohozyaistvennoi Mekhaniki*, Section 2, 96-119, Vol. XII. (Translated by W.R. Gill, National Tillage Machinery Laboratory, USDA-ARS, Auburn, AL).

Kepner, R.A., R. Bainer and E.L. Barger. 1972. *Principles of Farm Machinery*. Westport, CT: The Avi Publishing Co.

Khalilian, A., T.H. Garner, H.L. Musen, R.B. Dodd and S.A. Hale. 1988. Energy for conservation tillage in coastal plain soils. *Transactions of the ASAE* 31(5): 1333-1337.

Khat, L.R., V.M. Salokhe and H. Jayasuriva. 2005. Experimental validation of distinct element simulation for dynamic wheel-soil interaction. ASAE Paper No. 053120. Presented in Annual International Meeting, 17-20 July, 2005, Tampa Convocation Center, Tampa, Florida, USA.

Kiss, G.C. and D.G. Bellow. 1981. An analysis of forces on cultivator sweeps and spikes. *Transactions of the CSAE* 23 (1): 77-83.

Kondner, R.L. and J.S. Zelasko. 1963. A hyperbolic stress-strain response: cohesive soils. Journal of Soil Mechanics and Foundations Division, *American Society of Civil Engineers* 89 (SM1):115-143.

Koolen, A.J. and H. Kuipers. 1983. *Agricultural soil mechanics*. Berlin, Germany. Library of Congress Cataloging in Publication Data.

(Kostritsyn, A.K. 1956. Cutting of a cohesive medium with knives and cones.) Vsesoiuzz. Akad. Sel'skokhoziaistvennykh Nauk. Zeml. Mekh. Sborn. Trudov. (Leningrad) 3: 247-290, illus. *National Institute of Agricultural Engineering*, Engineering Translation 58.

Kuiper, H. and B. Kroesbergen. 1966. The significance of moisture content, pore space, method of sample preparation and type of shear annulus on laboratory torsional shear testing of soils. *Journal of Terramechanics* 3(4): 17-28.

Kushwaha, R.L. and C. Linke. 1996. Draft-speed relationship of simple tillage tools at high operating speeds. *Soil & Tillage Research* 39: 61-73.

Kushwaha, R.L. and J. Shen. 1995. Finite element analysis of the dynamic interaction between soil and tillage tool. *Transactions of the ASAE* 37(5): 1315-1319.

Lade, P.V. 1982. *Three Dimensional Behaviour and Parameter Evaluation for an Elasto-Plastic soil model*. A.A. Balkema, Rotterdam, Netherlands.

Lindstrom, M.J., W.W. Nelson, T.E. Schumacher and G.D. Lemme. 1990. Soil movement by tillage as affected by slope. *Soil & Tillage Research* 17:225-264.

Linke, C. and R.L. Kushwaha. 1992. High speed evaluation of draft with a vertical blade. ASAE paper No. 921019, St. Joseph, MI: ASAE.

Lowery B. and R.T. Schuler. 1991. Temporal effects of subsoil compaction on soil strength and plant growth. *Soil Science Society American Journal* 55: 216-223.

Luengo, O. and S. Singh. 1998. Modelling and identification of soil-tool interaction in automated excavation. IEEE/RSJ International Robotic Systems. Victoria, B.C. October 13-17.

Luth, H.J. and R.D. Wismer. 1971. Performance of plane soil cutting blades in sand. *Transactions of the ASAE* 14(2): 255-259, 262.

McKibben, E.G. and I.F. Reed. 1952. The influence of speed on the performance characteristics of implements. *Society of Automobile Engineers*. National Tractor Meeting, Milwaukee, Wis.

McKyes, E. 1978. The calculation of draft forces and soil failure boundaries of narrow cutting blades. *Transactions of the ASAE* 21(1): 20-24.

McKyes, E. 1985. *Soil Cutting and Tillage*. Amsterdam, The Netherlands. Elsevier Science Publishers.

McKyes, E. and O.S. Ali. 1977. The cutting of soil by narrow blades. *Journal of Terramechanics* 14(2): 43-58.

McKyes, E. and F.L. Desir. 1984. Prediction and field measurements of tillage tool draft forces and efficiency in cohesive soils. *Soil & Tillage Research* 4(4): 459-470.

McKyes, E and J. Maswaure. 1997. Effect of design parameters of flat tillage tools on loosening of a clay soil. *Soil & Tillage Research* 43: 195-204.

Michel, J.A., K.J. Fornstrom and J. Borrelli. 1985. Energy requirements of two tillage systems for irrigated sugar beets, dry beans and corn. *Transactions of the ASAE* 28(6): 1731-1735.

Mohsenin, N.N. 1970. *Physical Properties of Plant and Animal Materials*, 93. New York, NY 1001. Gordon and Breach Science Publishers,

Mouazen, A.M. and M. Nemenyi. 1999. Finite element analysis of subsoiler cutting in non-homogeneous sandy loam soil. *Soil & Tillage Research* 51: 1-15.

Mouazen, A.M. and H. Ramon. 2002. A numerical hybrid modelling scheme for evaluation of draught requirements of a subsoiler cutting a sandy loam soil, as affected by moisture content, bulk density, and depth. *Soil & Tillage Research* 63: 155-165.

Mulqueen, J., J.V. Stafford and D.W. Tanner. 1977. Evaluation of penetrometers for measuring soil shear strength. *Journal of Terramechanics* 14(3): 137-151.

Nichols, M.L. 1931. The dynamic properties of soil II. Soil and metal friction. *Journal of Agricultural Engineering* 12:321-324.

Nichols, M.L. 1932. The dynamic properties of soils, III. Shear values of uncemented soils. *Agricultural Engineering* 13 (8): 201-204.

Nichols, M.L. and C.A. Reaves. 1958. Soil reaction: to subsoiling equipment. *Agricultural Engineering* 39: 340-343.

Nikiforov, P.E. and M.I. Bredun. 1965. *The sliding friction of soil on metal and plastic surfaces*. Moscow, Russia: Nukai.

Niyamapa, T.K. and V.M. Salokhe. 1992. Soil failure under undrained quasi static and high speed triaxial compression test. *Journal of Terramechanics* 21(3):237-251.

O'Callaghan, J.R. and K.M. Farrelly. 1964. Cleavage of soil by tined implements. *Journal of Agricultural Engineering Research* 9(3): 259-270.

Ohu, J.O., G.S.V. Raghavan and E. McKyes. 1985. Peatmoss effect on the physical and hydraulic characteristics of compacted soils *Transactions of the ASAE* 15: 423-427.

Onwualu, A.P. and K.C. Watts. 1998. Draught and vertical forces obtained from dynamic soil cutting by plane tillage tools. *Soil & Tillage Research* 48: 239-253.

Owen, G.T. 1989. Subsoiling forces and tool speed in compact soils. *Canadian Agricultural Engineering* 31(1): 15-20.

Panwar, J.S. and J.C. Siemens. 1972. Shear strength and energy of soil failure related to density and moisture. *Transactions of the ASAE* 15: 423-427.

Payne, P.C.J. 1956. The relationship between the mechanical properties of soil and the performance of simple cultivation implements. *Journal of Agricultural Engineering Research* 1(1): 23-50.

Payne, P.C.J. and D.W. Tanner. 1959. The relationship between rake angle and the performance of simple cultivation implements. *Journal of Agricultural Engineering Research* 4(4): 312-325.

Perdok UD, van de Werken G. 1982. Power and labour requirements in soil tillage. *International Congress 12th of Agricultural Machinery Exhibition*, Landbouw RAI, Amsterdam, 55-70.

Perumpral, J.V., R.D. Grisso and C.S. Desai. 1983. A soil tool model based on limit equilibrium analysis. *Transactions of the ASAE* 26(4): 991-995.

Plasse, R., G.S.V. Raghavan and E. Mckyes. 1985. Simulation of narrow blade performance in different soils. *Transactions of the ASAE* 28(4): 1007-1012.

Plackett, C.W. 1984. The ground pressure of some agricultural tires at low and zero sinkage. *The British Society for Research in Agricultural Engineering*. 159-166.

Plouffe, C., C. Lague, S. Tessier, M.J. Richard and N.B. McLaughlin. 1999. Moldboard plow performance in a clay soil: simulation and experiment. *Transactions of the ASAE* 42(6): 1531-1539.

Raghavan, G.S.V., E. McKyes and B. Bealieu. 1977. Prediction of clay soil compaction. *Journal of Terramechanics* 14 (1): 31-38.

Reece, A.R. 1965. The fundamental equation of earthmoving machines. Symposium of Earthmoving Machines. *Institute of Mechanical Engineering*. 179(3F).

Rosa, U.A. 1997. Performance of narrow tillage tools with internal and strain rate effects. Unpublished Ph. D. thesis. Saskatoon, SK: Department of Agricultural and Bioresource Engineering, University of Saskatchewan.

Rosa, U.A. and D. Wulfsohn. 1999. Constitutive model for high speed tillage using narrow tools. *Journal of Terramechanics* 36: 221-234.

Roscoe, K.H., A.N. Schofield and C.P. Wroth. 1958. On the yielding of soils. *Geotechnique* 8(1): 22-53.

Rowe, R.J. and K.K. Barnes. 1961. Influence of speed on elements of draft of a tillage tool. *Transactions of the ASAE* 4: 55-57.

Schafer, R.L., and C.E. Johnson. 1982. Changing soil condition-The soil dynamics of tillage. In *Tillage Effects on Soil Physical Properties and Processes.* American Society of Agronomy Special Publication Number 44, 14-15. Madison.

Schmertmann, J.H. 1975. Measurement of insitu shear strength. In *Proceedings of the Conference on insitu measurement of soil properties*, 2: 57-138.

Schuring, D.J. and I.R. Emori. 1964. Soil deforming processes and dimensional analysis. Paper 897c. *Society of Agricultural Engineering*, New York.

Shen, J. and R.L. Kushwaha. 1998. *Soil-Machine Interactions: A Finite Element Perspective*. Saskatoon, Saskatchewan: Marcel Dekker Inc.

Shikanai, T. and M. Ueno. 2002. Simulation of soil resistance at plate penetration by the distinct element method. ASAE Paper No. 023046. Presented in Annual International Meeting, July 28-July 31, 2002, Hyatt Regency Chicago, Chicago, Illinois, USA.

Siemens, J.C., J.A. Weber and T.H. Thornburn. 1965. Mechanics of soil as influenced by model tillage tools. *Transactions of the ASAE* 8(1): 1-7.

Smith, J.L. 1964. Strength-moisture-density relations of fine grained soils in vehicle mobility research. Technical report No. 3-369. U.S. Army Engineer Waterways Experimental Station. Vicksburg, MS.

Smith, L.A. and J.R. Williford. 1988. Power requirement of conventional, triplex, and parabolic subsoilers. *Transactions of the ASAE* 31(6): 1685-1688.

Soehen, W. 1958. Fundamentals of pressure distribution and soil compaction under tractor tires. *Journal of Agricultural Engineering* 39: 276-281, 290.

Spoor, G. and R.J. Godwin. 1978. An experimental investigation into the loosening of soil by rigid tines. *Journal of Agricultural Engineering* 23: 243-257.

Stafford, J. V. 1979. The performance of rigid tine in relation to soil properties and speed. *Agricultural Engineering Research* 24(1): 41-56.

Stafford, J.V. and D.W. Tanner. 1983a. Effect of rate on soil shear strength and soil-metal friction, I. Shear strength. *Soil & Tillage Research* 3: 245-261.

Stafford, J.V. and D.W. Tanner. 1983b. Effect of rate on soil shear strength and soil-metal friction, II. Soil-metal friction. *Soil & Tillage Research* 3: 321-330.

Stewart, R.E. 1979. *Seven decades that changed America* (St. Joseph, Mich: American Society of Agricultural Engineers).

Summers, J.D., A. Khalilian and D.G. Batchelder. 1986. Draft relationships for primary tillage in Oklahoma soils. *Transactions of the ASAE* 29(1): 37-39.

Swick, W.C. and Perumpral. 1988. A model for predicting soil-tool interaction. *Journal of Terramechanics* 25(1): 43-56.

Tang, W.H. and K. Hoeg. 1968. Plane strain loading of a strain hardening soil. Contact Report No. 3-129, Report 5, Contract DA-22-079-eng-471. Cambridge, MA: Department of Civil Engineering, MIT.

Taylor, H.M. and G.F. Arkin. 1981. Root Zone Modification: Fundamentals and Alternatives. In *Modifying the Root Environment to Reduce Crop Stress,* ed. G.F. Arkin and H.M. Taylor, 3-17. St. Joseph, MI: ASAE Monograph No. 4.

Terzaghi, K. 1943. *Theoretical Soil Mechanics*. New York, NY: John Wiley & Sons.

Tupper, G.R. 1974. Design of the Stoneville parabolic subsoiler. Information sheet 1249. *Mississippi Agricultural and Forestry Experts*. Station of Mississippi State, Mississippi 39762.

Vanden Berg, G.E. 1961. Requirements for a soil mechanics. *Transactions of the ASAE* 4(2): 234-238.

Verma, B.P. 1971. Oscillating soil tools-a review. *Transactions of the ASAE* 14: 1107-1115, 1121.

Vetrov, Y.A. and V.P. Stanevski. 1972. The investigation of the factors of the speed of cutting soils. *Mining Construction and Highway Machines* 8: 21-26. Translated by W.R. Gill, National Tillage Machinery Laboratory, Auburn, AL.

Wells, L.G. and E.C. Burt. 1984. Response on selected soils to power tires at disparate moisture conditions. ASAE paper NO. 84-1546. St. Joseph, MI: ASAE.

Wells, L.G., and O. Treesuwan. 1977. The response of various soil strength indices to changing water content, ASAE Paper No. 77-1055, ASAE, St. Joseph, MI 49085.

Wheeler, P.N. and R.J. Godwin. 1994. Soil dynamics of single and multiple tines at speeds up to 20 KPH. In *Proceedings of the 2nd International Conference in Soil Dynamics*, Silsoe, Bedford: 108-109.

Wheeler, P.N. and R.J. Godwin. 1996. Soil dynamics of single and multiple tines at speeds up to 20 km h^{-1}. *Journal of Agricultural Engineering Research* 63: 243-250.

Wismer, R.D. and H.J. Luth. 1972. Rate effects in soil cutting. *Journal of Terramechanics* 8(3): 11-21.

Wolf, D., T.H. Garner and J.W. Davis. 1981. Tillage mechanical energy input and soil-crop response. *Transactions of the ASAE* 24(6): 1412-1419.

Wood, R.K. and D.A. Mangione. 1993. Tractor performance with radial-ply tires at rated deflection. USDA Hatch Project No. 958. OARDC Journal Article No. 91-93.

Wroth, C.P. and G.T. Houlsby. 1980. A critical state model for predicting the behavior Of Clays. In *Proceedings of the Workshop on Limit Equilibrium, Plasticity and Generaralized Stress-Strain in Geotechnical Engineering*: 592-627, New York, NY: ASAE.

Yong, R.N. and A.W. Hanna. 1977. Finite element analysis of plane soil cutting. *Journal of Terramechanics* 14(3): 103-125.

Zelenin, A.N. 1950. Basic physics of the theory of soil cutting, Akademia Nawk USSR, Moscow-Leningrad (NIAE Transaction)

Zeng, D. and Y. Yao. 1992. A dynamic model for soil cutting by blade and tine. *Journal of Terramechanics* 29(3): 317-327.

Zhang, Z.X. and R.L. Kushwaha. 1999a. Operating speed effect on the advancing soil failure zone in tillage operation. *Canadian Agricultural Engineering* 41(2): 87-92.

APPENDICES

Appendix-A: Tables of Analysis of variance

Appendix-B: Tables of Comparison between Experimental and Predicted Data

Appendix-C: Tables of Analyses of Regression Equations of Energy Components

Appendix-D: Load Cells Calibration Procedure

Appendix-E: Details of Speed Adjustment, Running Tool and Computer Program, and
Collecting High Speed Data

Appendix-F: Forth Program

TABLES OF ANALYSIS OF VARIANCE

Table A.1 Analysis of variance of the energy model

Source	DF	SS	MS	F	P	R^2	CV
Model	31	57126144.08	1842778.84	425.33	< 0.0001	0.99	4.97
Error	32	138641.73	4332.55				
Total	63	57264785.81					

Table A.2 Analysis of variance of energy model including interactions between variables

Source	DF	SS	MS	F	P
Moisture (M)	1	991622.62	991622.62	228.88	<0. 0001
Depth (D)	3	25361610.14	8453870.04	1951.24	<0. 0001
Speed (S)	3	27555975.22	9185325.07	2120.07	<0. 0001
M * D	3	170711.17	56903.72	13.13	<0. 0001
M * S	3	231656.78	77218.92	17.82	<0. 0001
D * S	9	2555772.00	283974.66	65.64	<0. 0001
M * D* S	9	258796.14	28755.13	6.64	<0. 0001

Table A.3 Results of t-test for different levels of moisture content

Statistical term	Value
Alpha	0.05
Error degrees of freedom	32
Error mean square	4332.55
Critical value of t	2.04
Least significant difference	33.52

Table A.4 Categorizing moisture content levels by t-test

t-grouping	Mean	N	Moisture Content (%)
A	1448.70	32	20
B	1199.75	32	14

Table A.5 Results of t-test for different levels of operating depth

Statistical term	Value
Alpha	0.05
Error degrees of freedom	32
Error mean square	4332.55
Critical value of t	2.04
Least significant difference	47.403

Table A.6 Categorizing depth levels by t-test

t-grouping	Mean	N	Depth (mm)
A	2202.80	16	160
B	1568.02	16	120
C	1011.97	16	80
D	514.12	16	40

Table A.7 Results of t-test for different levels of forward speed

Statistical term	Value
Alpha	0.05
Error degrees of freedom	32
Error mean square	4332.55
Critical value of t	2.04
Least significant difference	47.403

Table A.8 Categorizing speed levels by t-test

t-grouping	Mean	N	Speed (km h^{-1})
A	2345.62	16	24
B	1411.66	16	16
C	938.08	16	8
D	601.55	16	1

Table A.9 Analysis of variance for cohesion

Source	DF	SS	MS	F	Pr>F	R^2	C.V.	Root MSE	Mean
Model	2	39.69	19.84	23.12	0.015	0.94	12.16	0.93	7.62
Error	3	2.57	0.86						
Total	5	42.27							

Table A.10 Results of t-test for different values of cohesion

Statistical term	Value
Alpha	0.05
Error degrees of freedom	3
Error mean square	0.86
Critical value of t	3.18
Least significant difference	2.95

Table A.11 Categorizing cohesion values based on moisture levels by t-test

t-grouping	Mean	N	Average Moisture (% db)
A	11.25	2	14
B	5.95	2	17
B	5.65	2	20

Table A.12 Analysis of variance for adhesion

Source	DF	SS	MS	F	Pr>F	R²	C.V.	Root MSE	Mean
Model	2	11.38	5.69	24.73	0.013	0.94	16.95	0.48	2.83
Error	3	0.69	0.23						
Total	5	12.07							

Table A.13 Results of t-test for different values of adhesion

Statistical term	Value
Alpha	0.05
Error degrees of freedom	3
Error mean square	0.23
Critical value of t	3.18
Least significant difference	1.52

Table A.14 Categorizing adhesion values based on moisture levels by t-test

t-grouping	Mean	N	Average Moisture (% db)
A	3.95	2	20
A	3.65	2	17
B	0.89	2	14

Table A.15 Analysis of variance for soil internal friction angle

Source	DF	SS	MS	F	Pr>F	R²	C.V.	Root MSE	Mean
Model	2	6.30	3.15	2.70	0.213	0.64	3.06	1.08	35.32
Error	3	3.50	1.17						
Total	5	9.80							

Table A.16 Results of t-test for different values of soil internal friction angle

Statistical term	Value
Alpha	0.05
Error degrees of freedom	3
Error mean square	1.16
Critical value of t	3.18
Least significant difference	3.43

Table A.17 Categorizing soil internal friction angle values based on moisture levels by t-test

t-grouping	Mean	N	Average Moisture (% db)
A	36.5	2	17
A	35	2	20
A	34	2	14

Table A.18 Analysis of variance for soil external friction angle

Source	DF	SS	MS	F	Pr>F	R²	C.V.	Root MSE	Mean
Model	2	3.45	1.72	5.29	0.104	0.78	1.69	0.57	33.63
Error	3	0.98	0.33						
Total	5	4.43							

Table A.19 Results of t-test for different values of soil external friction angle

Statistical term	Value
Alpha	0.05
Error degrees of freedom	3
Error mean square	0.32
Critical value of t	3.18
Least significant difference	1.81

Table A.20 Categorizing soil external friction angle values based on moisture levels by t-test

t-grouping	Mean	N	Average Moisture (% db)
A	34.70	2	17
A	33.20	2	14
A	33	2	20

APPENDIX B

TABLES OF COMPARISON BETWEEN EXPERIMENTAL AND PREDICTED DATA

Table B.1 Difference between experimental and predicted values of soil-tool energy component

Moisture Content (%)	Depth (mm)	Experimental (J)	Predicted (J)	Difference (%)
14	40	30.93	9.08	70.63
14	80	225.45	274.40	21.71
14	120	501.56	480.23	4.25
14	160	599.20	626.57	4.57
14	40	31.95	9.08	71.56
14	80	228.48	2074.40	20.10
14	120	514.48	480.23	6.66
14	160	648.48	626.57	3.38
20	40	90.71	89.47	1.37
20	80	342.65	371.74	8.49
20	120	611.92	594.52	2.84
20	160	718.26	757.81	5.51
20	40	93.52	89.47	4.34
20	80	345.66	371.74	7.54
20	120	671.54	594.52	11.47
20	160	752.78	757.81	0.67

Table B.2 Difference between experimental and predicted values of soil-soil energy component

Moisture Content (%)	Depth (mm)	Experimental (J)	Predicted (J)	Difference (%)
14	40	13.97	14.25	2.04
14	40	14.54	14.25	1.96
20	40	38.30	39.04	1.93
20	40	39.78	39.04	1.86

Table B.3 Difference between experimental and predicted values of deformation energy component

Moisture Content (%)	Depth (mm)	Experimental (J)	Predicted (J)	Difference (%)
14	80	106.38	105.82	0.53
14	120	258.87	264.48	2.17
14	160	310.53	323.03	4.03
14	80	107.52	105.82	1.58
14	120	265.60	264.48	0.42
14	160	337.79	323.03	4.37
20	80	122.84	124.01	0.95
20	120	254.78	267.42	4.96
20	160	301.28	310.70	3.13
20	80	122.94	124.01	0.87
20	120	284.57	267.42	6.03
20	160	317.89	310.70	2.26

Table B.4 Difference between experimental and predicted values of all acceleration energy components (first approach)

Moisture Content (%)	Depth (mm)	Speed (km h^{-1})	Experimental (J)	Predicted (J)	Difference (J)
14	40	8	91.30	2.41	97.36
14	40	16	255.4	433.38	69.69
14	40	24	1139.90	1324.74	16.22
14	80	8	71.20	-12.71	117.85
14	80	16	485.10	489.71	0.95
14	80	24	1762.10	1452.50	17.57
14	120	8	75.90	186.97	146.27
14	120	16	555.40	760.82	36.99
14	120	24	1645.50	1795.06	9.09
14	160	8	586.00	601.43	2.63
14	160	16	1423.00	1246.72	12.39
14	160	24	2160.00	2352.40	8.91
14	40	8	88.97	2.41	97.29
14	40	16	292.25	433.38	48.29
14	40	24	1199.28	1324.74	10.46
14	80	8	53.69	-12.71	123.67
14	80	16	482.46	489.71	1.50
14	80	24	1952.96	1452.50	25.63
14	120	8	123.18	186.97	51.78
14	120	16	643.28	760.82	18.27
14	120	24	1907.58	1795.06	5.90
14	160	8	598.49	601.43	0.49
14	160	16	1459.49	1246.72	14.58
14	160	24	2214.69	2352.40	6.22

Table B.4 - Continued

Moisture Content (%)	Depth (mm)	Speed (km h⁻¹)	Experimental (J)	Predicted (J)	Difference (J)
20	40	8	233.02	255.27	9.55
20	40	16	588.97	450.03	23.59
20	40	24	940.34	1105.17	17.53
20	80	8	242.35	259.89	7.24
20	80	16	543.26	597.48	9.98
20	80	24	1395.51	1395.46	0.00
20	120	8	350.23	479.31	36.85
20	120	16	837.26	959.73	24.63
20	120	24	1950.40	1900.53	2.56
20	160	8	981.56	913.51	6.93
20	160	16	1647.99	1536.77	6.75
20	160	24	2547.46	2620.40	2.86
20	40	8	260.35	255.27	1.95
20	40	16	684.10	450.03	34.22
20	40	24	1037.25	1105.17	6.55
20	80	8	254.00	259.89	2.32
20	80	16	562.22	597.48	6.27
20	80	24	1552.72	1395.46	10.13
20	120	8	359.45	479.31	33.34
20	120	16	836.94	959.73	14.67
20	120	24	1887.10	1900.53	0.71
20	160	8	1002.56	913.51	8.88
20	160	16	1652.36	1536.77	7.00
20	160	24	2600.03	2620.40	0.78

Table B.5 Difference between experimental and predicted values of acceleration energy component – speeds of 16 and 24 km h^{-1} (2nd approach)

Moisture Content (%)	Depth (mm)	Speed (km h^{-1})	Experimental (J)	Predicted (J)	Difference (J)
14	40	16	255.40	340.42	33.29
14	40	24	1139.90	1341.74	17.71
14	80	16	485.10	450.09	7.22
14	80	24	1762.10	1482.67	15.86
14	120	16	555.40	754.39	35.83
14	120	24	1645.50	1818.22	10.50
14	160	16	1423.00	1253.32	11.92
14	160	24	2160.00	2348.41	8.72
14	40	16	292.25	340.42	16.4
14	40	24	1199.28	1341.74	11.88
14	80	16	482.46	450.09	6.71
14	80	24	1952.96	1482.67	24.08
14	120	16	643.28	754.39	17.27
14	120	24	1907.58	1818.22	4.68
14	160	16	1459.49	1253.32	14.13
14	160	24	2214.69	2348.41	6.04

Table B.5 - Continued

Moisture Content (%)	Depth (mm)	Speed (km h^{-1})	Experimental (J)	Predicted (J)	Difference (J)
20	40	16	588.97	457.30	22.36
20	40	24	940.34	1098.09	16.78
20	80	16	543.26	635.44	16.97
20	80	24	1395.51	1394.18	0.10
20	120	16	837.26	1008.22	20.42
20	120	24	1950.40	1884.90	3.36
20	160	16	1647.99	1575.62	4.39
20	160	24	2531.39	2570.24	1.53
20	40	16	684.10	457.30	33.15
20	40	24	1037.25	1098.09	5.87
20	80	16	562.22	635.44	13.02
20	80	24	1552.72	1394.18	10.21
20	120	16	836.94	1008.22	20.46
20	120	24	1887.10	1884.90	0.12
20	160	16	1652.36	1575.62	4.64
20	160	24	2600.03	2570.24	1.15

Table B.6 Difference between experimental and predicted values of acceleration energy component – speed of 8 km h^{-1} (2nd approach)

Moisture Content (%)	Depth (mm)	Speed (km h^{-1})	Experimental (J)	Predicted (J)	Difference (J)
14	40	8	91.30	124.09	35.89
14	80	8	71.20	-10.60	114.88
14	120	8	75.90	143.74	89.34
14	160	8	586.00	587.11	0.19
14	40	8	88.97	124.09	39.48
14	80	8	53.69	-10.60	119.74
14	120	8	123.18	143.74	16.69
14	160	8	598.49	587.11	1.90
20	40	8	233.02	253.54	8.80
20	80	8	242.35	198.78	17.98
20	120	8	350.23	433.06	23.65
20	160	8	981.56	956.37	2.57
20	40	8	260.35	253.54	2.62
20	80	8	254.00	198.78	21.74
20	120	8	359.45	433.06	20.48
20	160	8	1002.56	956.37	4.61

Table B.7 Difference between experimental and predicted values of acceleration energy component – speed of 8 km h^{-1} (exponential approach)

Moisture Content (%)	Depth (mm)	Speed (km h^{-1})	Experimental (J)	Predicted (J)	Difference (J)
14	40	8	91.30	84.04	7.97
14	80	8	71.20	84.04	18.03
14	120	8	75.90	84.04	10.70
14	160	8	586.00	592.25	1.07
14	40	8	88.97	84.04	5.54
14	80	8	53.69	84.04	56.53
14	120	8	123.18	84.04	31.77
14	160	8	598.49	592.25	1.04
20	40	8	233.02	283.23	21.55
20	80	8	242.35	283.23	16.87
20	120	8	350.23	283.23	19.13
20	160	8	981.56	992.06	1.07
20	40	8	260.35	283.23	8.79
20	80	8	254.00	283.23	11.51
20	120	8	359.45	283.23	21.20
20	160	8	1002.56	992.06	1.05

APPENDIX C

TABLES OF ANALYSES OF REGRESSION EQUATIONS OF ENERGY COMPONENTS

Table C.1 Analysis of regression equation of soil-tool energy

Source	DF	SS	MS	F	P>F	R^2	CV
Model	4	978888.04	244722.01	151.82	0.0001	0.98	10.02
Error	11	17731.08	1611.92				
Total	15	996619.12					

Table C.2 Analysis of regression equation of soil-soil energy

Source	DF	SS	MS	F	P>F	R^2	CV
Model	1	614.29622	614.29622	976.895	0.0010	0.99	2.97
Error	2	1.25765	0.62883				
Total	3	615.55387					

Table C.3 Analysis of regression equation of soil deformation energy

Source	DF	SS	MS	F	P>F	R^2	CV
Model	4	88743.39	22185.85	154.23	0.0001	0.99	5.16
Error	7	1006.96	143.85				
Total	11	89750.36					

Table C.4 Analysis of regression equation of soil acceleration energy (speeds of 8, 16 and 24 km h^{-1})

Source	DF	SS	MS	F	P>F	R^2	CV
Model	9	24035686.89	2670631.88	105.91	0.0001	0.96	16.49
Error	38	958198.29	25215.74				
Total	47	24993885.19					

Table C.5 Analysis of regression equation of soil acceleration energy (speeds of 16 and 24 km h^{-1})

Source	DF	SS	MS	F	P>F	R^2	CV
Model	7	13309077.47	1901296.78	57.09	0.0001	0.94	14.30
Error	24	799290.04	33303.75				
Total	31	14108367.51					

Table C.6 Analysis of regression equation of soil acceleration energy (speed of 8 km h^{-1})

Source	DF	SS	MS	F	P>F	R^2	CV
Model	4	1369938.02	342484.50	97.22	0.0001	0.97	17.67
Error	11	38750.82	3522.80				
Total	15	1408688.84					

Table C.7 Analysis of regression equation of soil acceleration energy - exponential approach (speed of 8 km h^{-1})

Source	DF	SS	MS	F	P>F	R^2	CV
Model	3	1389760.54	463253.51	293.69	0.0001	0.99	11.82
Error	12	18928.29	1577.36				
Total	15	1408688.83					

APPENDIX D

Load Cells Calibration Procedure

D.1   Load Cells Calibration of Low Speed Carriage

Before using the carriage for any experiments, load cells were calibrated to make sure about their accuracy. The common method is dead load method; in this method, each load cell after uninstallation from the carriage is bolted at one end to a U joint and freely hanged up from a lifter. In the next step, different dead loads are bolted to the lower end of the load cell through a chain and when they are lifted, corresponding force values in Newton are shown on the digital control board. In practice, beside the board, load cell of every channel was put in a circuit of a resistor with an excitation voltage by connecting two terminals directly to each other. If at zero load, the number on the digital screen was as expected (based on calculations), load cell was working properly. Then to double check the adjustment, a known weight of 2178 N was applied to the load cell and this time zero value was supposed to show up on the screen. If the value on the screen was different from zero, by turning the adjusting screw of that load cell, it was set on zero. This procedure was done for both loading and unloading cycles. Table D.1 shows different channels, their expected reactions, and their calibration values at zero and 2178 N.

D.2   Load Cells Calibration of High Speed Carriage

Each load cell was hanged from a U joint freely at zero load and the corresponding pot in the logger box for that particular channel was set on 23 by turning the screw of the pot. This number was showing on the screen of the computer when the Forth program was running and the calibration function was activated. Different dead weights were hanged to the lower side of the load cell and when the whole collection was lifted up by the lifter new numbers on the screen were indicating the response of the load cell to the hanged weights.

Since the tool carriage was designed to record different reactions from different load cells, the zero point set up for load cells was different. For example, Load cells of channels 1, 2, and 3 were designed to work under tension; therefore, their zero point was set at 23. Channels 4 and 5 were designed to work under compression; therefore, their zero load point was set at 284, which was the maximum number achieved at zero load by turning the screws on the pods.

Table D.1 Calibration values of different channels of low speed carriage

Channel	Load Cell	Force & reaction	Dead Loads (N) 0	2178	Resistive value ($k\Omega$)	Excitation Voltage (V)
7	1	Vertical Tension	5244	0	50.2	9.692
2	2	Vertical Compression	2760	0	50.2	9.692
3	3	Vertical Compression	2744	0	50.2	9.692
4	4	Draft Tension	2616	0	50.2	9.692
5	5	Draft Tension	2623	0	50.2	9.692
6	6	side way Tension & Compression	5241	0	50.2	9.692

Finally, channel 6, which was designed to measure side way forces, had to work under both tension and compression; therefore, zero point was set at 453. In this way, one-directional hanging method could be applied for load cells working in tension, compression, or both reactions. Table D.2 shows values indicated by load cells against different dead weights as well as their calibration equations.

Zero load was set at 23 because the maximum number for the maximum load was 1023, and since the maximum capacity of most load cells was 1000 Lbs, it was easier to

set zero point at 23. Therefore, for each pound of increase in weight, there could be one unit of increase in the corresponding number, which this was in accordance with the perfect linearity of the load cells. In the calibration equations of Table D.2, X shows data logger reading and F is the equivalent force in kgf.

Table D.2 Calibration values of different channels of high speed carriage

Channel or load cell	Force & reaction	Dead loads (kgf)				Calibration equations
		0	22.83	48.98	222	
1	Vertical Tension	23	49	80	281	
2	Draft Tension	23	73	133	527	$F = 0.4397X - 9.6491$
3	Draft Tension	23	73	133	526	$F = 0.4406X - 9.7167$
4	Vertical Compression	284	77	142	553	
5	Vertical Compression	284	73	135	527	
6	Side way Tension & Compression	450	503	565	971	

APPENDIX E

Details of Speed Adjustment, Running Tool and Computer

Program, and Collecting High Speed Data

Hydraulic system was to be checked for several things. The situation of the swash plate of the pump that determined applied speed was fixed by turning a nut that controlled the swash plate. A potentiometer installed concentrically with the adjusting screw of the swash plate indicated different numbers at which each of them presented a particular speed of the carriage. Those numbers had been previously calibrated with their corresponding speed that best suited that specific depth and moisture content and were calibrated by preliminary tests. Hydraulic system was to be run ideally for few minutes to let oil get a normal temperature in order to avoid extraordinary high oil pressure and consequently unexpected higher speeds.

The below procedure was followed to set up computer and the program before they could exchange any information with the logger.

1. Turning computer on in windows mode
2. Restarting computer in MS Dos mode
3. **C:\WINDOWS>CD..** Enter
4. **C:\>** Enter
5. **C:\>CD TDS** Enter. RS232 should have been connected to the logger at this point and power of the logger should have been turned on up to here
6. **C: TDS>PC** Enter

There would be a question about which program to be compiled; just press enter

7. Enter
8. **F8** To compile TDS file
9. **Run fast** To determine mode of collecting data

(1.88 second program).

10.   Enter

When the last line of the program, "run fast", was written on the screen and enter key was pressed, RS232 was disconnected from the logger, and all system was ready to run the tool and collect data.

By pressing start switch of the electric motor, hydraulic system was ready to receive commands from the electronic control box. On the electronic control box, high speed mode was chosen then the black button of high speed was pressed and finally, the green start button was pressed when the operator was ready to run the tool. Thus, high speed carriage started going forward as the tool was engaging within the soil. When the carriage was close to pass the second reed switch, red stop button was pressed by the operator to give the carriage enough distance to stop before it hits the end. All this took less than a second to occur. It was particularly important at lower depths (e.g. 40 and 80 mm) and higher speed (24 km h^{-1}) to stop the carriage manually. For higher depths (e.g. 120 and 160 mm) and lower speed (16 km h^{-1}), inertial force served as a powerful decelerator to brake the carriage after it passed the end reed switch.

Data collection was started when the reed switch, which was acting as triggering button, passed a magnet installed beside the beam and it was immediately indicated by turning the red light of the box on. Data acquisition was finished approximately 1.88 seconds later regardless of the tool running speed, and it was the time when the red light turned off.

After each experiment was performed, data were transferred and saved into the computer. The RS232 port on the logger was connected to the computer through a long cable, and the next procedure was followed to watch the data on the screen and to save them on the computer later.

1. **F1**   Shows main menu
2. +   To enter data file name (e.g. March1st)
3. **. Data**   All 1700 data lines of all 7 channels would quickly pass the screen
4. **F1**   Shows main menu

5. **X**   Exit from TDS

6. **CD**   Exit from Dos mode

7. **Exit**   enter into Windows environment

According to the above example procedure, data shown of the screen were saved in the TDS file under a file name of "March1st". In EXCEL, the file "March1st" could be opened through the C drive and TDS folder. The file was originally saved as a text file and could be saved on a floppy disc only as a text file. When the text file was opened in an EXCEL spread sheet, data could be saved as an EXCEL file for any further processing.

For the current research, raw data of each experiment were saved as both text and EXCEL files and were later processed to investigate the average speed and draft recorded during each experiment.

APPENDIX F

Forth Program

PROG81

(A/D DATA ACQUISTION PROGRAM ---DSDS November 2004

(High speed Data Acquisition system for Linear Soil Bin

(CREATED BY Denise Stilling for Reza

(digital output added by Wayne Morley

(MODIFIED FURTHER BY WAYNE MORLEY FOR 8 CHANNELS ONLY 7 RECORDED

(The program examines channel 7 to see when to begin; then in reads

(channels 0 to 7 and stores 0 -6 data at $9000.
(at the start and the end of the run and stored for determining
(rate of data acquisition.

(Assume data sensors connected to the A/D channels

(channel 0 -Hall's Effect Sensor --pulses --speed of travel divided by 2
(channel 7 -Trigger for the initiation of data acquisition
(channel 1 -Load cell for measuring force vertical A
(channel 2 -Load Cell for measuring force Draft A
(channel 3-Load cell for measuring force Draft B
(Channel 4 -Load Cell for measuring force vertical B
(Channel 5 -Load cell for measuring force vertical C
(Channel 6 -Load cell for measuring force Side Force
(
(
(
(The following code is a TDS2020 utility from Triangle Digitia1 services Ltd

($A-D.TDS ver 1.40 By Peter Rush 20 sep 93
([c] 1993 Triangle Digital services Ltd
(Analog to Digital routine for TDS2020, assembler code version

(Approx 27uS conversion time running from H8/532 PROM
(Approx 48us conversion time running from external PROM

: DENNYD ;(Dictionary pointer index word for debugging

DECIMAL
(---

CODE A-D (channel -n convert channel c 0-7, giving digital value n 0-1023
@R7+R3 MOVI,

R3 R4 MOVI, (two copies of channel no
B 7 ## R3 AND, (mask off channel number
B8##R3 OR, (select fast conversion
B $FFE8)) R3 MOVO, (store channel no
B $20## R3OR, (start conversion bit
B $FFE8)) R3MOVO, (start conversion
3 ## R4 AND, (mask off CH1 & CHO
R4 SHAL, (offset to A-D register
BEGIN,
B $FFE8)) 7 ## BTSTI, (await end of conversion
EQ N UNTIL,
$FFEO @R4 R3 MOVI, (get A-D result
5 ## R4 MOVI, (no of shifts less one
HERE $FB8A ! (start of loop
R3 SHLR, (normalise result
$FB8A@ R4 SCB/F, (loop back
@-R7 R3 MOVO, (keep result
END-CODE

(Dictionary pointer index for programming and debugging DSDS

(Memory pointers for storing data DSDS
$9000 CONSTANT STORAGE
$9000 VARIABLE PTR (Initializes PTR to current address for storing data
$9000 VARIABLE OPTR (Output pointer to access storage block
0 VARIABLE CTR (Increment each time PROGRAM1 is run)

PROG81

$0 0 2VARIABLE STARTIME
$0 0 2VARIABLE ENDTIME
$FF CONSTANT NODAQS (Determines number of samples to be taken

169

```
1 $81FO! (INITALIZE PORT A BIT 0 OUTPUT
: LEDOFF 0 $81EO ! ;
: LEDON 1 $81EO ! ;   DSDS
( Data Acquision
( Debugging words to see if A/D is working
:GET-A/D (A/D from channels 1to 4 and display to screen
7 0 DO I 32EMITIA-D.
LOOP
;

GET-A/DS ( A/D 100 samples from channels 1 to 4 and prints to screen
2000 0 DO I GET-A/D CR LOOP
;

: CHK-STORAGE (n---; checking size of storage area
0 DO I $9000 I 2*+ !LOOP;
: READ_STORAGE (end start --; prints from storage area
DO I 2* $9000 + @. CR LOOP;

( Iteratively running these words determined 13870 dwords space
( IE 3467 FOR 4 CHANNELS

( Data Acquisition word for PROGRAM1 DSDS
: GET-A/DS! ( Get A/D and store data slow approx 14+ seconds
1700 0 DO $9000 I 16 * + PTR ! 8 MS ( updating current pointer
7 0 DO I A-D PTR @ I 2*+ !LOOP
LOOP
;
:GET-A/DF! ( Get A/D and store data fast
1700 0 DO $9000 I 16 * + PTR ! (updating current pointer
7 0 DO I A-D PTR @ I 2*+ ! LOOP
LOOP
;
: DeltaTIME
ENDTIME 2@ STARTIME 2@ D-
;
( printing Data to the screen DSDS
: .DATA (prints space delimited data to screen

CR."TIME OF RUN" DeltaTIME 2DUP D.."TICKS " >SMH."SMH"
." TRIAL" CTR @ . CR
1700 0 DO I. 32 EMIT STORAGE I 16 * + OPTR !
7 0 DO I 2* OPTR @ + @. LOOP CR
LOOP
;
```

(Logic to control data acquisition
: RUNFAST (uses A-D without delay

LEDOFF
BEGIN 7 A-D 500 < UNTIL (waits for a value to be read from ch 8)
(THIS LINE ABOVE POLLS UNTIL AHIGH VALUE IS READ FROM CH 8)
(."TRIGGERED"

LEDON
(@TIME STARTIME 2!
GET-A/DF!
LEDOFF
(@TIM EENDTIME2!
1 CTR +!
; (captures 14 samples on each channels on 100 Hz signal)
: RUNSLOW (uses A-D routine with 8 M~ delay

PROG81

LEDOFF
BEGIN 7 A-D 500 < UNTIL (waits for a value to be read from ch 8)
(THIS LINE ABOVE POLLS UNTIL A HIGH VALUE IS READ FROM CH 8)
(." TRIGGERED"
LEDON
(@TIME STARTIME 2!
GET ..A/DS !
LEDOFF
(@TIME ENDTIME 2!
1 CTR +!
(captures14 samples on each channels on 100 Hz signal)

(To print data and capture to file, CAPTURE.DEF
(Select F1 then enter "+" use the numeric pad
(Enter .DATA from keyboard after values have been
(displayed, select Fl then enter "-" and data will have
(been captured as an ASCII file for future analysis)

: CAL (--; Displays 4 channels of A-D; use space to exit loop)

BEGIN
16 0 DO CR LOOP
7 0 00 CR ." Channel" I . 32 EMIT I A-D. CR LOOP CR

." Hit space bar to exit program" CR
500MS
KEY 32=
UNTIL;

(TO use program may need to adjust NODAQS and which channels you hook
(things up to otherwise enter PROGRAM1 undo serial interface run trial
(hook up serial interface run .DATA and select file capture from main menu

: HELP
." To CALIBRATE enter the command CAL" CR
." To RUN the program enter RUNFAST OR RUNSLOW and operate soil bin" CR
." TO CAPTURE data to a file hit F1 then '+' on numeric keypad" CR
." then type .DATA then hit F1 then '-' on numeric keypad" CR
" then exit to DOS and rename CAPTURE.DEF to your TRIALNAME" CR ;
" RUNFAST IS 2 SECOND PROGRAM RUNSLOW 14 + SECOND..